COOPERATIVE BEHAVIOR IN BEES, WASPS, AND BURGLARS

A Dissertation

Presented to the Faculty of the Graduate School

of Cornell University

in Partial Fulfillment of the Requirements for the Degree of

Doctor of Philosophy

by

Kathryn Joann Montovan

August 2013

COOPERATIVE BEHAVIOR IN BEES, WASPS, AND BURGLARS

Kathryn Joann Montovan, Ph.D.

Cornell University 2013

There are many aspects of social, colonial, and individual behavior that are puzzling and difficult to understand. Mathematical models provide an ideal tool for understanding the possible behaviors of systems under different hypotheses, often providing surprising insights about the actual effects of different model pieces. We use a number of different types of theoretical, mathematical and computational models to examine a few areas of insect and social behavior related to cooperation. First we consider a self-organized storage pattern in the comb of honey-bees. This pattern makes the colony more efficient and helps facilitate the survival and normal development of the brood (young bees). We explore how the colony level patterns can emerge and be maintained by thousands of bees performing tasks using simple rules that rely only on local information. We discuss how the results of these models demonstrate gaps in the current knowledge of honey bee behavior and motivate further research on queen movement patterns.

We then explore the evolution of restraint for the parasitoid wasp *Hyposoter horticola*, which parasitizes host egg clusters but utilizes only 30% of the eggs in each cluster. Since natural selection favors individuals with more offspring, it is puzzling that these wasps do not use more of the available resources. We use both theoretical models and empirical results to explore several plausible explanations for this behavior. We first consider whether the wasp's parasitism is reduced by physical/physiological constraints. Then, we explore selective pres-

sures that might favor submaximal parasitism behavior and discuss the most reasonable explanation for sub-maximal parasitism by *H. horticola*.

Last, we explore the related, but more general question of the evolution of cooperative behaviors. We use the iterated prisoner's dilemma to model the benefits and costs of cooperation for repeated interactions. We classify the population dynamics for interacting strategies to understand the conditions that favor greater levels of cooperation. We then explore the bifurcations of the system. These bifurcations show where small changes to parameter values produce qualitatively (and sometimes drastically) different population dynamics.

BIOGRAPHICAL SKETCH

Kathryn Joann Sullivan was born in Lincoln, NE and grew up spending summers in a small town in rural Nebraska and school years in St. Paul, Minnesota. She graduated from St. Paul Central High School in May 2001, and the University of Minnesota, Morris (UMM) in May 2005. At UMM, she primarily studied math and three dimensional studio art. In her last year, she participated in an REU internship at the Smithsonian Environmental Research Center (SERC) which led into two years of work as a lab technician, counting barnacles, grinding plant samples, attending seminars, and dreaming about using advanced mathematical modeling to test ecological hypotheses against data.

Her desire to learn ecological modeling and a lifelong interest in teaching motivated Kathryn to pursue a Ph.D. in applied mathematics at Cornell University. While at Cornell, Kathryn developed diverse skills in mathematical ecology in her studies and research and refined her teaching approaches while instructing in the math department and for Cornell Outdoor Education. Her aim is to become a professor at a small liberal arts school that values both excellence in teaching and research.

In May of 2009 Katie became Kathryn Joann Montovan when she married her wife, Maggie at the camp where they met. Katie looks forward to the next phase of her academic adventure which will take place at Bennington College, where she will be a professor teaching applied mathematics. Bennington College is a small school with highly interdisciplinary students where she will be able to develop effective teaching techniques in small classes of motivated students, perform research with students with multiple intersecting interests, and teach a wide variety of classes.

To my family:

For mastering the art of nodding and smiling supportively.

ACKNOWLEDGEMENTS

First, I would like to thank each member of my special committee. They have all played a essential role in my growth as a scholar throughout the last six years. Laura Jones helped me define my project, learn R, become a better writer, and was my mentor. Saskya van Nouhuys gave me the opportunity to do field research on my study system, helped me learn how to design, implement and write about experiments, and has taught me many essential lessons about academic writing and research. Kern Reeve introduced me to the fascinating world of behavioral models and has taught me how to think critically about biological systems, ask important questions and create models that fit the biology. Steve Strogatz accompanied me on an adventure into the mathematical world of cooperation cycles and nemesis strategies and taught me to simplify ideas into their most essential elements and how to find a niche within a well-studied field.

Chapter 1 is a joint project with Nathan Karst (now at Babson College), Tom Seeley, and Laura Jones. I would like to thank Tom for introducing me to the fascinating world of insect behavior and Nathan for being my co-pilot on this project. I would also like to thank the NSF-IGERT program for encouraging interdisciplinary research and supporting both Nathan and me while we did this project.

Chapter 2 is the result of close to a decade of work by many people. Saskya van Nouhuys has been studying the ecosystem for decades and provided uncountable observations and datasets that helped parametrize and test the models. Kern Reeve provided behavioral modeling expertise and Laura Jones considered the broader implication that landscape might play. Christelle Couchoux was very generous with her experimental data and performed some of the key studies presented here. David Muru helped perform the group fitness study

and Lucie Salvaudon helped with the egg cluster architecture study. Suvi Ikonen, Terhi Lahtinen, Mina Brunfeldt, and Eliza Metsovouri provided essential laboratory support. Funding from the Academic academy of Finland grant numbers 250444, 213547, 125553 to S. van Nouhuys and a travel grant from the Cornell University Department of Ecology and Evolutionary Biology funded my travel to Finland to perform experimental work and observations.

In Chapter 3, I present the results of a joint project with Steven Strogatz and Danielle Toupo. Another applied mathematics student, Isabel Kloumann, is working on a closely related project and provided great feedback and ideas on this project.

I would also like to thank the Cornell Graduate School, Dean Jan Allen, and the '2013 Spring Break Boot Camp' crew for jumpstarting my progress on my dissertation. In bootcamp I learned the secrets of being a productive writer and finishing a Ph. D. (i.e. "write every day" and "a good dissertation is a done dissertation"). This support was instrumental in my success in this final stage of my studies.

I want to say a sincere and heartfelt thank you to my family and friends for their support, encouragement, and guidance. They have forgiven me for many forgotten birthdays, inattentive phone calls, impatience and forgetfulness. They have also patiently calmed me down when I was upset, encouraged me when I was sure I couldn't succeed, and found ways to help me get what I needed to make it through. Each time, I have secretly promised to dedicate my dissertation to each of them. This dissertation is my christmas, birthday, and thank you gift for each of them for the past few years. Their support has made it possible, and I have completed it for all of them.

Last, but certainly not least, I would like to thank my wife, Maggie, who is my rock. She kept me level while I was pulled in multiple directions, laughing when things got too serious, and having fun in my spare moments. She too has forgiven a large amount of neglect as I focus on my studies, and for this I am grateful. During the stressful parts of graduate school, job applications and interviews, she has made sure that I eat regularly, make it to the gym, sleep, and don't live in a slovenly state of chaos. She has been an instrumental part of this dissertation. She does not know enough math or ecology to contribute to my research but she is my invisible coauthor in everything I do.

TABLE OF CONTENTS

LIST OF TABLES

LIST OF FIGURES

CHAPTER 1

INTRODUCTION

Cooperative behaviors are generally thought of as actions that impart a benefit to the group at a personal cost to the individual. These sort of behaviors have puzzled biologists, economists, behavioral scientists, ecologists, and social and political scientists for decades. Selfish individuals would seemingly benefit from being greedy and non-coorperative, but it is common to find cooperation in societies and ecosystems and many of these systems rely on this cooperation for their continued existence. In our society today we are more and more connected with each other and that provides opportunities for increased levels of generosity, but also wider reaching and more visible harm from greed. There is always a need for cooperation in societies, but we are encountering new challenges of changing human connectivity and it is more important than ever that we gain a better understanding of how we can facilitate and encourage generous and cooperative actions for the benefit of everyone. Climate change is a great example of a problem whose solution requires the cooperation of large groups of people but where individuals have motivation not to do their part. We contribute to this conversation by considering three specific (but unrelated) questions about individual behavior and the mechanisms that maintain cooperation under each set of circumstances.

Ecology is the study of how organisms interact with each other and their environments. The interactions are often complex and occur at different scales. For example, there are several species of small reef fish, often referred to as cleaner fish, that groom larger fish by removing dead skin and ectoparasites.

The host fish refrains from eating the cleaner fish and benefits from the cleaning, and the small fish gets an easy meal. Can we understand the implications of the mutually beneficial relationship for the relative population sizes for both cleaner fish and the larger 'hosts'.

Ecologists strive to understand similar larger implications of interactions between species for the composition, distribution, amount, and state of organisms within and among ecosystems. Targeted experiments can help us understand the direct interactions between individuals or the effects of the environment on specific species, but a theoretical framework is required to understand how micro-scale interactions combine to create different ecosystem compositions and population fluctuations.

Evolutionary biology studies the evolutionary processes that have produced the diverse array of species that currently inhabit the earth. We focus on the behavioral end of evolutionary biology which considers how certain behaviors may have evolved in response to the environment or other pressures. When these pressures are interactions with other species, we enter the realm of behavioral ecology which considers how species coevolve in response to each other.

In my work, I use mathematical models to test theoretical hypotheses about the interactions or evolutionary pressures that create observed, larger scale patterns. I am specifically interested in understanding cooperation, restraint and collective behaviors. I work closely with biologists to develop a set of reasonable hypotheses that could explain the phenomenon of interest. I then formulate these hypotheses as mathematical models, and use existing data and targeted

experiments to formulate and parametrize each model. These models make predictions that I compare with the biological data. In this way, I am able to consider abstract theories, make concrete predictions and understand whether each hypothesis is theoretically reasonable. I use a diverse set of mathematical and modeling tools, with an emphasis on game theory, computer-based simulation modeling, and dynamical systems analysis. This dissertation is comprised of three, somewhat disjoint, projects that are connected by their relevance to cooperative-like behaviors, with a focus on insect behavior.

Chapter 2 focuses on how self organization in honey bees can create beneficial patterns of storage in the comb. Self-organization is a process by which a global order arises from local interactions. Bees work together in many colony activities with each of thousands of bees following a fairly simple set of rules that combine to create beneficial colony-level structures. I consider a storage pattern that is formed on the inner combs of the hive. On these sheets of comb, the developing brood are clumped together into a central brood region, with pollen stored nearby, and honey in the periphery. Previous modeling work on these comb patterns discovered rules that can create a self-organized pattern on empty comb, but did not consider whether the self-organized patterns can be maintained after the brood mature and start to vacate their cells.

The currently accepted model of self-organized cell allocation pattern formation [18] does not maintain observed comb patterns, so I consider alternative hypotheses that could maintain the allocation patterns. I start the model with a well formed pattern and implement three sets of rules governing comb storage related bee behavior. These include simple rules for how the queen moves

across the comb and what criteria she uses to decide if an empty cell is acceptable for a new brood, where honey and pollen are placed when brought into the comb, and how honey and pollen are consumed from storage. I find a set of simple rules that maintain the self-organized storage patterns over realistic seasonal time-frames. This work motivates additional experimental work that is essential to truly understanding the maintenance of the comb pattern.

In chapter 3, I consider the reasonable evolutionary causes for submaximal resource use by the parasitoid wasp *Hyposoter horticola* in the Åland islands of Finland. The puzzle here is that the wasp parasitizes clusters of host eggs, but utilizes just a small fraction (roughly 30%) of each cluster, ignoring many seemingly good hosts, and marking the cluster to deter other wasps from using it. *H. horticola* lays it's eggs within the host butterfly larvae and it's offspring are dependent on the host throughout their larval development. I first use experimental data to consider whether the wasp is able to parasitize all of the eggs in the cluster. To do this we determine if the wasp has enough eggs and time to parasitize more hosts, the hosts are all available at the same time, the wasp can access all eggs in the mounded cluster, and if the hosts have undetected immunological defenses that eliminate some of the parasitoid eggs or larvae. We find that it is unlikely that the wasp's parasitism frequency is limited by physical or physiological constraints.

Since the wasp appears to be physically able to parasitize more eggs, the frequency of parasitism must be beneficial for some reason, otherwise the wasps would evolve higher parasitism rates. There are multiple established evolutionary theories that explain the evolution of submaximal resource use for other

species. The most relevant and notable theories are prudence, risk-aversion, and optimal foraging. For *H. horticola*, prudence takes the form of reduced parasitism to increase local host densities in future generations, and risk-aversion would mean parasitizing smaller fractions of multiple clusters to reduce the risk of losing all offspring. Both of these hypotheses turn out not to be applicable to *H. horticola* because of the large and well mixed populations of *H. horticola* in the Åland islands. The most plausible reason is that the wasp leaves each cluster after parasitizing a third of the eggs because this optimizes the wasp's limited time and gives her offspring the best chance of survival. My work eliminates many seemingly plausible hypotheses for the cause of this submaximal parasitism and suggests the most likely explanation for this behavior.

In chapter 4, I examine cooperation more generally by exploring the potential for stable levels of cooperation in the stochastic iterated prisoner's dilemma. I start by considering the interactions of just two strategies: any contender against the reigning champion. If the reigning champion is fairly cooperative but relatively unforgiving of defections, frequently retaliating by not cooperating after they opponent does not cooperate, then more cooperative contender strategies will be able to win and take over. If the reigning champion is too forgiving, then less cooperative strategies will take over. Thus, to end up with more cooperative populations, the strategies must not be too forgiving of defections.

We then consider a population with 3 types of people: everyone is either nice, mean, or police-like. Nice individuals are giving and cooperative with everyone, mean individuals take as much as they can from everyone, and police

retaliate against mean individuals and are nice when someone is nice to them. Our goal is again to explain the conditions that favor cooperation. The prevailing strategy depends on how forgiving the nice individuals are, how damaging the mean individuals are and the frequency of mistakes in the interactions (*e.g.* I mistakenly think you were mean to me when you meant to be nice). We again find that the population is taken over by more cooperative individuals if the nice strategy is not too forgiving of defections. When the nice individuals are more forgiving, stable populations with at least some cooperators are still possible. In this case, the population could settle to a state where there are enough police to keep the burglars from significantly harming the nice volunteers, and all three types have steady and non-zero population sizes. The prevailing strategy (or strategies) depends not only on the relative benefits and costs of cooperation, but also on how many mistakes the police make, and how forgiving the nice individuals are.

In this dissertation, I present studies of cooperative-like behaviors in three, very different, contexts. This is not a comprehensive study of cooperation, but does provide a deeper level of understanding about these types of cooperative behaviors. Colonies work together to create important colony-level organization and we explain how this organization can be maintained by thousands of bees following simple, local rules. This demonstrates the importance of understanding how self-organization can maintain order. Somewhat unrelatedly, parasitoids must somehow ensure that they do not wipe out their hosts and thus cause their own extinction in the process. Thus submaximal resource use benefits the species, but comes at a large cost to individuals who reduce parasitism. Under these circumstances there must be some mechanism that maintains low

parasitism rates (which are cooperative-like). Last, repeated interactions between individuals facilitate greater levels of cooperation despite the personal costs associated with cooperating. We explicitly describe the conditions under which cooperative strategies dominate the population and refine our understanding of population dynamics of cooperative, non-cooperative and retaliatory strategies in populations. This work adds to our current understanding of the maintenance of cooperation in three diverse contexts.

CHAPTER 2

LOCAL BEHAVIORAL RULES SUSTAIN THE CELL ALLOCATION PATTERN IN THE COMBS OF HONEY BEE COLONIES (*APIS MELLIFERA*)

Abstract

In the beeswax combs of honey bees, the cells of brood, pollen, and honey have a consistent spatial pattern that is sustained throughout the life of a colony. This spatial pattern is believed to emerge from simple behavioral rules that specify how the queen moves, where foragers deposit honey/pollen and how honey/pollen is consumed from cells. Prior work has identified a set of such rules can explain the formation of the allocation pattern starting from an empty comb. We show that these rules cannot maintain the pattern once the brood start to vacate their cells and bees refill these cells. We propose new, biologically realistic rules that better sustain the observed allocation pattern over time. Specifically, we consider an alternate model formulation of brood density-dependent honey and pollen consumption and an alternate model of queen movement which biases her walk toward the center of the comb in response to heat gradients on the surface of the comb. We analyze the three resulting models by performing hundreds of simulation runs over many gestational periods and a wide range of parameter values. We develop new metrics for pattern assessment and employ them in analyzing pattern retention over each simulation run. Applied to our simulation results, these metrics show alteration of an accepted model for honey/pollen consumption based on local information can stabilize the cell

allocation pattern over time. We also show that adding global information, by biasing the queen's movements towards the center of the comb, expands the parameter regime over which pattern retention occurs.

2.1 Introduction

Honey bee colonies benefit from a high degree of internal organization, in which thousands of bees work together to make decisions and create stable, colony-level patterns. Elements of colony-level organization and decision making rely on individual bees performing fairly simple actions; for example, foraging bees perform waggle dances that recruit others to desirable foraging locations in appropriate densities [31], and new colonies collectively choose the best nest cavity based on information gathered by many individual bees [95]. In this paper, we consider how the actions of individual bees can cause the self-organized creation and maintenance of a colony-level storage pattern for brood, honey, and pollen in a colony's combs.

Seeley and Morse (1976) described a general cell allocation pattern in the nests of honey bees: a dense brood clump surrounded by cells storing pollen, and with honey stored in periphery cells, mostly in the upper region of the comb [94]. This distribution of different types of cells confers several benefits to the colony. First, it helps ensure that a colony's brood are raised at the proper temperature. Tautz *et al.* (2003) showed that the temperature at which pupae are incubated has a significant impact on their ability to perform foraging functions as adults [104]. Fehler *et al.* (2007) connected temperature, colony efficiency,

and brood density by demonstrating that brood areas with larger percentages of open cells require more attention from workers in order to maintain an optimal brood rearing temperature [34]. Starks and Gilley (1999) deepened this connection between the temperatures and brood health in their observation that that worker bees themselves act to shield brood from temperature fluctuations by positioning themselves on particularly warm areas on the interior of the hive's walls [101]. Camazine (1990) argued that along with worker behavior, the physical distribution of different cell types can act to maintain proper temperature by suggesting that concentrating brood cells near the middle of the nest helps insulate the larvae from fluctuating environmental conditions [20]. Thus, an advantageous positions of brood cells frees workers from needing to perform some thermoregulation tasks.

Second, maintaining a ready supply of pollen near developing brood increases work efficiency by the nurse bees in a colony. Cralsheim *et al.* (1992) showed that the primary consumers of pollen are nurse bees which feed the brood [26], and Camazine (2001) noted that pollen storage near brood cells would theoretically reduce the time and energy spent by nurse bees in retrieving stored pollen [19]. Taken in total, the existing literature presents a convincing case for the effectiveness of a densely populated region of brood cells immediately surrounded by a ring of pollen storage cells, with honey storage cells filling the remainder of the comb.

Much work has been done to understand how this pattern is created within the nest, but none of this research has considered pattern maintenance after brood begin to vacate their cells. These newly emptied cells are then refilled

with brood, pollen or honey. Originally, it was believed that the pattern arises because each bee follows an internal blueprint, placing each product in its associated cells according to an overall plan [94, 93, 119, 18]. Camazine refuted this argument by observing that when empty comb is inserted into the brood region it is initially filled with both pollen and honey, but that fairly quickly these cells are emptied and filled with brood [18]. This observation led to cellular automata models [18, 19] and simplified differential equation models [20, 59] of self-organized pattern formation in which the storage patterns result from each bee following simple behavioral rules that do not rely on global information about the nest. These models are able to explain the creation of an idealized self-organized pattern on an initially mostly-empty sheet of comb, but they only consider the first 20 days or a single brood generation; the simulations based on these models stop before the first bees vacate their brood cells.

A more recent model for the storage pattern developed by Johnson (2009) combines the idea of self-organization with gravity-based templates (*i.e.*, blueprint-like rules) which bias the movement of nectar handlers towards the top of the comb and help produce a more realistic pattern with honey stored near the top of the comb [60]. This model includes two kinds of global information, templates for nectar storage and brood cells, but it too only considers the pattern formation before young bees start to vacate their cells (the first 20 days).

In this section we present an agent-based model that uses simple, local, biologically relevant rules to maintain storage patterns over multiple brood cycles. We start with the model developed by Camazine in 1991 [18], which can create a self-organized pattern on a nearly empty comb (now referred to as model 1)

and change some of the rules in biologically reasonable ways to create models that both initially create and then steadily maintain the comb allocation patterns once young bees begin to vacate their cells (models 2 and 3).

Our first modification is in the implementation of a rule that specifies that consumption of nectar and pollen is brood-density dependent. This behavioral rule is based on the observation that most of the stored pollen and a good amount of the stored honey are consumed by nurse bees feeding the brood [26]. These bees typically start their search for pollen or honey from a brood cell and would find nearby food cells more frequently than far away cells. In our model pollen, a storage cell can hold up to 15 loads of pollen or 25 loads of honey. In model 1 [18], when a bee is searching for a cell from which to consume nectar or pollen, the cell is chosen randomly from all of the cells in the comb, and the number of loads taken is linearly proportional to the local density of brood within a preset radius of up to four cells. Thus, when a cell is chosen, a greater number of loads are taken if there are many brood cells nearby. We argue that this is not realistic, because nurse bees cannot carry more nectar or pollen than other bees. Instead, they are more likely to choose cells close to the brood. Thus, we propose modifying the implementation of this rule to linearly increase the probability of choosing cells near brood based on the local brood density and then take only one load each time the cell is chosen (models 2-3). Thus cells near brood are more likely to be chosen but only one load is taken from each chosen cell.

Our second modification is in the way that the queen moves as she deposits brood (model 3). In the original model (model 1, based on [18]) and model

2, each time the queen moves she choses a random direction and moves one step. We consider the option that she senses heat gradients on the surface of the comb and modifies her direction of movement based on these heat gradients. These heat gradients result from a colony-level effort to maintain an acceptable temperature for brood survival and development [34, 104]. The workers in the colony maintain the temperature in the brood region by heating the caps of individual brood cells [16], entering empty cells within the brood region and heating adjacent brood through the cell walls [62], creating evaporative cooling [49], and using their own bodies to make a heat-shield [101]. These thermoregulatory actions, focused on the brood region, can create thermal gradients across the nest [57] that are qualitatively similar to the gradients measured in colonies of bees [8]. When the comb is full, as will be the case for most of our modeling, there is a well established temperature gradient from center to edge [63]. It has been shown repeatedly that bees are aware of and change their behavior in response to the temperatures that they experience [42, 113] and it is reasonable to believe that the queen can sense these thermal gradients and respond accordingly. There has been no research done on the queen's specific response to thermal gradients so we model them according to our best intuition and present this as an open question in honey bee behavior.

2.2 Methods

In a comb that has a well formed cell allocation pattern, the actions of the bees can either maintain or destroy this pattern over time. The difference between maintenance and destruction lies in the choice of parameters for key functions,

as well as in implementation choices for important pieces of the model. Since a significant amount of work has already been done on the formation of the pattern, we will focus on the ability of simple rules to maintain the storage pattern over realistic timeframes of multiple brood cycles. We begin by outlining the overall structure and computational aspects of the simulator and parameter selection scheme (Section 2.2.1). We then detail the three main components of the models we compare: queen movement and oviposition (Section 2.2.2), nectar/pollen collection and deposition (Section 2.2.3), and nectar/pollen consumption by all bees (Section 2.2.4). Finally, we will confirm that the proposed rules are also able to form the pattern on a nearly empty comb.

2.2.1 Model implementation

We implement the models using an agent based simulation model in Matlab [69]. The modeled comb is 45 cells wide by 75 cells tall with hexagonal cells, which matches the approximate number of cells on one side of a full depth Langstroth frame. We simulated a season of 60 days or 3 brood cycles, with a 12 hour day-night cycle. The simulation has hour-long time steps, where foragers deposit honey and pollen during the day, and bees consume honey and pollen and the queen lays eggs into suitable cells during all hours.

At the beginning of each hour, we determine the number of eggs the queen attempts to lay as she walks along the comb (see Section 2.2.2), and the amount of honey and pollen deposited and consumed (see Section 2.2.3). In order to avoid simulation artifacts caused by some tasks being preferentially performed

before others, we randomize the sequencing of deposition, consumption and oviposition events each hour. Brood mature in approximately 21 days and then vacate their cells [119], so in the model, the 21-day-old immature bees are randomly partitioned into 24 equally sized groups (up to rounding error), one of which vacates its cells at the end of each hour.

Unless specified, each model run was initiated with a completely full comb with an ideal pattern of a center region of brood, surrounded by a ring of pollen, and honey in all remaining cells. The assignment of type to each cell is deterministic and constant across all simulations. The brood region is a circular disk centered in the middle of the comb with radius 18 cell lengths. Around this brood region is a ring of pollen 4 cell lengths wide. The rest of the comb is filled with honey. Each storage cell has the capacity to contain up to 25 loads of honey or 15 loads of pollen. This is consistent with [91] and is between the estimates used in [18] and [60]. The initial amount of nectar in each pollen and honey cell was chosen uniformly randomly from the ranges of $1-15$ loads and $1-25$ loads, respectively. Similarly, the initial age of each brood cell is chosen uniformly randomly from $1-21$ days. While developing the model, we explored multiple capacities and found that changing the capacity of the honey and pollen cells within the established ranges (pollen: $15-20$ loads per cell, honey: $20-40$ loads per cell) did not qualitatively change the resulting allocation patterns.

Other parameter estimates for this system are somewhat speculative, so we consider a wide range of values for each model parameter. To sample the parameter space efficiently and enable analysis of model sensitivity to variation in parameter values, we used a Latin hypercube sampling structure. Latin hy-

Parameter	Description	Estimate	Range
n	Queen's cell visitation rate (cells per hour)	60 [18]	60 – 120
r_b	Brood requirement radius (cells)	4 [18]	1 – 4
r_n	Preferential nectar consumption radius (cells)	4 [18]	1 – 4
ω	Average honey collection (loads per day)	833 (Sec. 2.2.3)	1000 – 4000
ρ_{ph}	Ratio of pollen collection to honey collection	0.21 [18]	0.2 – 1.0
ρ_p	Ratio of pollen consumption to pollen collection	0.99 [18]	0.9 – 1.1
ρ_h	Ratio of honey consumption to honey collection	0.59 [18]	0.9 – 1.1
χ	Temporal distribution of daily nectar and pollen collection: uniform constant ($\chi = 0$), uniform random ($\chi = 1$) and Markov clumped random ($\chi = 2$)	NA	0 – 2
k	Model 1: Ratio of honey/pollen taken from cells fully surrounded by brood cells to honey/pollen taken from cells with no brood neighbors	10 [18]	5 – 20
k	Models 2 and 3: Ratio of probability that a cell fully surrounded by brood cells is chosen for nectar consumption to the probability that a cell with no brood neighbors is chosen	10 [18]	5 – 20

Table 2.1: Parameters used in simulations of models 1- 3 and the sensitivity analysis. The estimates from the literature were used as a starting point for parameter ranges. The reasoning for the given ranges based on the literature estimates are given within the relevant model description sections. For example, for queen cell visitations, the estimate is for the number of eggs laid per hour, so we inflated it to account for the queen rejecting cells, then extended the range for sensitivity testing. Similar reasoning explains the elevated range for w. The values for $\rho_{ph}, \rho_p, \rho_h$ apply most directly to the pattern formation phase of colony development, and were modified for the full comb.

percube sampling chooses m equally likely values for each parameter and then randomly selects (without replacement) from these values to create a unique parameter set for each of the m model runs [11, 32]. We create 200 unique parameter sets that we use to analyze all three models. Ranges for the key parameters in the model (Table 2.1) were chosen based on the relevant literature, with ranges extended to acknowledge uncertainty in parameter estimates. Reasoning for particular parameter choices is included in the related model sections

below.

As discussed in Section 2.1, we consider three agent-based models. While the details of each will be elaborated below, the main components and their similarities and differences are as follows:

Model 1: The queen performs a random walk across the comb and attempts to oviposit in suitable cells. Workers attempt to deposit honey and pollen in cells sampled uniformly randomly from all cells which are empty or partially full of the same material. Workers attempt to consume honey and pollen sampled uniformly randomly from all cells, with the number of loads taken proportional to the local density of brood cells.

Model 2: The queen performs a random walk across the comb and attempts to oviposit in suitable cells. Workers attempt to deposit honey and pollen in cells sampled uniformly randomly from all cells. Workers attempt to consume 1 load of honey or pollen at a time, with the probability a cell will be selected proportional to the number of neighboring brood cells.

Model 3: The queen performs a random walk biased towards the center of the comb and attempts to oviposit in suitable cells. Workers attempt to deposit honey and pollen in cells sampled uniformly randomly from all cells. Workers attempt to consume 1 load of honey or pollen at a time, with the probability a cell will be selected proportional to the number of neighboring brood cells.

When mathematically defining the exact mechanisms by which these ex-

tractions, depositions and ovipositions occur, it is convenient to have symbols to refer to certain classes of cells. At every time t, we can partition the cells of the comb into four subsets: $E(t)$, the empty cells; $H(t)$, cells containing honey; $P(t)$, cells containing pollen; $B(t)$, cells containing brood. We define $N = (45)(75) = 3375$ to be the total number of cells on the comb.

2.2.2 Queen movement and egg laying

In order to capture the variability in the queen's walk across the comb, we use one of two probability distributions to model the direction of her movement:

(1) uniform distribution on the interval $[-\pi, \pi]$ (random walk)

(2) wrapped Gaussian distribution with mean θ and standard deviation σ on $[-\pi, \pi]$ (biased random walk).

In both cases, the mean $\theta = 0$ represents the angle pointing the queen from her current position towards the center of the comb. Once a direction is chosen, the queen moves to the nearest cell in that direction.

While the uniform angle distribution is relatively straightforward, the exact mechanism by which we introduce a bias in the queen's movements towards the center of the comb is important. For simplicity, we implement an affine scaling of the standard deviation of the distribution as a function of the queen's

distance from the center of the comb of the form

$$\sigma = \sigma_o - (\sigma_o - \sigma_c)\frac{d}{d_{max}}, \tag{2.1}$$

where d is the distance in cell lengths from the center of the cell on which the queen is currently located to the center of the cell in the center of the comb, and $d_{max} = \sqrt{22^2 + 37^2}$ is the maximum distance from any cell to the center of the comb. The tunable parameters σ_o and σ_c describe the desired standard deviation when the queen is located at the center (origin) and corners of the comb, respectively. With σ_o sufficiently large, the wrapped Gaussian produces nearly uniformly random angles when the queen is near the center of the comb. If $\sigma_o > \sigma_c$, the queen's movement becomes increasingly biased towards the center of the comb as she moves farther away from it. We set $\sigma_0 = 5$ and $\sigma_1 = 2.828$. With this choice, the queen visits cells at the edge of the comb roughly half as many times as cells near the center of the comb. Figure 2.2.2(a) shows the number of visit to each cell for a typical random walk by the queen, and Figure 2.2.2(b) shows the number of visit to each cell for a typical biased random walk.

The number of cells visited by the queen in one hour, n, is determined by the Latin hypercube sampling for each model run and is between 60 and 120 cells per hour. This parameter range was chosen because the queen lays between 1000 and 2000 eggs in a day, with is equivalent to $42 - 84$ eggs per hour [74, 12, 18]. We selected a range from $60 - 120$ cells visited per hour because many attempts to lay eggs fail either because the cell is already in use or because it is too far from the nearest brood cell. In an empty comb the queen will lay roughly the desired maximum number of eggs and in a more full comb her efficiency decreases as she spends more time searching for suitable cells. The set of cells $A(t)$ which the queen finds acceptable are empty and within radial distance r_b

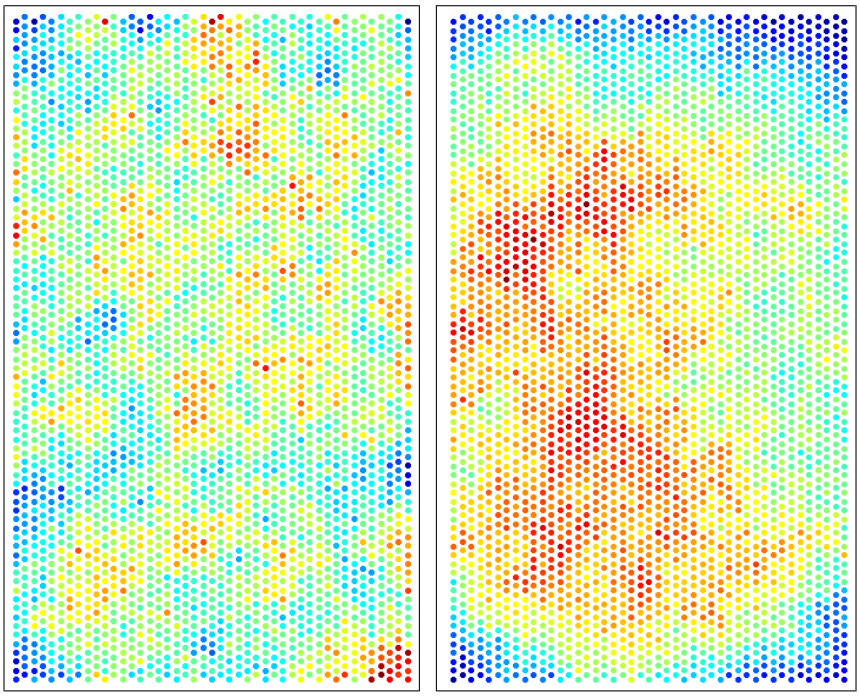

(a) Random walk (b) Biased random walk

Figure 2.1: Density maps of the number of queen visits per cell for 1,000,000 steps of the queen according to an example of the a) random walk and b) biased random walk. Red cells were visited most often and blue cells were visited least often.

from a brood cell. In symbols,

$$A(t) = \{e \ : \ e \in E(t), \min_{b \in B(t)} d(e, b) \leq r_b\}, \tag{2.2}$$

where $E(t)$ is the set of empty cells at time t, and $d(x, y)$ is the Euclidean distance measured in cell lengths between the center of cell x and the center of cell y. This distance threshold r_b is varied in the Latin hypercube sampling design between 1 and 4. The upper end of this range was chosen to match Camazine's model [18] and the shorter distances test the sensitivity of the models to this parameter.

2.2.3 Nectar and pollen collection and deposition

Both honey and pollen are deposited into cells which are empty or partially filled with the same substance as is being deposited. Pollen foragers and honey storers examine multiple cells when depositing loads of food [17] and deposit less honey and pollen when the comb is full [96]. To be consistent with these observations, each forager selects cells uniformly randomly from *all* comb cells and is allowed up to 6 attempts to find a suitable cell. Modeling deposition in this way serves two purposes. First, workers do not need to have global information about the location of all honey and/or pollen cells at a given time as they would if the cells were chosen randomly from the available honey/pollen cells and empty cells. Second, a worker aborting the search for an appropriate cell on this comb approximates the worker going to find an empty cell on another comb when the simulated comb is becoming overly full. This creates the random deposition with the desired decreased deposition rate for full combs. We note that this interpretation of how to model pollen and honey deposition conforms to the descriptions in Camazine [19].

In order to describe deposition in our agent-based model, we must describe the collection and deposition rates in terms of actions of individual bees. We calculate the number of individual loads of honey and pollen that are deposited into the comb each hour from established yearly totals and measured bee load capacity. A typical colony collects 60 kg of honey in a season, with 40 mg of honey in each load, 180 days in the summer season, and approximately 10 sheets of comb per colony [18, 19]. This results in approximately 833 loads on average entering each sheet of comb in the hive every day. This estimate was then in-

creased to account for the fact that, in our models, many attempts to deposit honey are unsuccessful because the chosen cells are full or partially full of the wrong substance. For each model run, the average number of loads of honey collected per hour ω was determined by uniform sampling between 1000 and 4000 loads per day for the Latin hypercube setup. The average number of loads of pollen collected per hour is chosen by Latin hypercube sampling [71, 11] as a fraction of the collected honey, $\rho_{ph} \in [.2, 1]$ so the total amount of pollen collected in a season is $\rho_{ph}\omega$. The ratio ρ_{ph} has been observed to be about 0.26 [18]. Our model extends this range to look at the sensitivity and consider potential changes in storage ratios for the full comb within the simulated nest.

Pollen and honey availability depends on seasonally variable flowers and weather dependent favorable foraging conditions. To capture this, we consider three different types of temporal variability in nectar foraging, with the method chosen at random for each model run. The amount of honey and pollen collected per day are either

(1) constant in time and equal ω and $\omega\rho_{ph}$, respectively. This represents an unrealistic environment with favorable foraging conditions each day and a constant amount of honey and pollen available each day.

(2) drawn uniformly randomly from $[0, 2\omega]$ and $[0, 2\omega\rho_{ph}]$, respectively. This represents an environment where foraging can occur each day, and there is always some honey and pollen available, but the daily amount varies somewhat from day to day.

(3) subject to a Markov process in which the amount of honey and pollen collected are either identically zero or equal to 2ω and $2\omega\rho_{ph}$, respectively,

with probability 0.70 that the amount collected on a given day will be the same as the amount collected the day before. This represents an environment where there spans of several days with unfavorable weather for foraging but on good days a constant amount of nectar and honey are available.

The transition probability in the Markov process model was chosen to create realistic fluctuations in food availability. This could be refined, but for our model we decided to keep this element fairly simple. In all of these cases, the total amount of food collected during the modeled season is set to the predefined amounts for each type of food. The daily amounts were then used to calculate the hourly collection rates which is simply one twelfth of the daily collection rates.

2.2.4 Nectar and pollen consumption

Food consumption is modeled by randomly choosing a cell in the comb and taking a load out of this cell if it contains the desired food type. We assume that consumption depends heavily on the number of nearby brood. The dimensionless brood density within distance r_n at a cell c is given by

$$D_{r_n}(c) = \frac{|\{b \ : \ b \in B(t), d(b,c) \leq r_n\}|}{3r_n(r_n+1)}, \tag{2.3}$$

where $B(t)$ is the collection of brood cells at time t, and $d(b,c)$ is the Euclidean distance measured in cell lengths from the center of cell b to center of cell c. The denominator is given by the observation that the total number of cells whose

centers are within r_n cell lengths a the center of a given cell on a hexagonal grid is $6 + 12 + \ldots + 6r_n = 6(1 + 2 + \ldots + r_n) = 6r_n(r_n + 1)/2$ (excluding the chosen cell itself).

The brood density dictates honey and pollen consumption in all models considered. In model 1, cell choice is uniformly random and the number of loads of nectar taken from a selected cell c is linearly dependent on the local brood density $D_{r_n}(c)$.

$$P(\text{cell } c \text{ chosen}) = \frac{1}{N} \tag{2.4}$$

$$n_L = \min(\text{loads left}, \lfloor 1 + D_{r_n}(c)(k-1) \rceil). \tag{2.5}$$

In models 2 and 3, cell choice is linearly proportional to the local brood density, and the number of loads of honey or pollen taken from a selected cell is constant.

$$P(\text{cell } c \text{ chosen}) \propto 1 + D_{r_n}(c)(\ell - 1) \tag{2.6}$$

$$n_L = 1. \tag{2.7}$$

In all models, cell choice for honey or pollen removal is taken over all comb cells, regardless of whether a cell is (partially) filled with the desired type of food or not. If the desired type is not found in the chosen cell, then another cell is chosen, with up to six cells being checked before the process is abandoned and the model moves on to the next task. Note that in both methods workers do not need to have global information as to the location of all honey and/or pollen cells at a given time.

Camazine originally set $r_n = 1$ and $k = 10$ [18]. Here we have expanded these

definitions to $r_n \in [1, 4]$ and $k \in [5, 20]$ in order to determine the sensitivity of each model to these parameters.

The amount of honey and pollen consumed over the entire modeled season is calculated as a ratio of amount foraged. Consumption is assumed to be constant throughout the season, and during all hours of the day. The ratios of pollen and honey consumption to collection (ρ_p and ρ_h, respectively) were chosen to be in the range of $0.9 - 1.1$ since our interest is in pattern maintenance after the comb fills. This range allows us to consider the phase when much of the incoming honey is being deposited in other non-brood combs. Within the nest, central combs contain brood and other combs are mostly used for the storage of honey [94]. Colonies have mechanisms that ensure that foraging does not exceed available storage capacity, which include comb building and colony splitting to create a new colony [119]. These mechanisms, combined with the use of a small number of combs for brood, should maintain the rate of incoming honey and pollen to these brood combs to, on average, replace the consumed honey and pollen. Thus on these combs, we expect to see ratios of consumption to collection close to 1 after the comb is full and the pattern is established. Otherwise, in time, the comb would become either overfull or completely empty.

2.2.5 Brood and Pollen Ring metrics

To assess the level of pattern retention during the simulation runs, we developed two metrics that describe the compactness of the brood region and the level of definition of the pollen ring (or gap of empty cells). The brood metric is

the average number of adjacent brood for each brood cell.

$$m_b(t) = \frac{1}{|B(t)|} \sum_{b \in B(t)} |\{x \ : \ x \in B(t), 0 < d(x,b) \leq 1\}|, \tag{2.8}$$

where $B(t)$ is the collection of brood cells at time t, and $d(x,b)$ is the Euclidean distance measured in cell lengths from cell x to cell b. Note that $m_b(t)$ is undefined if $|B(t)| = 0$, that is, if there are no brood on the comb at time t. We observed qualitatively that in simulations with brood compactness metric $m_b \geq 5.25$, the brood cells are sufficiently dense to fit the observed pattern.

The pollen metric is the average distance from each honey cell to the nearest brood cell, *i.e.*, the smallest number of cells visited when traveling from a honey cell to the nearest brood cell.

$$m_p(t) = \frac{1}{|H(t)|} \sum_{h \in H(t)} \min\{d(b,h) \ : \ b \in B(t)\}, \tag{2.9}$$

where $H(t)$ is the collection of cells containing honey at time t, and $d(b,h)$ is the Euclidean distance measured in cell lengths from the center of cell b to the center of cell h. Note that $m_p(t)$ is undefined if $|H(t)| = 0$, that is, if there are no cells storing honey on the comb at time t. In this case we observed that pollen metric $m_p \geq 12$ indicates a well-formed pollen ring, *i.e.*, one that forms a strong separation of honey cells from brood cells. In combination, these two metrics accurately describe how well the allocation adheres to the desired pattern. We use these metrics to assess the sensitivity in the model predictions over a range of reasonable parameter values.

2.2.6 Pattern Formation

In addition to testing pattern maintenance, we investigate the ability of each model to create the desired pattern on a nearly empty comb (similar to [19]). We perform the same simulations as above, but now set the initial comb storage pattern to be mostly empty with a clump of 7 brood cells (one brood cell with 6 adjacent brood cells) in the center of the comb. The parameter value ranges for some parameters were adjusted for the formation phase. We considered 100 parameter sets with the radius for the brood requirement (r_b) restricted to 2-4 since radii of 1 resulted in no new brood in the full (pattern sustenance model). We also restricted the ranges on the ratio of pollen collected to honey collected ($\rho_{ph} \in (.21, .45)$), the expected ratio of pollen consumption to pollen collection ($\rho_p \in (.9, 1.08)$), the expected ratio of honey consumption to honey collection ($\rho_h \in (0.49, 0.69)$, and the preferential consumption pressure near brood cells ($k \in (5, 15)$). These adjusted and narrower parameter ranges helped us look at the pattern formation locally near measured parameter estimates when the comb is being filled early in the season or in a new nest.

2.2.7 Sensitivity testing

We performed a global sensitivity analysis to assess the relative impact of each parameter on pattern retention for each of the 3 models. Because parameter estimates are uncertain, parameter ranges included maximum values up to a factor of 5 times larger than baseline values. For a complete list of parameters and their ranges, see Table 2.1. As Latin hypercube sampling is an efficient way

of sampling a large parameter space and our model is computationally intensive, we employed the same multidimensional hypercube used for parameter determination in our sensitivity testing [71, 11]. For each model scenario, 200 randomized parameter sets were generated by our hypercube. For each of these, we simulated 60 days; model metrics were then computed for days 20 – 60, and the values averaged. This time window includes multiple brood gestation periods, but omits transient dynamics due to comb initialization. We discard any run in which the brood clumping or pollen ring metric were undefined at any time between day 20 and day 60, leaving N_1, N_2 and N_3 viable runs for models 1, 2, and 3 respectively. Recall that the brood clumping and pollen ring metrics are undefined when there are no honey cells and no pollen storage cells, respectively, on the comb. These scenarios can occur, for instance, if the ratio of honey consumption to collection ρ_h is relatively large and relatively small, respectively.

After preprocessing the data, we scale each parameter value so that it is a percent of the observed parameter range in the N_i simulation runs, with 0.00 representing the minimum value and 1.00 representing the maximum value. We then perform multiple linear regression on the scaled data. We discard the intercept information from the linear regressions for both the pollen ring and brood region metrics, but note that the inclusion of this information in the regression is critical; without it, the least-squares method will produce a linear function for which each metric is equal to 0 when all parameters are equal to zero which is clearly not appropriate in the system modeled here.

We must interpret the remaining components, the so called elasticities of the metrics, with the scalings we have performed in mind. An elasticity value of

2 indicates that increasing the corresponding parameter from the bottom of its range to the top of its range increases the metric by 2 on average. (Notice that the the average metrics have not been scaled, so they should not be interpreted as percentages.) Similarly, an elasticity value of -3 indicates that increasing the corresponding parameter from the bottom of its range to the top of its range decreases the metric by 3 on average.

2.3 Results

Our results show that the cell allocation patterns of brood, pollen, and honey can be maintained over multiple brood gestation cycles by simple behavioral rules. To compare pattern retention across the 3 models, we first generated 200 parameter combinations using Latin hypercube sampling over the parameter ranges featured in Table 2.1. For each parameter combination, 3 separate 60 day simulations of the comb were completed, one for each model, with the initial state of each simulation being the ideal cell allocation pattern described in Section 2.2.1.

Comb snapshots: We begin by examining the cell allocation pattern across the comb. In Figure 2.2, we plot the comb at several points in time for models 1 – 3. The simulation run featured in each figure maximized the product $\overline{m_p} \cdot \overline{m_b}$, where $\overline{m_p}$ and $\overline{m_b}$ are the pollen ring and brood clumping metrics, respectively, averaged over days 20 – 60. While this product of averaged metrics is just one way we might define good performance in a simulation, we have found that it is a good indicator of pattern retention. Moreover, it is simple both in its form

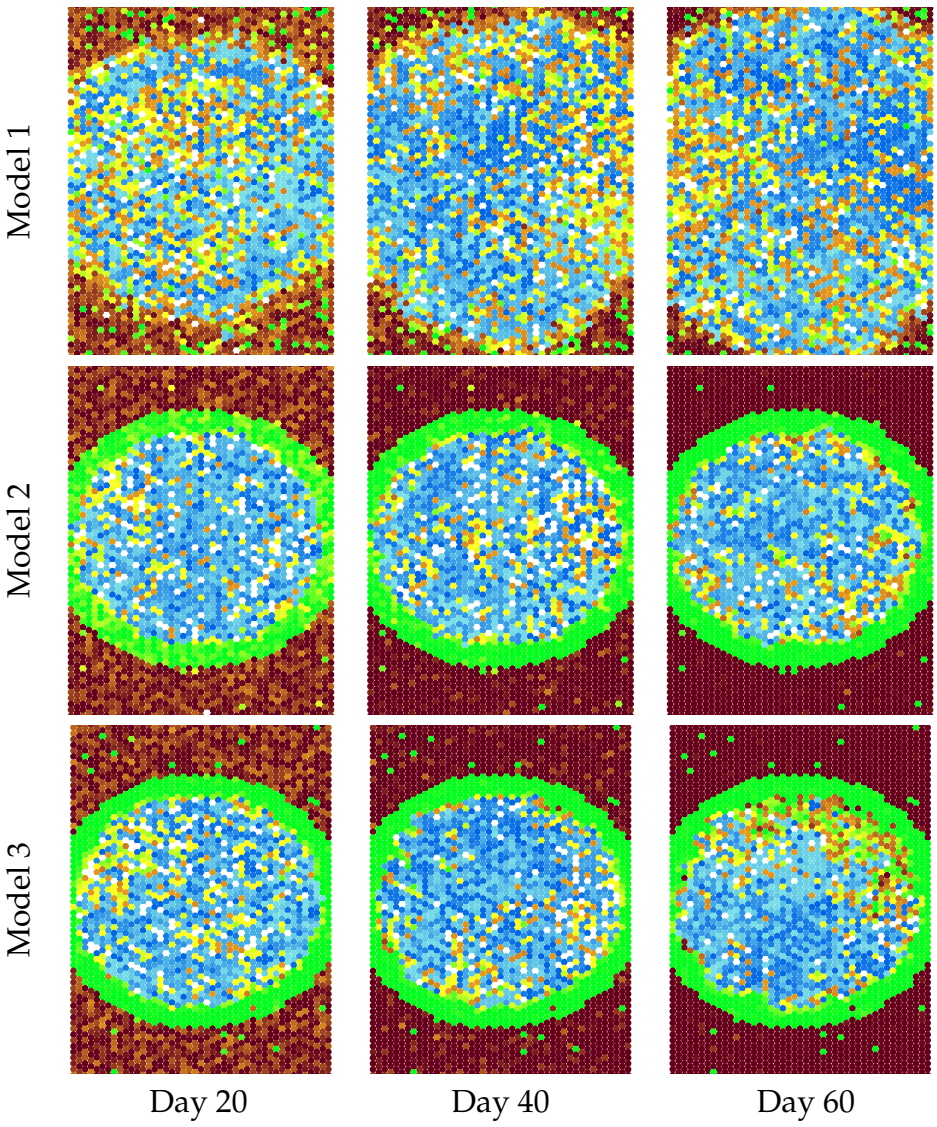

Figure 2.2: Snapshots of the simulation run for each model which maximized the product of time-averaged metrics $\overline{m_b} \cdot \overline{m_p}$ with contents plotted at day 20, 40 and 60 in columns 1, 2, and 3, respectively. Cells containing brood are blue; cells containing pollen are green; cells containing honey are brown; empty cells are white. Darker shades of each color represent older brood or fuller honey and pollen cells. For model 1 (row 1): $n = 61, r_b = 2, r_n = 2, \omega = 3475, \rho_{ph} = 0.9638, \rho_p = 0.9151, \rho_h = 1.0668, \chi = 1, k = 10$. For model 2 (row 2): $n = 97, r_b = 4, r_n = 1, \omega = 1150, \rho_{ph} = 0.2764, \rho r_p = 0.9362, \rho_h = 1.0970, \chi = 0, k = 15$. For model 3 (row 3): $n = 90, r_b = 3, r_n = 1, \omega = 1000, \rho_{ph} = 0.9719, \rho_p = 1.0206, \rho_h = 0.9854, \chi = 0, k = 16$.

and its computation. We average only after the first 20 days so as to not allow the initial ideal pattern to unduly influence the value of the averaged metrics.

Monitoring the simulations at days 20, 40, and 60 in Figure 2.2 allows us to easily compare across all 3 models. In Figure 2.2 (row 1), we see that model 1 has a fairly well defined and compact brood region at day 20. By day 40, this region has deteriorated, with the brood being both more diffuse and with honey storage cells occurring more frequently in the brood region. At day 60, the region containing brood has expanded considerably and is fair less densely populated with brood cells than at the previous snapshots. Pollen and honey storage cells are intermixed throughout the comb.

We compare these trends to the behavior of model 2 in Figure 2.2. Here we observe a compact brood region and well defined pollen ring across the 60 days of simulation. Some honey storage cells do encroach on the brood region, but most of these are converted to brood cells between snapshots, indicating the phenomenon is transient. A likely scenario is that the cell containing honey was recently vacated by an immature bee; due to preferential removal, this cell stays empty or almost empty much of the time, which increases the probability that the queen will lay an egg in it when she is next at the cell. Figure 2.2 shows that model 3 produces qualitatively similar results to model 2.

Metric time series comparison: In order to tease apart quantitative differences in qualitatively similar patterns, we plot the pollen ring and brood clumping metrics over time in Figure 2.3. Here we plot only the 20 simulations runs for each model that maximize the product $\overline{m_p} \cdot \overline{m_b}$, where again $\overline{m_p}$ and $\overline{m_b}$ are the

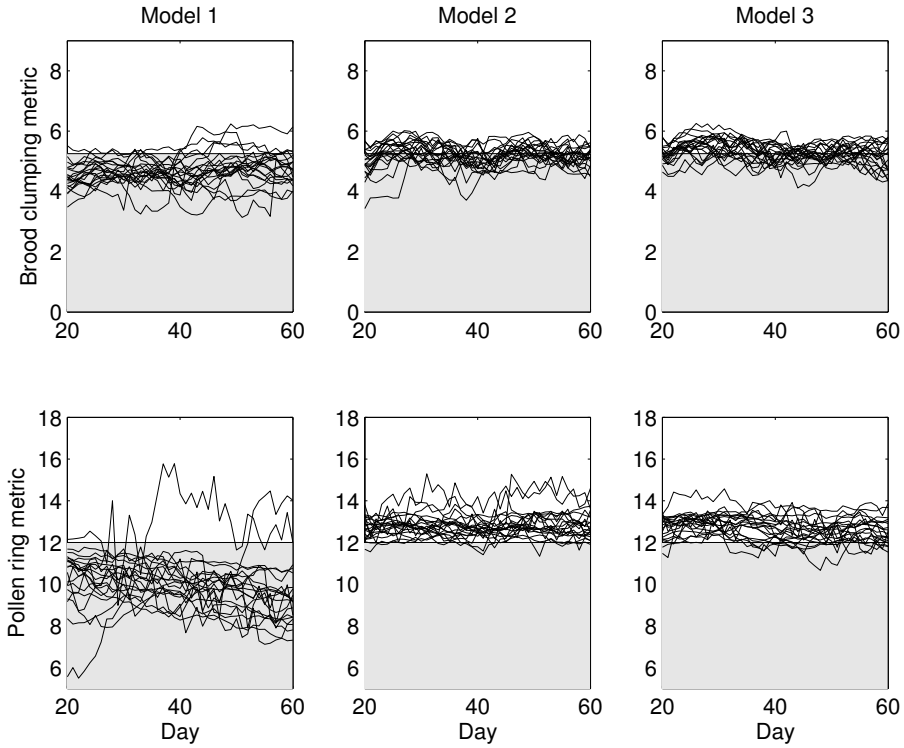

Figure 2.3: Trajectories of the brood clumping metric and pollen ring metric the 20 best simulation runs for each model. Recall that if the brood clumping metric is above 5.25 and the pollen ring metric is above 12, then the pattern is considered to be well formed.

pollen ring and brood clumping metrics, respectively, averaged over days 20 – 60. Under model 1, the brood clumping metric seems to stabilize up to probabilistic fluctuations after day 20, albeit it to a value that is below our threshold of $m_b(t) = 5.25$. This agrees well with our observations in Figure 2.2: model 1 produces a brood region up to and including day 60, but the region is relatively diffuse. Most traces of the pollen ring metric are monotonically decreasing up to probabilistic effects even up to day 60. This is good agreement with our results in Figure 2.2, as we noted that the diffuse brood region is increasingly infiltrated by honey storage cells. We note that one trace of the pollen ring metric exhibits a wild swing from low to high over the course of 20 days. In this simulation,

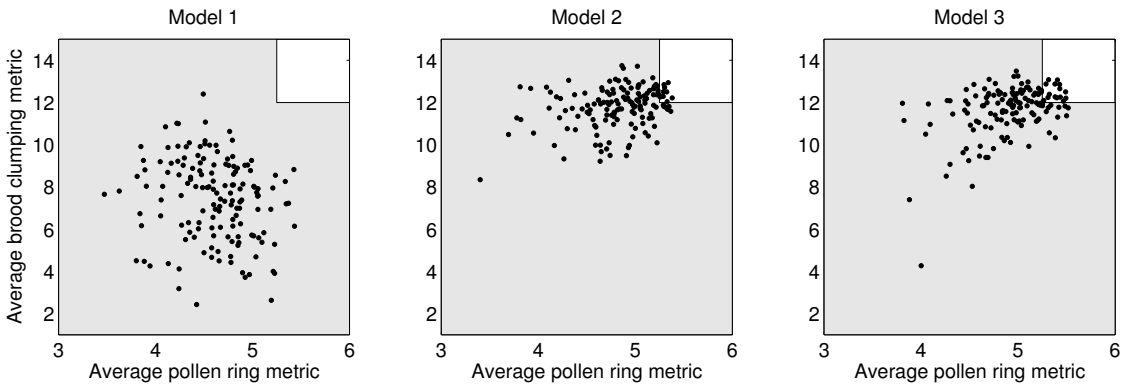

Figure 2.4: Brood clumping and pollen ring metrics on day 60 for each of the 200 simulations of models 1, 2 and 3. The gray region represents metric combinations that result in a poorly defined cell allocation pattern.

the comb contains no honey storage cells from day 11 to day 14. When a few honey storage cells begin to appear day 14, they are at first quite close to the brood patch, but as new groups of brood begin to emerge, the average distance between the few honey cells and the remaining immature brood cells begins to grow quite quickly, leading to a spuriously high metric. As the vacated brood cells begin to fill with honey at approximately day 40, the pollen ring metric begins to decrease to a more reasonable range, both because these new honey storage cells are relatively close to the brood cluster, and because a larger number of honey storage cells implies that outliers contribute less to the average minimum distance from honey to brood. This example and others like it motivate us to disregard any simulation run which at any point has an undefined pollen ring or brood clumping metric, as the metrics of these simulations cannot be trusted to convey accurate information about the retention of the pattern.

Metric space comparison: Note that Figure 2.3 shows both models 2 and 3 exhibit brood clumping and pollen metrics that are relatively constant and above

their respective thresholds from day 20 to day 60. As there is relatively little change over time in the brood clumping and pollen metrics, we can sacrifice the temporal component of the data in Figure 2.3 and plot each of the 20 runs for each model in metric space as seen in Figure 2.4. Here we plot the average brood clumping metric versus the average pollen ring metric for all simulation runs which do not have undefined pollen ring or brood clumping metric at any time between day 20 and day 60 for each of the 3 models. All averages are performed over the interval from day 20 to day 60. Similar to Figure 2.3, a point in a gray region in Figure 2.4 represents a simulation run in which one or both of the metrics averaged from day 20 to day 60 was below threshold. We note that although the results in Figure 2.3 might lead us to expect that there are simulation runs of model 1 in which the average brood clumping metric between day 20 and day 60 is above threshold (and similarly for the pollen ring metric), Figure 2.4 indicates that no simulation run of model is above threshold with respect to both averaged metrics. After introducing the revised honey/pollen rule in model 2, we observe 9 simulation runs that are above threshold with respect to both metrics. The parameter combinations leading to this outcome are listed in Table 2.2. If in addition we bias the queen's movement towards the center of the comb as in model 3, we observe 16 simulation runs that are above threshold with respect to both metrics. The parameter combinations leading to this outcome are listed in Table 2.3. The significance of the parameter combinations that lead to pattern retention in models 2 and 3 will be discussed in Section 2.4.

Figure 2.3 seems to indicate that there is a significant difference between the mean of the time-averaged pollen ring and brood clumping metrics of model 1 and the corresponding means of models 2 and 3. We can quantitatively confirm

Run No.	n	r_b	r_n	ω	ρ_{ph}	ρ_p	ρ_h	χ	k	$\overline{m_p}$	$\overline{m_b}$
1	108	3	1	1420	0.5	1.07	1.05	1	9	5.32	12.5
2	97	2	3	1945	0.76	0.99	1.08	1	19	5.29	12.51
3	70	4	3	3370	0.33	0.94	1.09	0	18	5.3	12.84
4	75	2	3	2275	0.67	1.08	0.92	0	14	5.26	12.26
5	116	3	1	3520	0.81	1.06	1.04	0	16	5.38	12.22
6	112	2	1	3445	0.73	0.99	0.95	0	13	5.29	12.29
7	88	3	1	1210	0.32	1.06	0.99	1	9	5.3	12.72
8	119	4	4	1165	0.57	1.03	1	1	19	5.33	12.03
9	97	4	1	1150	0.28	0.94	1.1	0	15	5.34	12.94

Table 2.2: Model 2 parameter contributions that result time averaged metrics $\overline{m_p}$ and $\overline{m_b}$ that are both above their respective thresholds.

Run No.	n	r_b	r_n	ω	ρ_{ph}	ρ_p	ρ_h	χ	k	$\overline{m_p}$	$\overline{m_b}$
1	102	4	4	1885	0.94	0.96	1.03	0	12	5.4	12.22
2	90	4	2	1930	0.51	0.96	1.08	0	16	5.29	12.88
3	90	3	1	1000	0.97	1.02	0.99	0	16	5.41	13.07
4	110	3	3	2140	0.88	0.92	0.97	0	15	5.43	12.85
5	108	3	2	3580	0.22	1.05	1.02	0	14	5.26	12.1
6	118	4	2	2440	0.36	0.9	1.01	2	14	5.43	12.66
7	89	2	3	1300	0.25	1.03	1.1	0	9	5.49	12.5
8	103	3	1	1015	0.68	1.06	0.92	2	9	5.38	12.27
9	112	2	1	3445	0.73	0.99	0.95	0	13	5.47	12.06
10	88	3	1	1210	0.32	1.06	0.99	1	9	5.32	13.08
11	79	4	3	3790	0.24	0.99	0.91	1	19	5.25	12.01
12	104	2	2	3415	0.41	0.98	0.93	1	17	5.31	12.24
13	70	2	2	2830	0.64	0.91	1.01	2	6	5.49	12.2
14	105	3	1	3865	0.37	0.95	1.09	1	9	5.38	12.88
15	101	1	4	3220	0.97	1	1.05	0	17	5.44	12.25
16	99	1	3	1585	0.95	1.02	1.02	2	9	5.32	12.39

Table 2.3: Model 3 parameter contributions that result time averaged metrics $\overline{m_p}$ and $\overline{m_b}$ that are both above their respective thresholds.

this intuition by performing one-way ANOVA. The results for the test applied to the time-averaged pollen ring metric are seen in Figure 2.4. We preprocess the data by removing every run in which the pollen ring metric was undefined at any time between day 20 and day 40. Recall that the pollen ring metric is undefined when there are no honey storage cells on the comb. We conclude form the results of the ANOVA test that it is highly unlikely that the observed pollen ring metrics from models 1, 2, and 3 are drawn from distributions with the same mean. A multicomparison test shows that the mean time-averaged pollen met-

Source	DF	Sum of squares	Mean squares	F ratio	F probability
Within groups	2	7.2365	3.61825	24.51	8.08×10^{-11}
Between groups	441	65.1077	0.14764		
Total	443	72.3442			

Table 2.4: One-way ANOVA test results for the average pollen ring metric over day 20 to day 60. It is highly unlikely that the average pollen ring metrics from the simulation runs of models 1, 2, and 3 were drawn from distributions with the same mean. ANOVA tests for average brood clumping were even more pronounced.

ric of model 1 is significantly different than that of models 2 and 3, while the mean time-averaged pollen metric of models 2 and 3 are not significantly different. We performed an identical analysis for the brood clumping metric and found an even more pronounced difference between the models.

Sensitivity testing: As discussed in Section 2.2.7, the use of Latin hypercube sampling for parameter selection enables us to perform a straightforward sensitivity analysis via multiple linear regression. A graphical summary of this analysis is seen in Figure 2.5. Here we include only the analysis of models 1 and 2, because the sensitivity profiles of models 2 and 3 are qualitatively similar.

For both models 1 and 2, the brood clumping metric is relatively inelastic with respect to most parameters, with the notable exception in both models being the brood clumping metric's dependence on n, the number of oviposition attempts per hour. In both models, increasing the number of oviposition attempts per hour increases the average brood clumping metric. This agrees with our intuition, as increasing the number of oviposition attempts per hour increases the likelihood that the queen will be place an egg in a recently vacated brood cell.

The elasticity of the pollen ring metric varies quite widely between model 1 and model 2. For most parameters, an identical increase in parameter value in

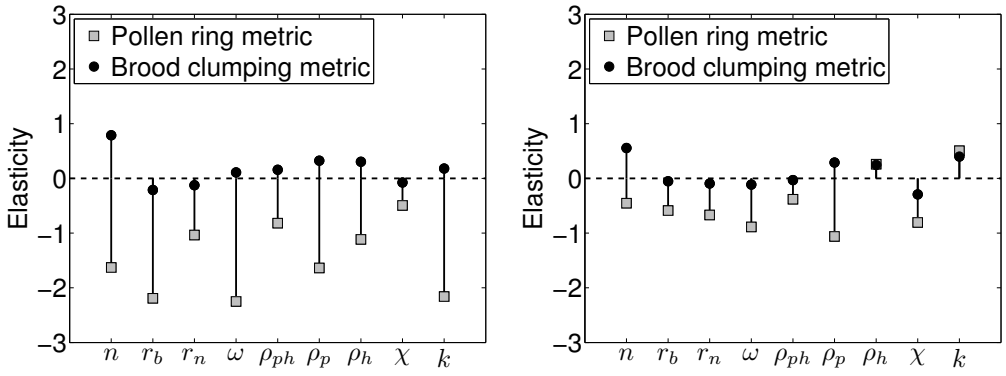

(a) Model 1 (b) Model 2

Figure 2.5: Sensitivities for models 1 and 2. The sensitivity of models 2 and 3 were qualitatively similar. The "elasticity" is the proportional change in the value of the metric relative to the change in the parameter value. A positive elasticity indicates that the metric increases with the parameter while a negative elasticity indicates that the metric decreases with increases in the parameter. See Table 2.1 for parameter definitions and ranges.

model 1 and model 2 will on average simply result in a larger decrease in the pollen ring metric in model 1 than in model 2. However, there are cases where identical parameter increases will result in an increase in pollen ring metric in model 2 and a decrease in pollen ring metric in model 1. Perhaps most notable is the parameter k. Recall that in model 1, the parameter k represents the number of loads of honey/pollen that will be removed from a cell completely surrounded by brood if it is chosen for consumption, while in model 2, the parameter k represents the ratio of the probability that a cell completely surrounded by brood will be chosen for consumption to the probability that a cell with no brood neighbors will be chosen for consumption. The elasticities of k in models 1 and 2 are markedly different. Increasing k in model 1 leads to a substantial decrease in the pollen ring metric, while increasing k in model 2 results in a moderate increase in the pollen ring metric.

The elasticity analysis also features some results that might seem at first counterintuitive. For instance, increasing r_b, the upper bound on the minimum distance from a brood cell at which the queen will oviposit, results on average in a decrease in both brood clumping metric in both model 1 and model 2. While it might at first seem that larger r_b would result in a denser brood region, our results here show that larger r_b more often allows the queen to oviposit well outside the current brood region, thus lowering the brood clumping metric. With that being said, many simulation runs with $r_b = 1$ eventually had no brood on the comb, and so were not included in this sensitivity analysis. This is especially relevant in model 1, where all simulations with $r_b = 1$ eventually had no brood on the comb. Together, these illuminate a natural tension: there is a parameter threshold below which the patten disintegrates, but on average increasing the parameter decreases one or both of the parameter metrics. It bears remembering that the elasticities featured in Figure 2.5 are simply linear fits over the entire observed parameter range. We allow, and expect, the parameters to have nonlinear effects on the metrics that are not captured by this sensitivity analysis, as well.

Model validation: While our work here is primarily focused on pattern retention over multiple brood gestation cycles, it is also important to confirm that the models investigated here are capable of forming the cell allocation pattern from a nearly empty comb. Our modeling framework contains the same general pattern formation processes that Camazine described [18], but to check that our models would in fact create the initial pattern of a compact brood region surrounded by a ring of pollen, we performed simulations starting with an empty comb for all three models for the first twenty days. Figure 2.6 shows an example

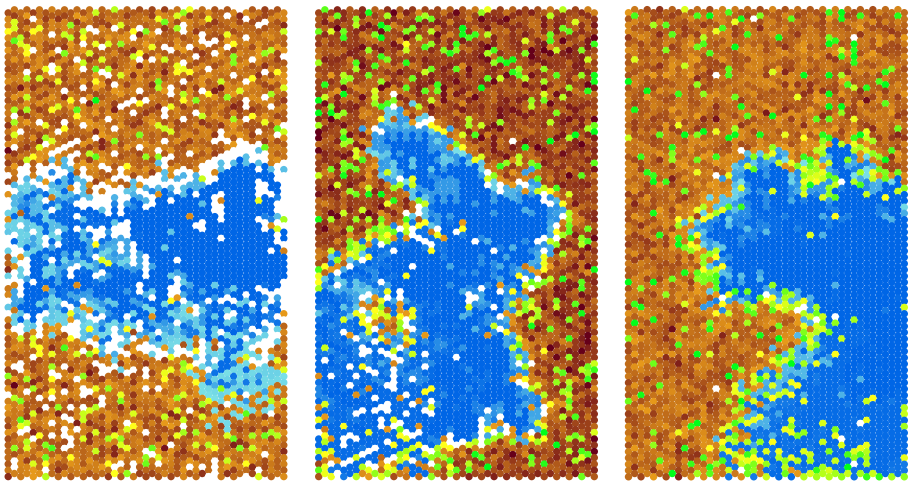

(a) Model 1 (b) Model 2 (c) Model 3

Figure 2.6: Day 20 of a simulation run demonstrating that each model is able to create the desired pattern on an empty sheet of comb. Model 1 has parameters $n = 79, r_b = 3, \rho_h = 3, \omega = 1930, \rho_{ph} = 0.2536, \rho_p = 1.0436, \rho_h = 0.6799, \chi = 2, k = 13$, model 2 used parameters $n = 79, r_b = 3, \rho_h = 3, \omega = 1930, \rho_{ph} = 0.2536, \rho_p = 1.0436, \rho_h = 0.6799, \chi = 2, k = 13$, and model 3 used parameters $n = 86, r_b = 3, \rho_h = 4, \omega = 1480, \rho_{ph} = 0.3748, \rho_p = 1.0345, \rho_h = 0.6900, \chi = 2, k = 10$.

of a well formed pattern for each model at day 20. For model 1, our simulations reproduced Camazine's results [18]. All three models are able to form the initial pattern for a range of parameter values. The final pattern is not perfect, but the compact brood region forms and the pollen ring is visible.

Given the stochastic nature of the simulation, there is the natural question as to whether a given simulation of a particular parameter combination is representative of the behavior in general. Figure 2.7 shows metric traces for 20 simulations of one parameter combination applied to models 2 and 3. The traces of both metrics are relatively tight, and in particular, all traces are qualitatively

similar in that all exceed the metric thresholds most of the time. All brood metrics were within 15% of the mean, and all pollen ring metrics were within 5% of the mean.

2.4 Discussion

This study is the first to consider how cell allocation patterns can be maintained over multiple brood gestation cycles. We acknowledge that our work here is a drastic simplification of what is a rich and complex natural phenomenon, and that the patterns created and maintained by the models we present in many cases capture only some of the qualitative aspects of cell allocations observed in the wild. For instance, we ignore the existence of other combs in the colony, the highly complex and variable availability of nectar and pollen, the extreme shifts in colony population over the course of a season, anisotropies introduced by gravity, and myriad other effects. Yet it is exactly this extreme simplification that makes our results interesting; pattern formation and retention, at least in a qualitative sense, are achievable with only a few simple rules. Below we present the level to which pattern retention occurs in each of the three models and discuss the significance of the rules and information that were necessary to introduce in order to achieve a given level of pattern retention.

Figure 2.2 shows anecdotally that model 1 is not capable of maintaining the pattern over a 60 day period, while models 2 and 3 are. In order to more precisely discuss the quality of an observed pattern, we have introduced a brood clumping metric $m_b(t)$ in Equation 2.8 and a pollen ring metric $m_p(t)$ in Equation

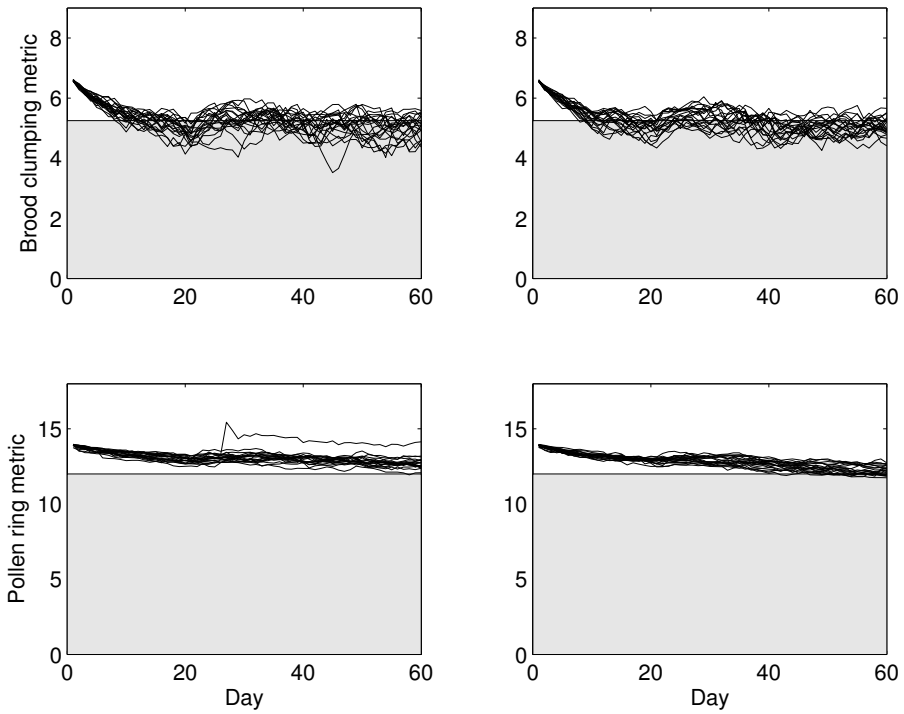

Figure 2.7: To test the consistency of the model, 20 replicate simulations were performed for the parameter sets that resulted in the highest average metrics for models 2 (left panels) and model 3 (right panels). For model 2, this was $n = 97, r_b = 4, \rho_h = 1, \omega = 1150, \rho_{ph} = 0.2764, \rho_p = 0.9362, \rho_h = 1.097, \chi = 0, k = 15$. For model 3: $n = 90, r_b = 3, \rho_h = 1, \omega = 1000, \rho_{ph} = 0.9719, \rho_p = 1.0206, \rho_h = 0.9854, \chi = 0, k = 16$. Trajectories of the brood clumping metric (top panels) and pollen ring metric (bottom panels) for these twenty simulations show a tight fit for the pollen ring metric with a mean average metric (over the last 40 days) of 12.98 ± 0.30 S.D. for model 2, and 12.64 ± 0.23 S.D. for model 3 with all of the runs maintaining an average brood clumping metric above the desired 5.25. The brood metric is more variable with a mean metric of 5.13 ± 0.17 S.D. for model 2, and 5.14 ± 0.15 for model 3. Only six model 2 and four model 3 runs had an average brood clumping metric above the desired 5.25, but all of the runs had an average brood clumping metric above 4.79.

2.9. We average these metrics over days 20 to 60 to form $\overline{m_p}$ and $\overline{m_b}$, respectively, in order to discard transients and smooth out stochastic effects. Through observations of well formed patterns and the associated brood clumping and pollen ring metrics, we say that a simulation with $\overline{m_b} \geq 5.25$ and $\overline{m_p} \geq 12$ exhibits a well formed pattern.

These thresholds for the pattern metrics agree with anecdotal evidence. Of the 200 simulation runs of model 1 performed, none exhibited a well formed pattern. To make model 2, we modify model 1 to by changing the honey/pollen consumption rules as described in Section 2.2.4. Here we observe 9 of the 200 simulation runs exhibit a well maintained pattern. We emphasize that rules for oviposition, honey/pollen consumption, and honey/pollen deposition in model 2 are based solely on local information available to each bee. The 9 parameter combinations that resulted in a well formed pattern in model 2 are listed in Table 2.2. It is tempting to interpret the data listed there as definitive indicators of the types of parameter combinations that are amenable to model 2 maintaining the desired pattern. But we take any such interpretation with a grain of salt, as our sampling is probabilistic in nature and our parameter space is very large. With this warning in mind, we can make several observations. We note that n, the number of oviposit attempts made by the queen in an hour, is between 70 and 119. The observed minimum here is roughly 20% higher than the minimum allowable value, perhaps indicating that small values of n lead to poor pattern retention. This would agree well with the sensitivity analysis of model 1 featured in Figure 2.5(b). Similarly, the parameter r_b, the maximum distance from an existing brood cell at which the queen will oviposit, never assumes value $r_b = 1$. Here we can be more definitive, because each model 1

simulation in which $r_b = 1$ results in a comb without brood cells at some time between day 20 and day 60. The parameter ω, representing the number of loads of honey/pollen collected per day, achieves a large portion of its range, as do parameters ρ_{ph}, ρ_p, and ρ_h. Interestingly, the nectar collection schedule indictor χ, never assumes value $\chi = 2$ which would indicate that honey/pollen collection was subject to a Markov process. This may indicate that model 2 is not capable of maintaining the pattern in the presence of such variability. Finally, parameter k, representing the strength of preferential choice of honey/pollen cells near brood, does not assume values in the bottom 25% of its allowable range, perhaps indicating that pattern retention fares better when stronger preference is given to cells near brood. This is in good agreement with the sensitivity analysis featured in Figure 2.5(b).

In model 3, we incorporate the preferential consumption rule of model 2 and additionally bias the queen's random walk towards the center of the comb as described in Section 2.2.2. While we have presented literature that details several behaviors of honey bees perform in response to temperature and temperature gradients, there has been, to our knowledge, no work on the effect of temperature gradients on the queen's walk. Thus, while we may speculate that the queen may be using such gradients to inform her movements across the comb and hope that empiricists investigate this hypothesis, we must for the time being treat the queen's biased random walk as an introduction of *global* information into the model and acknowledge that this introduction makes pattern formation and retention somewhat less impressive.

We observe that 16 of the 200 simulation runs of model 3 exhibit a well

formed pattern. These parameter combinations are listed in Table 2.3. As with model 2, the parameter n, the number of oviposit attempts made by the queen in an hour, does not assume any value in roughly the bottom 20% of its allowable range. Note that in contrast to model 2, the parameter r_b, the maximum distance from an existing brood cell at which the queen will oviposit, assumes values in its allowable range. Similarly, the nectar collection schedule indicators χ and k, representing the strength of preferential choice of honey/pollen cells near brood, now assume values in their full range. In all, these expansions in parameter ranges which result in a well formed pattern together seem to indicate that pattern retention is more robust in model 3 than in model 2.

Much of our current understanding of self-organization in biological systems is on the emergence of global order from initial disorganization through local interactions between individuals [20, 18, 19, 91]. Our work extends this conversation to consider the additional requirements for maintaining order after it has been established. In some systems, maintenance could reasonably be expected from any process which can create order. However in honey bees, the rules change fairly significantly after the initial pattern formation phase and make it more difficult to maintain the pattern than to form it on an empty comb. This is likely the case for many other patterns in nature. We hope this work opens a larger discussion about whether the local interactions maintaining order are the same as those that initially allowed for self-organization, or whether new mechanisms must be investigated.

CHAPTER 3

THE PUZZLE OF SUB-MAXIMAL RESOURCE USE BY A PARASITOID WASP

Abstract

Heritable traits that increase individual fitness will dominate a population. It is therefore puzzling when individuals use just a small fraction of limited available resources. Submaximal resource use has been studied extensively for a variety of exploiter-resource systems, but typically these investigations consider only one of the many plausible explanations for the behavior. We study this question by considering all plausible reasons that the well-characterized and extensively-studied specialist parasitoid wasp, *Hyposoter horticola*, might parasitize only a third of the eggs in each of its host's egg clusters and then apply a deterrent marking which is respected by other *H. horticola* females. First we consider the possibility that the parasitoid is prevented from parasitizing all the hosts by biological constraints, such as egg limitation and physical inaccessibility of some hosts, by testing four hypotheses using experimental approaches. Next, we consider the possibility that selection favors submaximal parasitism by testing three hypotheses (*e.g* optimal foraging, cooperative benefits of unparasitized hosts, and avoiding density-dependent hyperparasitism) using a combination of theoretical models and experimental data. We find that for *H. horticola*, the most reasonable explanation is that submaximal resource use and deterrent markings maximize the wasps foraging efficiency across a landscape.

3.1 Introduction

There are strong individual benefits to being greedy, so for exploiter-resource relationships to persist, something must keep the exploiter from overexploiting its resource [73, 67, 120]. This could be a biological constraint that limits how many, or which, resources are exploitable. For instance, phenological asynchrony between an exploiter and its prey [40, 47, 111], or spatial refuge for the prey [28] would protect a fraction of the prey population. Alternatively, the exploiter may practice submaximal resource consumption. For example, a predator might increase its lifetime fitness through prudent resource use [118], or individuals could use bet-hedging strategies to increase geometric mean fitness [27], or, a parasite could be very selective in its choice of hosts [13]. Among exploiters, those that are parasites have the most direct motivation to make sure the hosts can survive long enough to support or transmit their offspring. Submaximal resource use in this context means parasitizing just a fraction of the hosts, when many more could be parasitized.

We examine submaximal resource use as it relates a specific kind of parasite, *i.e.* the parasitoid wasp, *Hyposoter horticola* in the Åland islands of Finland. Parasitoids are parasitic insects that are free living as adults, but live, while developing, attached to or within a single host organism, which eventually kill the host. *Hyposoter horticola* is an egg-larval parasitoid of the butterfly *Melitaea cinxia*. The wasps locate host egg clusters in the weeks before they are ready to be parasitized [107], use landmarks to remember their locations [110], parasitize a fraction of hosts in each egg cluster when the eggs near hatching and become susceptible, then mark the egg cluster to deter other females [24]. In

this way, *H. horticola* parasitizes roughly one third of nearly every host cluster on the landscape [108] with each cluster parasitized by a single female [24]. Our goal in this paper is to explain why *H. horticola*, which is clearly resource limited, parasitizes such a low fraction of the available hosts, takes the time to mark the clusters it parasitizes, and, when considering a new cluster, respects the deterrent markings of other wasps of the same species.

This puzzling set of behaviors could theoretically persist under a number of basic evolutionary scenarios. In this paper, we consider seven plausible reasons for submaximal parasitism by *H. horticola* (Table 3.1). We carefully consider each hypothesis and use a combination of theoretical, empirical, and modeling evidence to show that many of these hypotheses cannot explain parasitism restraint for *H. horticola*. This sort of careful comparative analysis of multiple plausible behavioral hypotheses with experimental data and empirical observations is rarely attempted. Each behavioral hypothesis has been studied individually as it relates to particular systems, but not altogether for the same system. This is because, in many systems, there is insufficient data for testing multiple hypotheses or the interactions between species are prohibitively complex, resulting in intractable models. The *M. cinxia – H. horticola* system is an ideal model system because the interaction between the species is direct, with one parasitoid supported by and eventually killing a single host, and has been extensively studied over 15 years [66, 108, 109]. Understanding the cause of submaximal parasitism in this system could help advance understanding of the evolution of restraint in exploitation more generally. In addition, the careful study of restraint in such a tractable system contributes to the larger literature on submaximal exploitation.

	Hypothesis	Short Explanation	Test
Biological Limitations	Wasp Egg Limitation	To parasitize the full host cluster, the wasp must have enough eggs. There is strong selective pressure toward not being egg-limited, but it is possible that the wasp is unable to produce more eggs.	Data from Couchoux *et. al.* (in prep)
	Host Egg Architecture	The host eggs are laid in mounded piles, and the wasp may not be able to oviposit into the inner eggs of the cluster. In this case, there would be strong selective pressure toward longer ovipositers, but this might not be possible.	Experiment 1
	Host Egg Defense	The host eggs may protect themselves against parasitism in ways that are hard to detect (such as killing parasitoid eggs quickly after oviposition).	Experiment 2
	Ephemeral resource	There is a short window of opportunity during which host eggs are susceptible to parasitism. It is possible that only a fraction of the eggs are available at a time, or that the eggs are susceptible for such a short period of time that the wasp cannot parasitize them all.	Experiments 3 and 4
Behavioral Response to Evolutionary Pressures	Cooperative benefits	The gregarious host caterpillars depend on group cooperation for foraging and developing an adequate winter nest for survival. If parasitism decreases host performance and too many caterpillars are parasitized it is possible that the whole cluster will suffer severely.	Experiment 5
	Optimal Foraging	Over time the wasp experiences decreasing parasitism efficiency at a given egg mass, and after a while, it is beneficial for the wasp to spend time and energy finding an unparasitized cluster.	Model results and Experiment 6
	Avoiding Hyperparasitism	The wasp might parasitize a small fraction of the cluster to avoid heavy losses due to density-dependent hyperparasitism.	Experiments 2 and 7

Table 3.1: An overview of the hypotheses that will be tested with a short explanation of each and the main test of the hypothesis.

3.1.1 Potentially Plausible Explanations

Multiple physical and physiological limitations could restrict the wasp's ability to parasitize hosts (see table 3.1). First, the wasp may be egg limited with only enough eggs at a given time to parasitize a third of a host egg cluster, or only enough eggs in its lifetime to parasitize a small fraction of encountered hosts resulting in choosiness about which hosts to accept [13, 48]. Second, the butterfly mounds its eggs in piles and this physical arrangement may protect the inner eggs from parasitism [50, 115, 53]. Third, the individual eggs are only susceptible to parasitism for a short period of time. If the eggs develop asynchronously, then many of them could be in a non-susceptible phase while the wasp is present [41, 40, 14]. Alternatively, if the eggs mature synchronously the wasp may only have enough time to parasitize a small fraction of the hosts. Last, the host eggs may have immune defenses that kill the wasp egg/larvae or otherwise prevent the wasp from ovipositing. One problem with all of these physical/physiological constraints is that while all of them would explain why only a fraction of the eggs are parasitized, none of them explain why the wasp spends precious time applying a deterrent marking to host clusters or why other individuals respect the marking when it is present.

If none of the above mechanisms constrains parasitism, the wasps are physically/physiologically able to parasitize more host eggs in each cluster and we must then look at evolutionary pressures that could select for wasps exhibiting restraint. Submaximal exploitation in other resource-exploiter systems is supported by a number of classical ecological or evolutionary explanations: prudent predation [98, 117], bet-hedging [37, 38, 54], and optimal foraging [103].

Prudent predation/parasitism is a form of group selection and is based on the idea that restrained harvesting strategies increase resource availability for future generations. For this to benefit the individuals practicing prudence, the species must live in small subpopulations with extremely limited mixing [98, 117]. The ideal circumstance for prudence is a territorial predator consuming a stationary resource that is renewed from within the predator's range [72] with a ratio of benefits to costs of prudence that is large compared to the ratio of maximum number of individuals in each territory (the group) to the number of territories (or groups) [105]. Prudence explains reduced predation in some predator-prey systems [118], but does not work in many systems because of the strict requirements for territoriality and resource renewal [46] and the relative delay in and weakness of the benefit compared to other factors such as increased number of offspring resulting from increased resource use [72].

Due to these strict requirements, the parasitoid wasp *H. horticola* is far from the ideal system for the prudent predation theory. Individual wasps have large, overlapping ranges with a small number of distinct populations and a large number of wasps in each population. Though the host butterfly lives as loosely connected networks of local populations in a fragmented landscape [44], the wasp disperses widely among the local host populations. There are two lines of evidence suggesting this. First, they are found in virtually all local host populations, colonizing new host populations the same year they originate even when these new populations are at least one kilometer from other known populations [108]. Second, while there is allelic variation in microsatalite markers when *H. horticola* is sampled throughout Åland, there is little evidence of spatial genetic structure across the Åland islands [61]. Thus, prudence is unlikely to be favored

in this system.

Another possibility is that the wasps are parasitizing a small fraction of each cluster so that they can reduce their risk by spreading their eggs between multiple host clusters or multiple habitat patches. Bet-hedging (or risk aversion) is the idea that highly variable survival rates give individuals who decrease the variability in the survival of their offspring a competitive advantage. There are two basic kinds of variability of survival that can lead to risk aversion: spatial and temporal. In temporally variable environments, behaviors that reduce the year-to-year variability in survival increase the geometric fitness [38]. Seed banks are an example of this type of risk spreading [22, 114]. In spatially structured environments with larger population sizes, risk-averse behaviors that reduce an individual's within year variability in fitness do not appreciably increase the expected fitness of the genotype because the gene is effectively already spread across the landscape. If the population size is extremely small, then bet-hedging decreases the probability of extinction of a particular genotype in a population [37, 54] and can have selective benefits. When populations are extremely small, risk-averse lineages may have a competitive advantage, but when the population becomes larger this advantage disappears.

H. horticola parasitizes roughly a third of the eggs in each host cluster. The host nests have spatial and temporal variability in the chance of whole cluster mortality due to summer drought, winter severity, and predation [64, 106]. The observed parasitism rates could reflect a choice to divide a limited number of eggs among multiple clusters to decrease survival variability. For one wasp, dividing her eggs among more clusters might reduce the variance in offspring

[54]. But selection acts on the mean fitness of alleles, so the geometric mean fitness of any one female isn't the quantity that matters. What matters is the total reproductive success of all females carrying the allele, and since the population of *H. horticola* wasps is large the expected fitness would remain virtually the same. Thus, selection would not favor this type of risk averse behavior. In addition, risk-aversion would not explain why deterrent markings are employed and respected.

The third possible theory is optimal foraging, which assumes that the foraging behavior of individuals evolves to maximize their fitness [84]. In a heterogeneous landscape, foraging individuals must make decisions about how to move through the landscape and optimize their fitness in response to the local abundance of resources. If a forager depletes resources in an area, then the individual will experience diminished efficiency as it spends longer at a particular site. An individual who is foraging optimally will balance this decreasing efficiency against the time and energy costs of searching for new foraging sites [21]. At some point, the expected efficiency of relocating will equal the current efficiency in the site, and at this point it will be beneficial to leave the site to find another. Optimal foraging models maximize net energy gained per unit time for the predator and are especially useful when there is variability or depletion in prey quality or abundance at a site. These models typically require that the individual's fitness depends on the foraging behavior, is passed on to offspring, and evolves more quickly than relevant conditions change [84]. There are many examples where predators leave a foraging location before resources are depleted because of diminished foraging efficiency [87, 72, 88]

For *H. horticola*, there would be some optimal time to leave one host egg cluster to search for another, unparasitized, cluster. This optimal leaving time would determine the fraction of the cluster parasitized. For optimal foraging to predict submaximal exploitation, individuals must suffer decreased efficiency or increased costs when they spend too long parasitizing a larger fraction of each host cluster. The cost of leaving is that there is competition over host clusters and there is a good chance that the wasp will not find another susceptible host cluster. The most basic optimal foraging model that we will consider posits that *H. horticola* experiences decreasing efficiency with additional time at a cluster because it is more likely to encounter host eggs that it has already parasitized. In addition, there are two, more specialized, density-dependent costs that could further decrease the parasitism rates. The first is that highly parasitized nests of gregarious host larvae may not be able to function as they should, and suffer higher rates of whole cluster mortality. The second is if the hyperparasitoid *Mesochorus stigmaticus* (parasitoid of the parasitoid) of *Hyposoter horticola* responds positively to local parasitoid density, spending more time at highly parasitized clusters. For the gregarious behavior model it would be beneficial to apply and respect deterrent markings. Either optimal foraging model could explain why deterrent markings are applied and respected if the wasps are marking as a signal to themselves (which happens to be beneficial to other wasps as well).

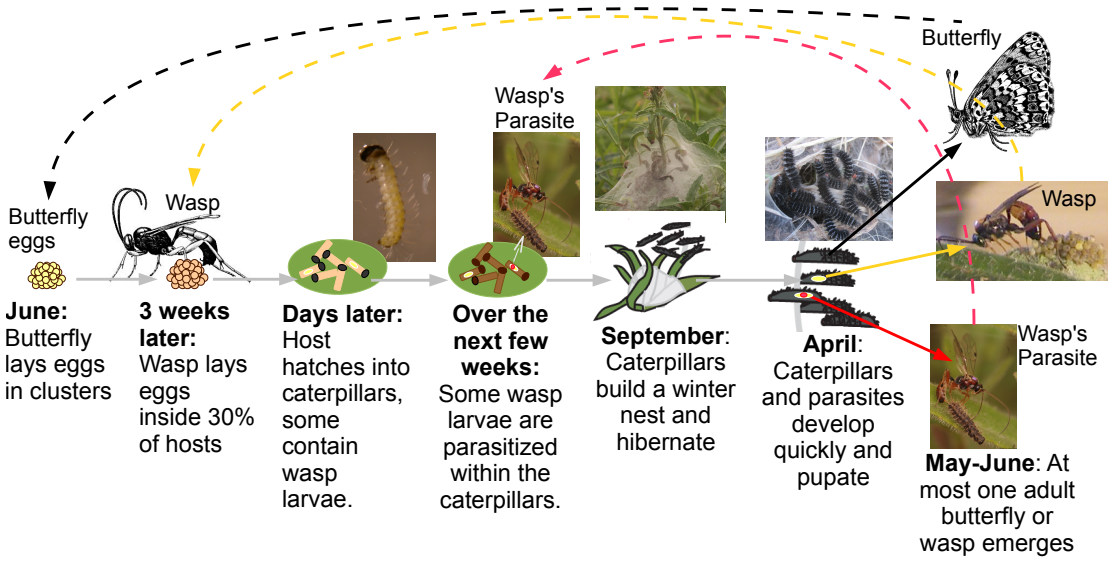

Figure 3.1: Diagram of key species interactions between the host *M. cinxia*, the parasitoid *H. horticola* and its parasitoid *M. stigmaticus*. Drawings of the wasp and butterfly were creates by Zdravko Kolev, photographs by Saskya van Nouhuys

3.1.2 Research System

The host of the parasitoid *H. horticola* is the checkerspot butterfly *Melitaea cinxia* (Lepidoptera: Nymphalidae) which has a Eurasian distribution. In the Åland islands of Finland it lives in small and extinction prone populations in networks of habitat patches of small dry meadows [110, 108, 66]. Suitable habitat for the butterfly is comprised of about 4000 habitat patches within an area 3500 km^2 [82, 45]. There are 300 to 500 local butterfly populations and all habitat patches are surveyed each year [44].

Individual butterflies lay clusters of 150-200 eggs on the leaves of the host plants (*Plantago lanceolata* and *Veronica spicata*) in June [66, 108]. These eggs take approximately two to three weeks to develop. Shortly before hatching, most

of the local host populations of *M. cinxia* in Åland become parasitized by *H. horticola*, which is a mobile, and solitary egg-larval endoparasitoid wasp [108, 66, 61, 107]. *Hyposoter horticola* has no hosts other than *M. cinxia* [97]. Females typically spend 20 to 60 minutes at each host cluster, parasitize roughly a third of the eggs, then mark the leaves around the egg cluster. This mark deters other conspecific wasps from parasitizing the remaining eggs [24].

All host eggs then hatch into caterpillars, some of which contain the parasitoid larvae. The caterpillars spin a communal silken web on the food plants. During the summer, the hyperparasitoid, *Mesochorus stigmaticus*, parasitizes some of the *H. horticola* larvae contained in the caterpillars. The caterpillars continue to live gregariously and in the fifth larval instar at the end of the summer when they diapause through the winter in a dense silken nest [108, 66]. In the spring, they moult twice and the fully developed caterpillars disperse to pupate for 2-3 weeks under vegetation. Just before pupation of the caterpillar would happen, the parasitoid and hyperparasitoid consume the host, kill it, and pupate. The butterflies and the wasps emerge in early June.

3.2 Methods and Results

In the following sections we present both the tests and the results of each hypothesis for submaximal parasitism (Table 3.1). We start by considering four possible biological reasons that the wasp might not physically or physiologically be able to parasitize all of the host eggs in a cluster.

3.2.1 Wasp egg limitation

Parasitoids which are egg limited (i.e. they don't have enough eggs to parasitize all of the hosts they encounter in a patch or lifetime), often reduce their parasitism rates by becoming choosy about which hosts they will accept [13, 48]. If *H. horticola* females did not have enough eggs at any one time to parasitize a full host egg cluster then that would explain observed parasitism rates but would not explain the deterrent marking behavior. *H. horticola* has a 10 day pre-ovipositional period in which eggs are developing and the wasp does not actively forage. Once mature, female wasps contain about 550 eggs ($\bar{x}$ = 550, SD = 173) in their ovaries and oviducts [25]. Thus, each wasp generally has plenty of eggs to parasitize the 100 to 200 host eggs in each host cluster.

3.2.2 Host Egg Cluster Architecture (Experiment 1)

Some insects effectively protect their eggs from parasitism by creating a mound where inner eggs are inaccessible to the parasitoid ovipositor [50, 115, 53] with up to half of the eggs protected in the inner layers of optimally shaped piles [36]. Since *M. cinxia* butterflies lay their eggs in mounds, the inner eggs may be protected from parasitism by *H. horticola*. We test this hypothesis (experiment 1) by comparing rates of parasitism of hosts from each part of the cluster (inner and outer).[1] Eleven host egg clusters were laid on plants by lab-reared butterflies under laboratory conditions and exposed to parasitism in the laboratory by one

[1]Experiment 1 was designed by S. van Nouhuys, performed by L. Salvaudon and analyzed by K. J. Montovan

H. horticola wasp each (see Appendix A.1 for more details). Seven wasps were used for this experiment, with three wasps each parasitizing a single cluster and the other four parasitizing two clusters each. Immediately after parasitism the outer layer of eggs was separated from the rest of the cluster. Both groups were reared to second instar and individuals were dissected to determine the parasitism level. The overall mean parasitism frequency for the clusters was 46% (±18% SD). The difference between the mean parasitism frequency of the two groups was −5.2% (±14.6% SD) with inner and outer eggs being parasitized equally. The wasps parasitized both groups of eggs and there is no meaningful difference in the parasitism rates. Thus, there is no evidence that mounding protects the inner eggs.

3.2.3 Host egg immunological defense (Experiment 2)

Hosts often defend themselves against endoparasitoids by encapsulating parasitoid eggs or small larvae [65]. Encapsulation of *H. horticola* by *M. cinxia* has never been observed (van Nouhuys, personal observation) and generally the immune response of very young insects (embryo) is weak [39, 33]. However, it is possible that if parasitoid eggs are encapsulated or killed in another way at a very early stage they would not be detected upon dissection. If this were the case we might expect that such early investment in immune response, which comes at a cost [92, 2] would be absent from *M. cinxia* populations that lack the parasitoid *H. horticola*.

To test this hypothesis, we compared the rate of parasitism by *H. horticola*

from Åland presented with egg clusters from Åland and egg clusters from Morocco (experiment 2).[2] *Hyposoter horticola* is not present in the Moroccan population of *M. cinxia*. The only known parasitoid of that population is *Cotesia melitaearum* (van Nouhuys, personal observation), which is also present in Åland, and which parasitizes older *M. cinxia* larvae [61]. Thus, in Morocco the hosts would not benefit from investment in early defense mechanism against the parasitoid.

For this experiment caterpillars were collected from several nests in the Moroccan highlands and also Åland, then were reared under laboratory conditions to pupation (see details in Appendices A.1 and A.2). Both types of butterflies (from Åland and Morocco) were mated and allowed to laid eggs on potted host plants *Veronica spicatta*. When the eggs were about two weeks old and just about ready to hatch, we exposed them to parasitism, each by a single wasp from Åland. We dissected the host larvae when 1-2 weeks old to determine the parasitism frequency in each host egg cluster. In total 26 egg clusters (11 from Åland and 15 from Morocco) were parasitized, each by a different wasp from the Åland population (see Table A.1 for summary results).

We compared the fraction of *M. cinxia* eggs parasitized in clusters from Åland and Morocco by wasps from Åland using a t-test. The wasps parasitized eggs from both origins at the same frequency (28% ± 17% SD, $t = -0.0047, df = 19.458, p = 0.9963$). Thus, we do not find evidence that there is locally evolved resistance in Åland restricting the parasitism.

[2]Experiment 2 was designed by S. van Nouhuys, performed by S. van Nouhuys and C. Couchoux, and analyzed by C. Couchoux

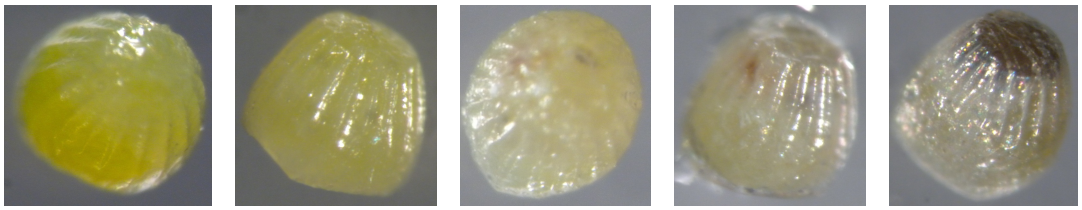

(a) Yellow (b) Creamy (c) Speckled (d) Grey-topped (e) Black-topped

Figure 3.2: Photographs of an egg from each visual maturity classes

3.2.4 Ephemeral resource use (Experiments 3 and 4)

Temporal asynchrony of the adult parasitoids with the susceptible stage of the host can create a short 'window of opportunity' [41, 40, 14]. *Hyposoter horticola* parasitizes its hosts while they are newly formed larvae still in the egg. *Melitaea cinxia* eggs start out as bright yellow, and when a cluster is completely bright yellow the wasps won't (or can't) parasitize it. As the eggs mature they change to a creamy color, then develop a couple of dark specks, then the top of the egg turns grey and later, just before the host larvae emerges, the top of the egg is nearly black. Figure 3.2 shows pictures of eggs in each of these five visible developmental phases. The host larvae become susceptible shortly before they emerge from their eggs. When the larvae start to hatch, the wasps are no longer interested in the cluster. If the window of opportunity for parasitism is short, and the eggs hatch asynchronously, then the parasitoid may only have enough time to parasitize a small fraction of the host eggs in a cluster before they hatch.

For example, if it takes the wasp one minute to parasitize each egg in a 100 egg cluster but all of the eggs in the cluster are only available for 30 minutes, then a wasp would be able to parasitize only 30% of the cluster before the entire

cluster hatches. Alternatively, host eggs may develop at slightly different rates, so it is likely that some eggs become susceptible first, and as they develop and hatch, others become available. Thus, if the wasp spent only a limited amount of time at a cluster, only a fraction would be available for parasitism. For example, again say there is a cluster of 100 eggs, but now eggs are susceptible to parasitism for 100 minutes, but at any time only 30 eggs are 'ripe'. Then a wasp visiting the egg mass could parasitize all of the susceptible eggs (30% of the cluster), and would then have to decide whether to wait for others to develop or move on to another cluster.

In order to test the hypothesis that the wasps are constrained by the developmental rate of the host egg, we first determined which visible phases of egg development are parasitized by the wasp (experiment 3).[3] 19 host egg clusters were exposed to parasitism, each by a single *H. horticola* wasp (see Appendix A.1 for details on how the wasps and host egg clusters were obtained). 11 wasps were used for the experiment, two parasitized three egg clusters, four each parasitized two clusters, and four parasitized a single cluster. Directly after parasitism the eggs were separated based on visual appearance into four groups: yellow/creamy, speckled, grey-topped, and black-topped.

The fraction of eggs parasitized in different categories of egg maturity were compared using a generalized linear model with a binomial error distribution and logic link function in the statistical software R [86]. Whether or not an egg was parasitized was modeled as a function of the cluster id and the maturity of the egg classified into four groups (creamy, speckled, grey-topped, and black-topped, see Fig. 3.2). We found that all of the egg maturity levels tested were

[3] I designed, performed and analyzed this study

susceptible to parasitism. The wasps would not probe the cluster until the eggs were more mature, so we were unable to test the susceptibility of less mature eggs (yellow). There was no significant difference in the parasitism of the four developmental phases of the eggs, but the levels of parasitism were significantly different in some of the clusters. This could be due to a number of factors unrelated to the development of the eggs (*e.g.* slight changes in lighting or laboratory conditions, differences between wasps, accessibility of egg cluster, *etc.*).

Now that we know that the last four categories of eggs are susceptible to parasitism, we want to determine if the wasp is limited by the fraction of the cluster that is in a susceptible phase or by the total time each cluster is susceptible. To answer both questions, I took hourly photographs of ten egg clusters over the last one to five days of development (experiment 4). For each cluster, I made a conservative estimate of the number of hours that essentially all of the eggs in the cluster were in one of the last three visible phases of development (speckled, almost black topped, black topped). The minimum window of susceptibility of an egg cluster was approximately 28 hours (mean=64 hours, standard deviation=38 hours). Wasps can probe approximately 1 egg per minute (computed in Appendix A.3). This window of opportunity is long enough for the wasps to find the cluster and parasitize much more than 30% of the host eggs. Thus, we did not find that the wasps were constrained by the rate of development of eggs, or synchrony of egg development in a cluster.

Therefore, the wasps have enough eggs in the ovary and oviduct to parasitize a whole cluster. All of the eggs in the cluster are physically accessible to the ovipositor, and the eggs are susceptible to parasitism for more time than the

wasp attends to the cluster. Although it is conceivable that some hidden factor could be keeping females from parasitizing more hosts than they do, we have tested all the factors for which there is any evidence in this system or others, so the reasonable assumption is that the female could parasitize more host eggs. The observed 30% frequency is then a behavioral decision rather than the result of a physical/physiological constraint. The following models consider the plausible evolutionary reasons that the wasp might behave in this way.

3.2.5 Cooperative benefits of unparasitized hosts (Experiment 5)

Many insect species that live gregariously during development, even those that are not social as adults, benefit from being in large groups as larvae [23]. *Melitaea cinxia*, the host of *H. horticola*, lives gregariously through their whole larval development and group size is positively associated with development rate, foraging success, and overwintering survival [106, 64]. In general, parasitized insects which continue to grow after being parasitized may perform poorly due to the cost of harboring the developing parasitoid larva [15, 83]. In a gregarious setting, if parasitized individuals are frail and do not contribute as much to the group, then the individual fitness of all members of highly parasitized groups could decline. This reduced fitness could favor the evolution of parasitoid restraint.

To determine the effect of parasitism frequency on host performance, we

manipulated the fraction of larvae parasitized in a nest in a replicated laboratory experiment and measured the rate of development, size at diapause, production of silk, and size at pupation of the hosts and parasitoid (experiment 5).[4] The host egg clusters were laid by *M. cinxia* butterflies under laboratory conditions on potted plants, then exposed to parasitism in the field, and brought back to the laboratory. Since young parasitized *M. cinxia* caterpillars are indistinguishable from unparasitized ones the actual fraction parasitized of each constructed nest was not known until the end of the experiment. To ensure a well distributed range of group parasitism frequencies, groups of a set size were constructed by mixing caterpillars from field parasitized clusters with caterpillars that were not exposed to parasitism. Aggregate groups of larvae were left undiluted, mixed 1:1, or from only unparasitized host nests. For the pre-diapause study, we used newly hatched caterpillars to construct 39 composite replicated groups of 40 larvae ranging in parasitism from 0 to 65%. They developed in these groups under laboratory conditions, making their silken winter nest, and going into diapause. At diapause, the larvae were weighed and dissected to determine the actual fraction parasitized in each nest. To assess the winter silk, the groups of caterpillars were sorted (blind to the level of parasitism) into 5 groups based on the amount of silk produced. Post-diapause larval growth was determined using another set of 30 lab-reared and field-parasitized composite groups of 25 larvae with 0 to 60% of host larvae parasitized in each group. These larvae were monitored as they developed from breaking diapause until metamorphosis.

Parasitism frequency did not have an effect on the rate of development to diapause of the host ($p - value = 0.3211$) or post-diapasue to pupation for *H.*

[4]Experiment 5 was designed by Saskya van Nouhuys, and performed and analyzed by David Muru.

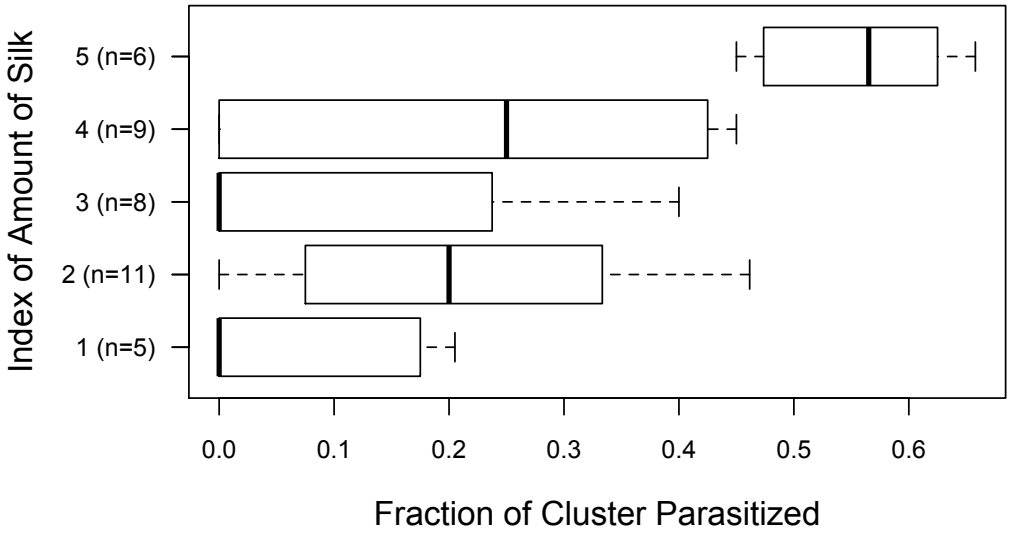

Figure 3.3: A box plot of the distribution of parasitism rates that result each index of winter silk production. Silk production is measured on a scale of 1 (least silk) to 5 (most silk). The group with the highest amount of silk production (5) is significantly different from the 4 lesser categories ($p < 0.001$) according to ANOVA analysis in R [86].

horticola ($R^2 = 0.03906$), the weight at diapause of *M. cinxia* ($R^2 = 0.009408$) or pupation of *H. horticola* ($R^2 = -0.004704$), or mortality of *H. horticola* ($R^2 = -0.02778$). Somewhat surprisingly, we found that larval groups with the highest fraction parasitized created the most silk for their winter nests (Fig 3.3). We did not test the actual performance of the winter nests but believe that the amount of silk is a fairly good indicator of the quality of the winter nest [64].

3.2.6 Optimal Foraging (Model results and Experiment 6)

There are many examples where predators leave a foraging location before resources are depleted because of diminished foraging efficiency [87, 72, 88]. *H.*

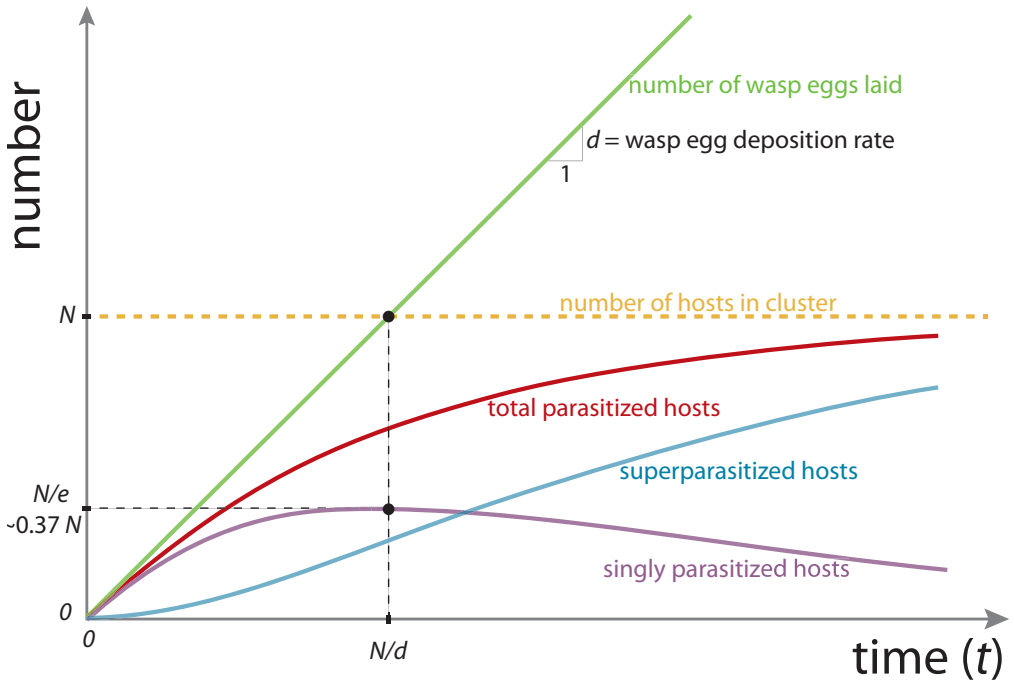

Figure 3.4: For any process involving random selection with replacement (like for *H. horticola*) there is a growing chance that the same item will be encountered multiple times. The green line shows the number of times the wasp probes the cluster, while the red line shows the total number of eggs probed (at least once). In this figure, we assume that the wasp lays an egg every time it probes. As the wasp parasitizes more eggs in the cluster the number of singly parasitized hosts increases to a maximum at N/d then decreases as these hosts become multiply parasitized. This creates a decreasing parasitism efficiency (number of hosts parasitized per unit time spent). This figure was created by Saskya van Nouhuys.

horticola experiences diminishing foraging efficiency as it spends more time at a host cluster because it becomes more likely to encounter previously parasitized hosts and only one wasp larvae can develop within each host. *H. horticola* is much larger than the host eggs and probes eggs randomly, making multiple somewhat haphazard passes across the eggs, and continuing to probe a few times when its ovipositor is no longer near eggs before turning around to make another pass [Montovan, Pers. Obs.]. Thus the wasp randomly probes eggs,

with seemingly no way to avoid encountering previously parasitized host eggs, which are not useful for the parasitoid. As *H. horticola* spends more time at an egg cluster it parasitizes a greater fraction of the eggs and it becomes more likely that the wasp will probe eggs that it has already parasitized (Figure 3.4). Since only one *H. horticola* larvae can develop within each host, the wasp's efficiency (number of ovipositions per unit time) decreases as it spends more time at each egg cluster. We hypothesize that under some circumstances this simple manifestation of optimal foraging would be enough to explain the 30% parasitism frequency of *H. horticola*.

In order to test the idea, we construct an optimal foraging model. We estimate the fraction of hosts parasitized ($g(t)$) when the wasp spends t minutes at a host cluster containing α host eggs using a Poisson distribution. This distribution expresses the probability that a particular egg is probed when the wasp spends t minutes probing the cluster. We use the probing efficiency, b (in eggs probed per minute at a cluster) to calculate that the wasp probes approximately bt eggs during its visit. Then, according to the poisson distribution, the probability that an egg is not probed is $e^{-\lambda}$ where lambda is the expected number of events in the timeframe, *i.e.* the number of eggs the wasp probes divided by the number of eggs in the cluster. Thus, the expected parasitism frequency is $g(t) = 1 - e^{-bt/\alpha}$. Since α is large, this is a reasonable approximation to the more realistic binomial distribution. We estimate b from laboratory data (see Appendix A.3 for details). The expected number of the eggs in the cluster that are probed at least once is

$$\alpha g(t) = \alpha(1 - e^{-bt/\alpha}) \tag{3.1}$$

This parasitism frequency function assumes that only one wasp parasitizes each cluster and that if the host is parasitized multiple times, one, and only one wasp larvae survives. In this case, wasps might try to avoid laying multiple eggs in each host because it is a waste of time and eggs. On the other hand, if multiple parasitisms of the same host kills all the wasp larvae, then there would be stronger selection for individuals that avoid super parasitism (through egg-checking or lower parasitism rates). To understand the frequency or multiply parasitized hosts, we expose host eggs to parasitism and dissect the host larvae soon after hatching to count the number of parasitoid eggs they contain (experiment 6). We expose host egg clusters (laid on potted plants by *M. cinxia* butterflies from Åland) to parasitism in the laboratory to parasitism by one wasp or multiple wasps and also put the eggs in the field to be parasitized. A total of 35 parasitized clusters were then dissected to determine the likelihood of multiple parasitisms (superparasitism) within single host larvae. These dissections show that although only one wasp reaches maturity within a given host, superparasitism does occur and is detectable in the lab. The observed superparasitism rates were compared to the expected rates under the assumptions of random probing (solid black line in Fig. 3.5) and were found to be lower than expected assuming purely random oviposition for all treatments: parasitized by a single wasp, multiple wasps, or in the field by an undetermined number of wasps. Since the wasp appears to probe the eggs randomly (and somewhat haphazardly), this suggests that the wasp is able to detect previously parasitized eggs and avoid superparasitism to some extent.

We tested this hypothesis by fitting the same data set to a non-linear model of random probing with a probability z of detecting previous parasitism and

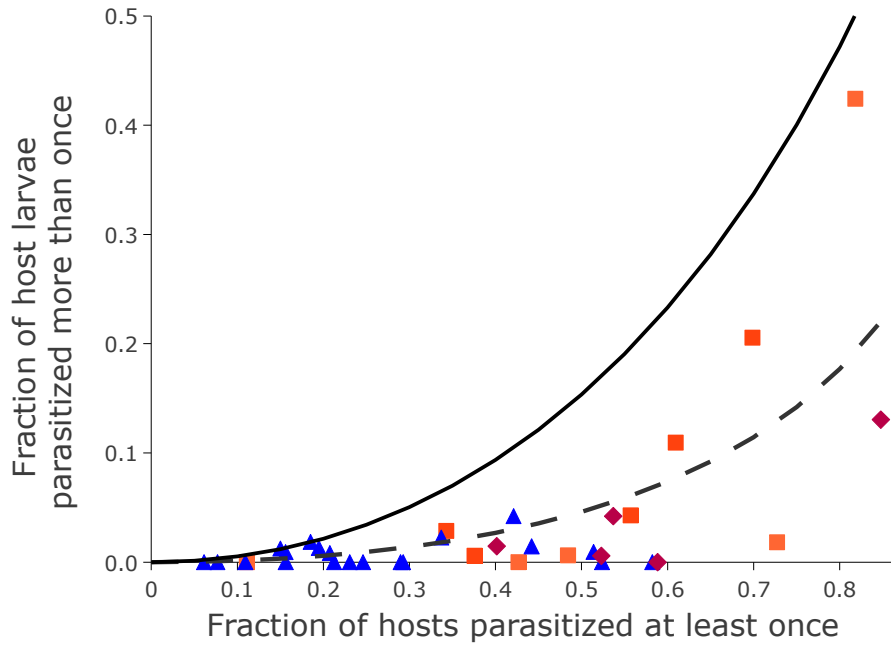

Figure 3.5: Frequency of *M. cinxia* host larvae containing multiple *H. horticola* eggs from a lab study with a single parasitoid (blue triangles), multiple parasitoids (orange squares), and field parasitism in Åland, Finland (pink diamonds). The solid black line is the expected fraction containing multiple eggs if oviposition happens randomly and the wasp does not check eggs for prior parasitism. The dotted grey line shows the best fit line for the data, where the fitted parameter (z) is the expected probability of detecting a previous parasitism and not laying an egg (here $z = 0.7471$, $p - value < 0.001$).

avoiding superparasitism. We found that the wasp detects and successfully avoids superparasitism approximately 75% of the time (dotted grey line in Fig. 3.5). The detection probability is significantly different than zero ($p - value < 0.001$). See Appendix A.4 for more details about the model.

Given the clear avoidance of superparasitism, it seems likely that there is an increased probability that all larvae will die in multiply parasitized hosts. To consider this possibility, we will look at the two two extremes. Above we

defined the fraction parasitized ($g(t)$) according to the assumption that each parasitized host (multiply or singly) supports one wasp larvae. We now will consider what happens at the other end of the spectrum when multiply parasitized hosts yield no wasp larvae. For this we define $g_2(t)$ to be the fraction of the cluster that is parasitized exactly once.

According to the poisson distribution with an additional probability of detecting previous parasitism (z), the fraction parasitized once is $g_2(t) = \frac{e^{-\lambda}}{z}(e^{z\lambda} - 1)$ where $\lambda = {}^{bt}/_{\alpha}$ (see more details about how we derived this expression in Appendix A.4). The expected number of host eggs parasitized exactly once is then

$$\alpha g_2(t) = \frac{\alpha e^{-{}^{bt}/_{\alpha}}}{z}(e^{{}^{btz}/_{\alpha}} - 1) \tag{3.2}$$

We use these parasitism functions ($g(t)$ and $g_2(t)$) to calculate the parasitism efficiencies for both scenarios: the expected number of hosts parasitized per unit time in a cluster. A similar approach was employed for parasitoids foraging for hosts in [55], however, this study was focused on confirming the model through experiments and did not explicitly define the equation $g(t)$. Often the cost of searching for new resources is included in optimal foraging models [21]. In our model we include the cost of searching in terms of time, but ignore any difference in mortality between time spent searching and ovipositing because the main causes of death for the parasitoid are roughly uniformly present during both searching and parasitizing. To get the parasitism efficiency ($w(t)$), we divide the number of eggs parasitized in each cluster ($\alpha g(t)$ or $\alpha g_2(t)$) by the total time the wasp spends searching for (t_s) and parasitizing (t) each cluster. The searching time (t_s) is the time to the next susceptible and unparasitized cluster, so it will depend on the local host and parasitoid density and will be greater

Parameter	Estimate	Source
b, probing efficiency	0.81 – 1.12 eggs/minute	Appendix A.3
α, number of eggs per cluster	100-200	[108]
t, time at cluster (min)	20-60	van Nouhuys, Pers. Obs.
t_s, searching time (min)	unknown, best guess: > 30	

Table 3.2: Parameter estimates from the literature or experimental data.

when there is more competition over host clusters. The time spent probing each cluster (t) is the wasp's decision variable on which selection acts. As the local parasitoid density increases relative to the local host density, competition over host clusters will be more intense and wasps will encounter and increased number of parasitized, marked, and thus unavailable clusters before eventually finding a host cluster at the right phase of maturity and not already parasitized.

$$w(t) = \frac{\alpha g(t)}{t_s + t} = \frac{\alpha(1 - e^{-bt/\alpha})}{t_s + t} \tag{3.3}$$

$$w_2(t) = \frac{\alpha g_2(t)}{t_s + t} = \frac{\alpha e^{-bt/\alpha}(e^{btz/\alpha} - 1)}{z(t_s + t)} \tag{3.4}$$

We use these models to predict optimal parasitism frequencies. To maximize the fitness with respect to t, we differentiate $w(t)$ and solve for t when $\frac{dw(t)}{dt} = 0$, and $\frac{d^2w(t)}{dt^2} < 0$. The functions were too complex to solve analytically, so we found the optimal value of t using the numerical solver FindRoot in Mathematica [1]. This required us to define each parameter explicitly, and made it necessary to individually look at the effects of each parameter on the optimal frequency of parasitism. To understand these effects, we varied one parameter at a time. All other parameters were held constant at $\alpha = 200$ eggs/cluster, $b = 1$ egg/min,

and t_s = 0.5 hours. For the second model, the probability of detecting previous parasitism was held constant at z = 0.7471.

Figure 3.6 shows the resulting optimal fraction parasitized for both parasitism functions, $g(t)$ (solid lines) and $g_2(t)$ (dashed lines), over realistic ranges of α (Fig 3.6a) and b (Fig 3.6b). When super parasitism kills all wasp larvae (dashed lines) the optimal parasitism rate is lower and approaches 62.8% for large t_s. The model predicts that as host clusters get larger (bigger *alpha*), the fraction parasitized should decrease slightly and if the wasp probes the eggs more quickly (bigger b), the fraction parasitized should increase slightly. We see that the optimal fraction parasitized is not very sensitive to changes in α or b. Since there is a large amount of uncertainty in the value of t_s, two ranges (small and large) were investigated (Fig 3.6c and 3.6d). For small values of t_s and realistic values of α and b, both models predict an optimal fraction parasitized close to the observed 30%. However, the optimal parasitism rate is sensitive to the search time t_s, which is a parameter that we do not know. For the model based on $g(t)$, relatively small parasitism frequencies are only predicted when the searching time t_s is fairly short, otherwise, the model predicts much more parasitism than is observed for this system. Including death due to superparasitism in our model (dashed lines) lowers the optimal parasitism rates and creates a larger range of search times, t_s, for which we would expect to see the wasp parasitize close to 30% or each cluster. Thus, optimal foraging with decreasing efficiency due to random probing can explain the observed submaximal parasitism frequencies if the wasp's searching time is relatively short. If superparasitism kills all wasp larvae contained in the host then slightly longer search times could also result in parasitism frequencies close to 30%.

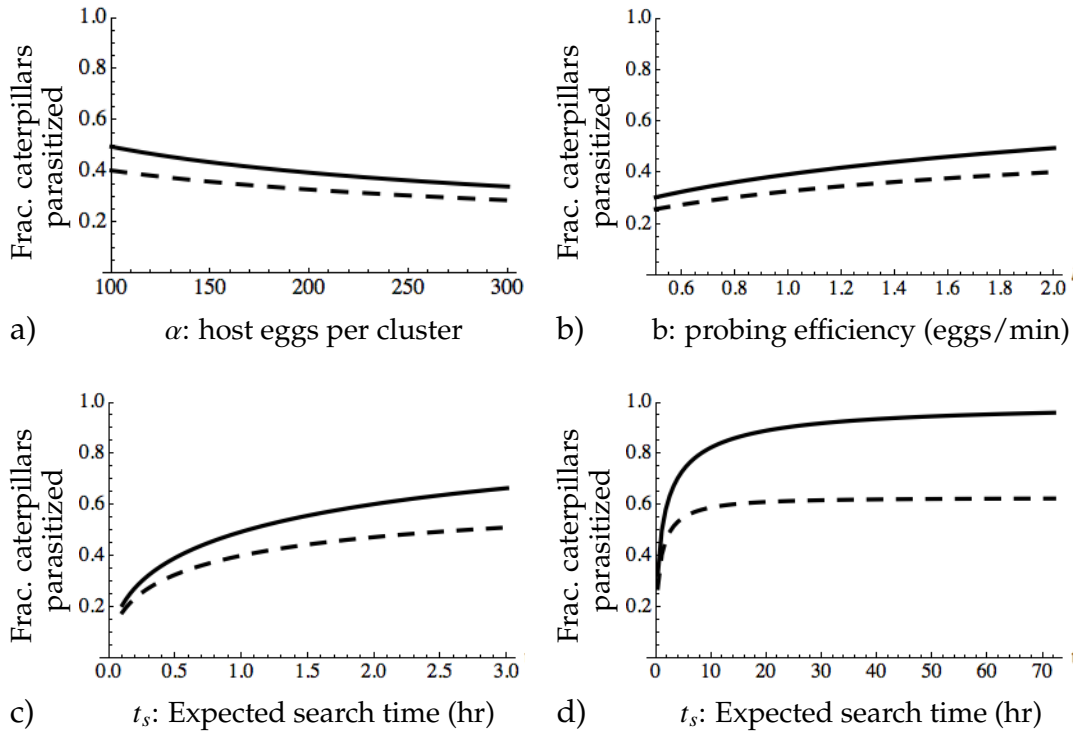

Figure 3.6: Numerically determined optimal values for t (amount of time spent probing each host egg cluster) over a range of realistic parameter values for the optimal foraging model with parasitism function $g(t)$ (Eqn. 3.3) shown as a solid line, and $g_2(t)$ (Eqn. 3.4) shown as a dashed line. For each graph one variable was varied and the rest were held constant at α = 200 eggs, b = 0.9 eggs per minute, t_s = 0.5 hours. These plots show how the optimal parasitism frequency changes with a) α, b) b, and c) the searching time for the next cluster, t_s, when searching times are fairly short and d) much longer timeframes.

3.2.7 Avoiding Hyperparasitism (Experiments 2 and 7)

Just as parasitism can affect the evolution of host behaviors, hyperparasitism can change the behavior of parasitoid hosts, potentially causing reduced parasitism in order to avoid positively density dependent hyperparasitism [7, 30]. *Hyposoter horticola* has one hyperparasitoid, *Mesochorus stigmaticus*. This solitary endoparasitoid probes second to fourth instar *M. cinxia* host caterpillars,

laying eggs inside any first or second instar *H. horticola* larvae contained inside. Multiple *M. stigmaticus* females visit host nests over several weeks during the summer, spending minutes to hours exploring and parasitizing the wasp larvae inside their butterfly hosts [van Nouhuys unpublished data]. Most host clusters are hyperparasitized with the frequency of hyperparasitism ranging from 0% (very rarely) to 51% of local populations of *H. horticola* larvae being hyperparasitized [66]. Our question is whether there is evidence that pressures of hyperparasitism can theoretically cause selection for reduced fraction of hosts parasitized by *H. horticola*, and whether there is evidence that this occurs in this system.

We look at this question in three different ways. First, we consider whether hyperparasitism by *M. stigmaticus* is in fact density-dependent (experiment 7). Then, we combine the observed density-dependent hyperparasitism pressures with our optimal foraging model (Eqn. 3.3) from section 3.2.6 to determine how large an effect this additional pressure might have on the wasp's behavior. Last, we compare the parasitism frequencies of *H. horticola* from populations with (Åland) and without (Estonia) *M. stigmaticus* to see if the population has a lower parasitism frequency in the presence of the hyperparasitoid (experiment 2).

We determined the hyperparasitism frequency for a range of parasitism frequencies in two different ways. First, we collected 16 nests that experienced natural parasitism and hyperparasitism in the autumn of 2007, kept them in the laboratory for winter diapause, reared them in the spring, and then counted the emerging number of *M. cinxia*, *H. horticola*, and *M. stigmaticus*.[5] Each nest was from a different local host population. Second, to extend the observed levels of

[5]These experiments were designed and performed by S. van Nouhuys.

parasitism and standardize for nest size and location, in the summer of 2009 we constructed nests of 60 *M. cinxia* prediapause caterpillars that ranged in fraction parasitized by *H. horticola* from ten to sixty percent, and placed them in the field to be naturally hyperparasitized by *M. stigmaticus*.[6] The groups were constructed by mixing caterpillars from egg clusters that had been placed in the field to be parasitized naturally by *H. horticola* with caterpillars from egg clusters of the same laboratory origin that had not been exposed to parasitism. Nests containing naturally parasitized caterpillars were left undiluted (N= 7), diluted 1:1 (N= 7), and diluted 2:1 (N=7). The nests were randomized and placed in natural locations in five different habitat patches. After three weeks in July (when *M. stigmaticus* is active in the field) the nests were brought back into the laboratory and reared. The number of caterpillars that became adult butterflies, *H. horticola* or *M. stigmaticus*, were recorded.

The data suggest that wasps suffer higher hyperparasitism losses for parasitizing more hosts (Fig 3.7a). The host clusters had a 72.2% chance of being hyperparasitized by *M. stigmaticus*. To understand the effects of hyperparasitism on the wasp's expected number of offspring, we consider the fraction of hosts within each cluster that were parasitized by *H. horticola* and not hyperparasitized by *M. stigmaticus* and thus emerge as *H. horticola* ($H(p)$) as a function of the initial fraction that were parasitized by *H. horticola*, p (Fig 3.7b). We fit a second order polynomial curve with a intercept at $(0, 0)$ because it would be nonsensical for a larger fraction to emerge as *H. horticola* than were originally parasitized (p). The second order linear model determines whether the data has a linear or second order relationship. The second order term was not significant

[6]This experiment was designed and performed by S. van Nouhuys, and both experiments were analyzed by K. J. Montovan.

($p = 0.29$). Thus, the best fitting function for *H. horticola* offspring production as a function of the frequency of *H. horticola* parasitism (p) is the line $y = 0.4573331p$ (shown in Fig 3.7b, $p - value < 0.001$).

The expected fraction of hosts that yield *H. horticola* is then the fraction that emerge from non-hyperparasitized clusters plus the fraction that emerge from hyperparasitized clusters.

$$H(p) = 0.278p + 0.722(0.4573p) = 0.6082p \tag{3.5}$$

The data supports a hyperparasitism function that linearly decreases the benefits of high parasitism frequencies to the wasp. This would affect the population sizes, but would not change the predicted optimal foraging strategy. We show this by demonstrating how hyperparasitism ($H(p)$ would fit into the optimal foraging model presented earlier (Eqn. 3.3). This is accomplished simply by using $H(p)$ to modify the fraction of the cluster that becomes *H. horticola*.

$$w_h(t) = \frac{\alpha H(p)}{t_s + t} = \frac{\alpha H(1 - e^{-bt/\alpha})}{t_s + t} = 0.6082w(t)$$

Since the data for the first test of this hypothesis is noisy, we confirm the results by using an entirely different approach to test whether parasitism frequency has evolved in response to density-dependent hyperparasitism. To do this we compare the behavior of *H. horticola* from Åland with those from an area free of *M. stigmaticus* (experiment 2).[7] In Estonia, the parasitoid *H. horticola* is present but *M. stigmata*, the hyperparasitoid, is absent (van Nouhuys, personal observation). We collected *M. cinxia* from an Estonian population that is 250 km

[7]This experiment was designed by S. van Nouhuys and performed by S. van Nouhuys and C. Couchoux

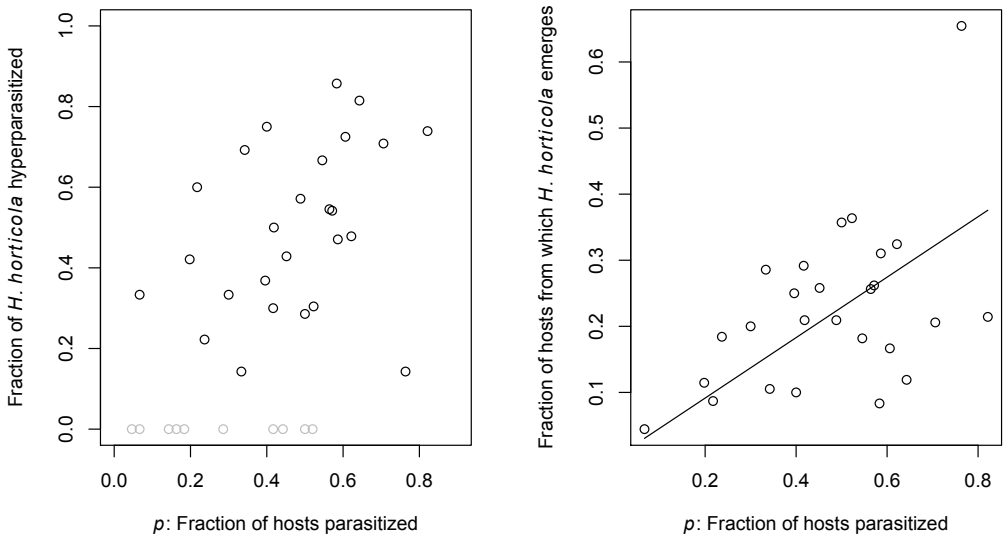

(a) Fraction of *H. horticola* hyperparasited

(b) Fraction of hosts parasitized and not hyperparasitized

Figure 3.7: a) The fraction of *H. horticola* that are hyperparasitized by *M. stigmaticus* as a function of the cluster parasitism frequency. Hyperparasitism is density-dependent and increases with p, the fraction parasitized by *H. horticola*. The fitness of *H. horticola*depends on the number of hosts parasitized by *H. horticala* that are not hyperparasitized. Gray circles show clusters that were not found by the hyperparasitoid. Figure b) shows the fraction of each host cluster that is parasitized by *H. horticola* and not hyperparasitized as a function of the fraction originally parasitized by *H. horticola*. Two functions were tested for goodness of fit (linear and second order polynomials with (0,0) intercepts). The best fit function is $y = 0.4573x$ ($R^2 = 0.8198$).

by sea from Åland and well outside of the distance that *H.horticola* can travel over water. There, the butterflies feed on *Veronica spicata*, and live in a similar climate to Åland, though the landscape structure is less fragmented [70]. If *H. horticola* has evolved to parasitize at a low frequency to avoid a positively density dependent hyperparasitoid in Åland, then we might expect individuals from the Estonian population not to exhibit such a constraint, and to parasitize a larger fraction of the hosts in each cluster.

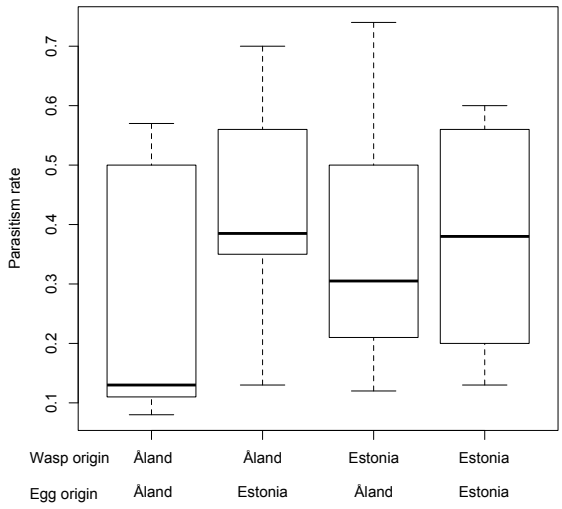

Figure 3.8: The fraction parasitized by *H. horticola* from Åland and Estonia of *M. cinxia* egg clusters from Åland and Estonia. In an analysis of variance there are no significant differences between treatments.

We collected 11 post diapause *M. cinxia* nests from Paldiski, Estonia in spring 2012. The larvae were reared to pupation into butterflies or wasps. The rearing, egg collection, and experimental protocol are described in Appendix A.2. In the fully crossed experiment, *H. horticola* from Åland were offered *M. cinxia* eggs from Åland (n = 11) and *M. cinxia* eggs from Estonia (n = 10) and wasps from Estonia were offered *M. cinxia* eggs from Åland eggs (n = 14) and *M. cinxia* eggs from Estonia (n = 14). A different wasp was used to parasitize each egg cluster. We compared the frequency of parasitism in egg clusters from the two origins by wasps from the two origins using a generalized linear model with the statistical software R [86]. The frequency of parasitism of the egg cluster was modeled as a function of egg cluster origin (Åland, Estonia), wasp origin (Åland, Estonia) and the interaction between wasp and egg origin. See table A.1 for the mean and standard deviation of the fraction parasitized for each treatment.

On average the fraction parasitized was 36% of the eggs in a cluster. This

ranged from 0.08 to 0.74, which is a larger spread than we usually find because the egg clusters were relatively small and the weather was cloudy so the wasps did not behave consistently under the laboratory conditions. There was no difference in the frequency of parasitism between egg origins or between wasp origins, and no interaction between egg and wasp origin (Fig. 3.8). The data do not support the hypothesis that *H. horticola* wasps from Åland behave differently than those from Estonia. Thus, there is no evidence that wasps from Åland have evolved restrained parasitism behaviors because of pressure from the hyperparasitoid *M. stigmaticus*.

3.3 Discussion

Host-parasitoid relationships are tightly coupled so there is strong selection for the host to develop defenses against parasitism. Specialist parasitoid wasps (such as *H. horticola*) experience this strong pressure to develop ways around the hosts defenses. This can lead to an arms race between the host and the wasp. This type of antagonistic coevolution can lead to a variety of outcomes including the Red Queen dynamic, in which both organisms evolve to keep up with the other, but neither ever gets ahead [90, 68].

We would expect that simple biological constraints would be an effective deterrent only if the parasitoid is not well adapted to the host, or is unable to adapt in the necessary ways. Since *H. horticola* has an extremely narrow host range, probably entirely limited to *M. cinxia* and certainly limited to *M. cinxia* in the study area, we were not surprised to find that the wasp is physically able

to parasitize all of the eggs in a cluster. That is, *Hyposoter horticola* typically has enough eggs, is not prevented from oviposition by the mounded egg architecture, short window of susceptibility or asynchrony in the development of eggs within each cluster. While it is possible that a fraction of the hosts have defenses against parasitoid which prevent parasitism or killed the wasp before our detection, our comparison with eggs from Morroco, which does not have *H. horticola*, does not support this idea.

One complication to these findings is that although each wasp generally has enough eggs to parasitize all of the hosts in multiple clusters, it could still be egg limited in its lifetime. This kind of parasitoid egg limitation causes some parasites to be selective in host use patterns, thus leaving many hosts unparasitized in order to find the best hosts [13, 48]. However, *H. horticola* is large compared with the host eggs and probing happens haphazardly making it unlikely that wasp has any information about the quality of particular eggs that it could use to choose among eggs within each host cluster. The wasps could be reserving eggs for better egg clusters, but we do not think that this is the case because *H. horticola* treats large and small clusters the same [24]. Furthermore, choosiness due to lifetime egg limitation would not explain why wasps leave a deterrent marking that other individuals respect.

We have shown that the wasp is not constrained by biology and is able to parasitize all of the eggs in any host egg cluster. Thus a behavioral explanation is most likely to explain why it does not parasitize more of each cluster. Theoretically, prudence and risk-aversion are not applicable to this system because in Åland, *H. horticola* has large population sizes that are reasonably well-mixed

across the landscape. Experimentally we have shown that the development and survival of wasps from highly parasitized clusters are similar with those from lesser parasitized nests.

There was no evidence that survival and fitness decrease for more heavily parasitized cluster. Although *M. cinxia* caterpillars live gregariously and rely on cooperative contributions to survive, the fraction parasitized did not affect the pre-diapause or post-diapause developmental rates or weights of the *M. cinxia* caterpillars. The most surprising result in this experiment, which warrants further study, was that highly parasitized clusters produced significantly more silk for their winter nests. This suggests that the parasitoid might induce the host to invest more into nest building than it would otherwise. Parasitoids are known to induce host behaviors that benefit the parasitoid [43]. In this case, the induced behavior could increase the chances that these clusters survive through winter at some energy/resource cost to the hosts later in life.

Optimal foraging models show the most promise for explaining restraint in resource use. We considered an optimal foraging model, which assumes that selection favors wasps that leave each cluster at the optimal time. In the most basic model, their efficiency decreases solely because the wasp probes randomly and only one larvae can develop within each host. As the wasp spends more time at the cluster she finds fewer and fewer eggs that she has not yet parasitized. The model with one parasitoid surviving in each parasitized host predicts drastically submaximal parasitism frequencies close to the observed 30%, only when the searching time required to find the next susceptible and unparasitized cluster is short (around 30 minutes). When all wasp larvae die in mul-

tiple parasitized hosts then the optimal parasitism rate lowered and, based on our data determined probability of avoiding superparasitism, never gets about 63% even for very long search times. Adding the effects of hyperparasitism to either model does not change these results.

The predictions of the optimal foraging models depend sensitively on the local density of hosts and *H. horticola* wasps. Since only one wasp parasitizes each cluster, the number of clusters it must check before finding one that is both susceptible and not already parasitized will depend on the local density of host egg clusters and foraging wasps. Thus, the search time, t_s, will vary spatially as a function of these densities. Estimates for t_s are currently unknown. There is indirect evidence that supports conflicting views of the intensity of competition. First, essential every host cluster is parasitized in the landscape even though it is available for a relatively short period of time (one to several days in a one year life cycle). This suggests that there is a high level of competition over clusters. Secondly, *H. horticola* wasps locate host clusters in advance, remember their locations, and monitor these clusters as they develop [110]. Multiple individuals know about and compete for each cluster (Couchoux and van Nouhuys, in prep). This suggests that there is a large degree of competition over clusters, but also that wasps are likely to secure multiple clusters. If they expected to parasitize at most one cluster in their lifetime then we would expect to see them finding and guarding host clusters to ensure that they will get to parasitize at least one cluster. Further studies of the level of competition are needed to conclusively understand this mechanism.

To test the idea that density-dependent hyperparasitism may have led to

the evolution of low rates of parasitism, we compared parasitism frequencies in Åland to those in regions that lack the hyperparasitoid and found that there were no significant differences in parasitism frequencies of *H. horticola* individuals from Estonia and Åland. Thus, while density dependent hyperparasitism would explain the deterrent marking behavior, there is no evidence to support the idea that the wasp should have or has evolved lower parasitism frequencies in the presence of the hyperparasitoid *M. Stigmaticus*.

Within a relatively low range of searching times, t_s, optimal foraging theories explain both the fraction parasitized, and the deterrent marking of clusters. These models assume that the wasp leaves each cluster when additional parasitism would reduce its expected fitness. Thus if another (essentially identical) wasp approaches the same, now previously parasitized, cluster, it will also maximize its fitness by leaving to search for another cluster. Explaining why wasps would take the time to perform deterrent markings is more difficult. It could be that the wasps leave the marking for themselves, and that others pay attention to it because it benefits them too. Other parasitoids are known to mark clusters and modify their search behavior in response to these pheromone markings [81, 10, 35, 102], and that some parasitoids recognized their own markings and use them to inform their actions [52].

In addition to the cost of wasted eggs and time laying multiple eggs in the same host, there could be additional costs related to what happens within hosts that have been parasitized more than once. For other species of parasitoids, avoidance of multiply parasitizing hosts is associated with changes in patch exploitation strategy [112]. We know that only one *H. horticola* can develop within

each host, but it is unknown what happens within multiply parasitized hosts. There are a few distinct options: a) only the first parasitoid larvae survives, b) one of the parasitoid larvae survives, c) both/all parasitoids die and the host survives, or d) the host and parasitoids all die. If the first parasitoid larvae kills all additional larvae, then there would be less motivation to mark the cluster unless the wasp left it for themselves. It is more likely that one of the later three options actually occurs, and that parasitism by another wasp would kill some (or all) of the first wasp's larvae, providing strong pressure for avoiding superparasitism [99, 85, 56] by parasitizing a smaller fraction of the cluster and applying and respecting deterrent markings. In our second optimal foraging model we see that if all parasitoids die in multiply parasitized hosts and the wasp cannot effectively avoid superaparasitism then the optimal parasitism rate is between 18% and 60% for all realistic parameter values and approaches 63% for very long search times.

Any time an individual restricts its own use of an available resource that it needs to survive and reproduce we wonder about what motivations that individual might have. This paper illustrates that while there are potentially many plausible explanations for submaximal resource use, nature is complicated and careful examination can show that many explanations are not reasonable. We have carefully considered all reasonable hypotheses for submaximal parasitism by *Hyposoter horticola* and show that most of them are not plausible. We conclude that the only reasonable explanation is that the *H. horticola* practices submaximal parasitism and deterrent markings as a way to forage optimally for hosts, but recognize that the plausibility of this hypothesis is dependent on a relatively short searching time t_s. There are many other parasitoids, espe-

cially egg parasitoids, that utilize just a small fraction of the available hosts (*e.g.* [27, 53, 89, 116]) and it is likely that some of them have similar evolutionary causes for their behaviors, but few parasitoid systems have been studied well enough to know. This work illuminates the relative importance and limitations of accepted theories for submaximal resource use. In this, as in many circumstances, individual selection (though optimal foraging and efficiency optimization or another mechanism) is a stronger motivator than bet-hedging (risk-aversion) or group selection and should be carefully considered when thinking about the evolutionary causes of any submaximal resource use.

CHAPTER 4

COOPERATION IN A REPETITIVE AND OFTEN MISTAKEN WORLD

Abstract

Altruistic individuals incur a cost for helping others so we would expect that under most reasonable circumstances natural selection should select against altruism. Why then are cooperative and altruistic behaviors so common in social and biological systems? In this chapter we will focus on the conditions under which direct reciprocity through repeated interactions supports the evolution of cooperation. Despite extensive work to understand cooperative behaviors, a rigorous overarching theory for cooperation through direct reciprocity remains elusive. We use simplified models to provide analytical insights about the evolution and stability of cooperation that help explain results from more complex computer simulations. We fully classify the population dynamics for a population consisting of any two stochastic reactive strategies. For populations with three set strategy types (non-cooperative defectors, mistaken tit-for-tat, and generous tit-for-tat), we describe the stability of each fixed point and find that the level of generosity in the generous tit-for-tat strategy can drastically change the population dynamics.

4.1 Introduction

The prevalence of altruistic behaviors in humans and animals is deeply puzzling because they impart benefits to an opponent at a personal cost to the cooperator. Cooperative dilemmas arise when individuals interact with others and are better off in a situation of mutual cooperation than mutual defection, but yet there is an incentive to defect. This incentive could be of three forms: i) it is better to defect when playing against a cooperator, ii) it is better to defect when playing against a defector, or iii) it is better to be the defector when a cooperator and defector interact [6, 29, 77]. Non-cooperation is most tempting when all three conditions are met, which happens in the class of games known as the *prisoner's dilemma*. This makes the prisoner's dilemma a particularly compelling context for understanding the evolution of altruism [76, 77].

In the prisoner's dilemma, two individuals independently choose to cooperate (C) or defect (D). As a convention the cooperator gets a reward, R, each time it interacts with another cooperator, and a sucker payoff, S, against a defector. A defector suffers a punishment, P, when playing against another defector, and gets a temptation, T, when interacting with a cooperator. We restrict out work to the well studied payoffs $T = 5, R = 3, P = 1, S = 0$ which were originally defined by Robert Axelrod [3, 4] (shown in Table 4.1). Thisensures that a pair

	C	D
C	3, 3	0, 5
D	5, 0	1, 1

Table 4.1: The Axelrod 5 – 3 – 1 – 0 payoff matrix.

of cooperators does better than a pair of defectors and also that defection is the dominant strategy for both players, *i.e.* for a single game, each does better by defecting regardless of what their opponent does. We are interested in repeated interactions so it is worthwhile to note that these payoffs also ensure that mutual cooperation (payoff $R = 3$) is better on average than retaliatory cycles (alternating between payoffs of $S = 0$ and $T = 5$).

Defecting is the dominant strategy for the prisoner's dilemma which means that each player should selfishly defect. So how can we understand high levels of cooperation in real-world prisoner's dilemma interactions? Direct reciprocity (through repeated interactions), indirect reciprocity (through reputations), spatial selection, multi-level selection and kin-selection all can favor cooperation [77]. We focus our work on direct reciprocity through repeated interactions. With repeated interactions players can adjust their strategy in response to their opponent's last action (*i.e.* a reactive strategy). This provides an opportunity for individuals to play strategies that reward cooperation and punish defection.

The repeated prisoner's dilemma has been studied extensively but there are still many open questions related to the population dynamics of multiple competing strategies. In the early 1980s, Robert Axelrod considered optimal strategies for the repeated prisoner's dilemma and showed that when there is a high enough probability that players will interact again, there is no best strategy, *i.e.* if the opponent's strategy is known, a response strategy can be carefully crafted to exploit its weaknesses and win the repeated game [5]. Since there is no single best strategy for the iterated prisoner's dilemma, Axelrod set out to find the best strategy among those designed to do well by inviting experts to sub-

mit strategies to a computer tournament. He found that the strategy with the highest average score was *tit-for-tat* (TFT) which is a strategy that cooperates in the first round and copies the opponents last choice for all other rounds [3, 4]. This strategy cooperates with cooperators and others playing TFT, but defects against defectors and is thus able to benefit from mutual cooperation without being exploited by defectors.

Although tit-for-tat does well in Axelrod's computer tournaments, it has a fatal flaw: two competing TFT individuals who make occasional mistakes can get stuck in long retaliatory cycles where they alternate between payoffs $S = 0$ and $T = 5$. This is worse than always cooperating ($R = 3 > \frac{5+0}{2}$). Since real (non-computer) individuals make mistakes it is reasonable to ask what the best strategy would be when individuals make occasional mistakes. To answer this question, Bendor *et. al* (1991) performed a round-robin tournament similar to Axelrod's except that there were occasional mistakes. They found that tit-for-tat was outcompeted by a more generous (forgiving) version of TFT [9]. Generous tit-for-tat ($GTFT$) is a stochastic strategy which cooperates after the opponent cooperated and cooperates after an opponent defects with probability q.

In general, stochastic strategies are defined by the probabilities that the player cooperates after the opponent cooperated (p) and cooperates after the opponent defected (q). Each strategy is represented as an ordered pair (p, q) within a continuous strategy space of reactive strategies. This space includes the non-stochastic strategies tit-for-tat, (TFT, $p = 1, q = 0$), always defect ($AllD$, $p = 0, q = 0$) and always cooperate ($AllC$, $p = 1, q = 1$) as well as all possible probabilistic responses to the opponents last move ($0 < p < 1, 0 < q < 1$).

The stochasticity creates a diverse array of potential strategies while still being analytically tractable. The expected payoffs of repeated interactions between two stochastic strategies are calculated using the stationary distribution of the associated Markov process as described in [75].

This provides a way to compare the fitnesses of different stochastic strategies in a population, but to understand how the frequency of each strategy will change we need a population model. One way to model the relative frequencies of each strategy is to assume that the population size of the strategy changes in proportion to the difference between the strategies' fitness and the average fitness across the population. The standard model for this type of population chance is defined by the replicator replicator equations [51]. Let x_i represent the proportion of the population playing strategy i. Then, if a population has n strategies, then the expected payoff for strategy i is

$$f_i = \sum_{i=1}^{n} E_{ij} x_j \tag{4.1}$$

where E_{ij} is the expected payoff of strategy i against strategy j. The change in population frequency for strategy i is

$$\dot{x}_i = x_i(f_i - \phi) \tag{4.2}$$

where ϕ is the average fitness of the population, *i.e.* $\phi = \sum_{i=1}^{n} x_i f_i$. Since each x_i is a proportion, $x_n = 1 - \sum_{i=1}^{n-1} x_i$. This simplifies the system to $n - 1$ dimensions.

In 1992, Nowak and Sigmund used replicator equations to investigate the population dynamics of competing stochastic strategies by performing computer simulations of 99 randomly chosen stochastic strategies plus one strategy close to TFT [79]. These simulations showed the mixed population was

quickly taken over by strategies that are close to *AllD*. Then, a strategy close to TFT takes over. The population then shifted to a more generous TFT strategy. Nowak and Sigmund found that, for the Axelrod $5-3-1-0$ payoffs, this $GTFT$ strategy is typically close to $(1, 0.3)$. This strategy is generous enough to end costly retaliatory cycles fairly quickly, but is not overly sensitive to exploitation by defectors. In their simulations, $GTFT$ was not taken over by any other strategies.

We reproduced this model and found that while a large fraction of the simulation runs eventually end up at a generous TFT strategy, the rest end stop at a non-cooperative strategy near *AllD* (Figure 4.1). The difference seems to be the presence of a strategy that is close enough to TFT to enable the population to become predominately generous TFT (Figure 4.2).[1] It is not well-understood why the end states in Figure 4.1 are confined to the regions near *AllD* and near generous TFT. In this chapter, we provide analytical results to help explain the general behavior of the simulation models. Since the interesting population changes typically occur when there are mainly two strategies (a reigning champion and a new contender), we start by looking at the population dynamics between any two competing stochastic strategies. Our analytical results fully classify the evolutionary population dynamics for any two competing strategies according to the replicator equations. We characterize the dynamics and find envelope functions for the region where bifurcations can occur. This work provides intuition about interacting strategies that is helpful when consider more complex systems with more than two distinct strategies.

We then consider the possibility that three main strategies are driving the

[1] Danielle Toupo performed the modeling and created both of these figures.

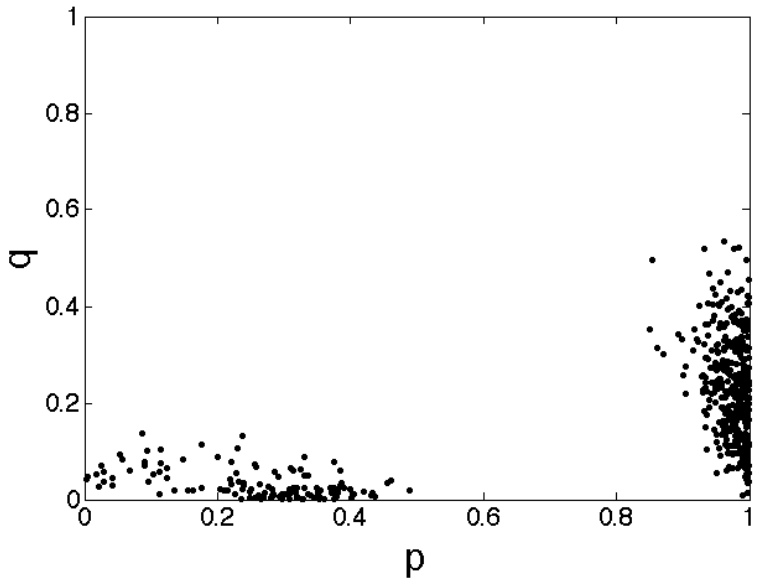

Figure 4.1: The final strategy for each of 500 simulation model runs, with the same model as described in [79]. Each simulation starts with a population with 99 random strategies (p, q) and the strategy mistaken TFT $(1-\epsilon, \epsilon)$. For all 500 simulations the prevailing strategy in the end is either close to *AllD*, (0,0), or generous TFT, (1,0).

population dynamics. We focus on the strategies always defect ($AllD : (0, 0)$), mistaken tit-for-tat ($\epsilon - TFT : (1-\epsilon, \epsilon)$) and generous tit-for-tat ($GTFT : (1, \hat{q})$). We determine the population dynamics for different probabilities of mistakes (ϵ) and forgiveness ($\hat{q}$) and show that the level of cooperation in the population depends on the initial population densities of all three strategies, the level of generosity ($\hat{q}$), and probability of mistakes (ϵ).

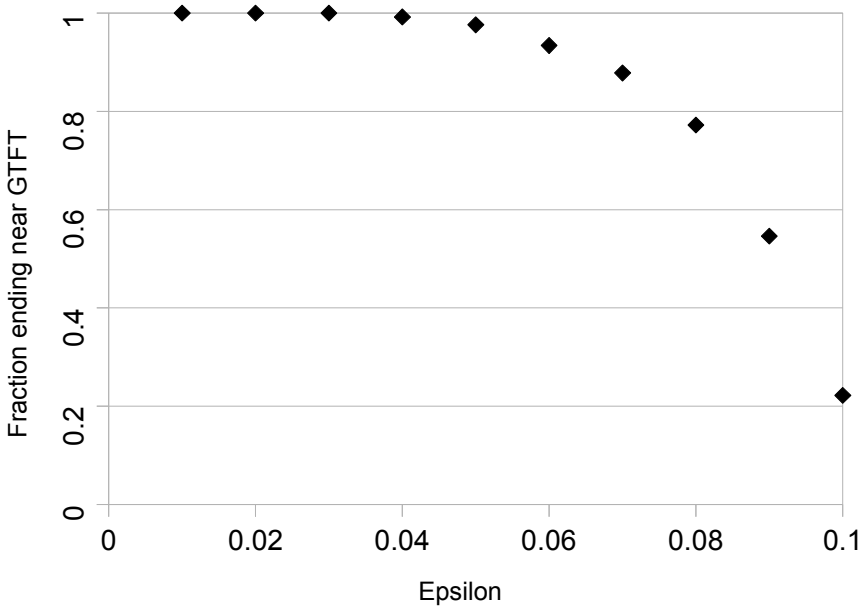

Figure 4.2: Results from the simulation model described in [79], with each simulation starting with a population with 99 random strategies (p, q) and the strategy mistaken TFT $(1 - \epsilon, \epsilon)$. Each datapoint shows the fraction of 600 simulation model runs that reach a cooperative end state. Once the added strategy is close enough to TFT essentially all of the simulation runs have a cooperative end-state.

4.2 Two-strategy Iterated Prisoner's Dilemma

In the simulations of Nowak and Sigmund [79] of populations of 100 strategies, the population tended to contain one prevailing strategy (with all other strategies existing at very low population densities). In this circumstance, a thorough understanding of how a prevailing strategy will perform against any single contender could help us understand the observed end-states in the more complicated simulation model.

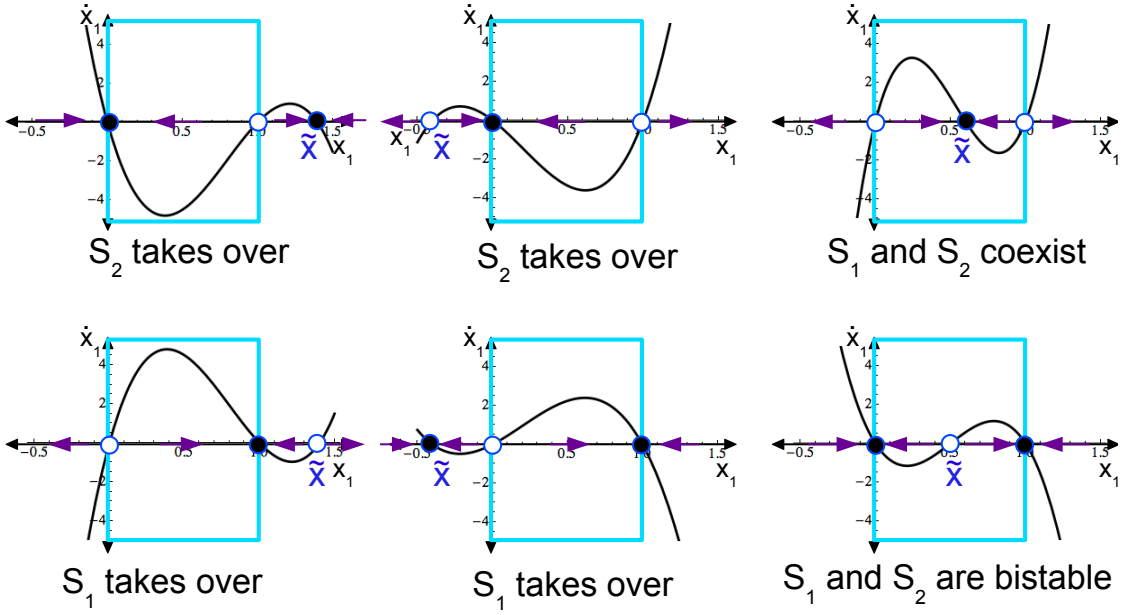

Figure 4.3: All possibilities for two-strategy replicator dynamics. x is the proportion of the population that uses strategy S_1, $\dot{x}$ is the change in the population proportion of strategy S_1. When $\tilde{x} \notin (0,1)$, strategy S_1 takes over when $\frac{d}{dx}\dot{x}|_{x=0} > 0$ (bottom left and middle panels) and strategy S_2 takes over when $\frac{d}{dx}\dot{x}|_{x=0} < 0$ (top left and middle panels). When $0 < \tilde{x} < 1$, the two populations stably coexist at an intermediate level if $\frac{d}{dx}\dot{x}|_{x=0} > 0$ (top right panel) and are bistable if $\frac{d}{dx}\dot{x}|_{x=0} < 0$ (bottom right panel).

We consider the possible population dynamics for two interacting strategies: a set strategy (the reigning champion) $S_2 = (p_2, q_2)$ against any other contending strategy, $S_1 = (p_1, q_1)$. Let x be the proportion of the population that is the strategy S_1, then $1 - x$ is the proportion of the population that plays strategy S_2. For this two player interaction, the replicator equations (equations 4.1 and 4.2) produce a one-dimensional system where $\dot{x}$ is at most a degree-three polynomial in terms of x. The points $x = 0$ and $x = 1$, which correspond to single strategy populations, are always fixed points. The change in population density for strategy S_1 is:

$$\dot{x} = x(xE_{11} + (1 - x)E_{12} - \phi) \tag{4.3}$$

with average fitness ϕ:

$$\phi = x(xE_{11} + (1-x)E_{12}) + (1-x)(xE_{21} + (1-x)E_{22}) \tag{4.4}$$

Here $\dot{x}$ is a degree-three polynomial in terms of x, which always has fixed points for single-strategy populations ($x = 0$ or $x = 1$). There are four distinct types of behavior when both populations start with non-zero densities. These can be characterized by the location of the nontrivial fixed point ($\tilde{x} \neq 0, \tilde{x} \neq 1$) and the slope of $\dot{x}$ when $x = 0$ (*i.e.* $\frac{d}{dx}\dot{x}|_{x=0}$). The possible types of population dynamics for the function $\dot{x}$ are shown in Figure 4.3 and are:

- strategy S_1 always takes over when $\frac{d}{dx}\dot{x}|_{x=0} > 0$ and $\tilde{x} \notin (0, 1)$.
- strategy S_2 always takes over when $\frac{d}{dx}\dot{x}|_{x=0} < 0$ and $\tilde{x} \notin (0, 1)$.
- both strategies coexist when $\frac{d}{dx}\dot{x}|_{x=0} > 0$ and $\tilde{x} \in (0, 1)$.
- the strategies are bistable, with initial population densities determining which takes over. This happens when $\frac{d}{dx}\dot{x}|_{x=0} < 0$ and $\tilde{x} \in (0, 1)$.

To understand the population dynamics for the prisoner's dilemma with the Axelrod payoffs (Table 4.1) by plotting the reigning champion strategy (S_2) in the $p - q$ plane (Figure 4.4). We then divide the strategy space according to the dynamics of strategy S_2 against contending strategies located in each region. As described above, there are up to four distinct regions: the competing strategy, S_1, 1) eliminates S_2 (green regions in Fig. 4.4), 2) is eliminated by S_2 (pink regions in Fig. 4.4), 3) coexists with S_2 (blue regions in Fig. 4.4), and 4) is bistable with S_2 (yellow regions in Fig. 4.4).

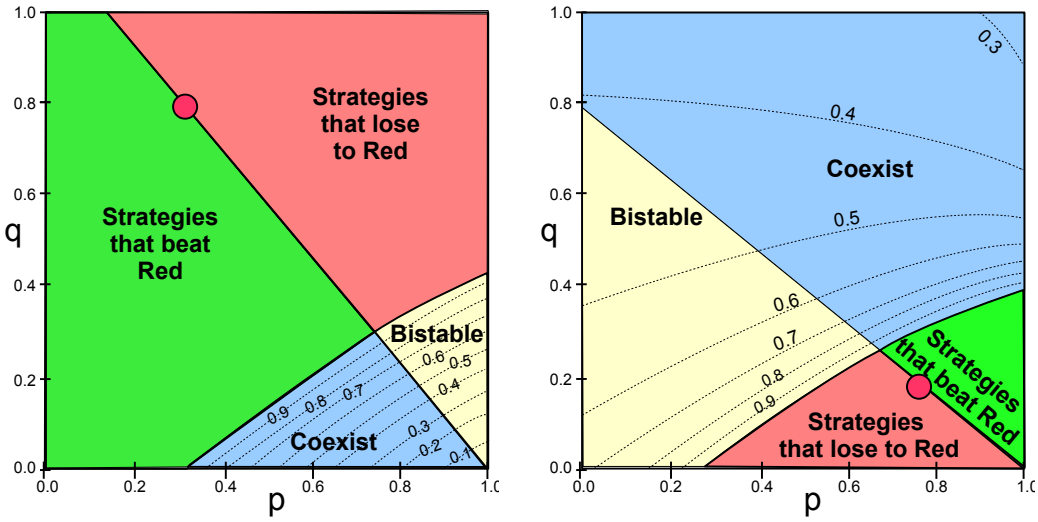

(a) $\tilde{s}$ is above the critical curve

(b) $\tilde{s}$ is below the critical curve

Figure 4.4: Population dynamics for two competing strategies. The strategy S_2 is plotted as a red point (and referred to as 'red' in region labels) and the regions describe what happens when S_2 competes with any strategy S_1 contained in that region. We have plotted two examples: one with S_2 above the critical curve (subplot 4.5(a)), and the other with S_2 below the critical curve (subplot 4.5(b)). The illustrated patterns are consistent for all choices of S_2 that are sufficiently far from the critical curve (between the blue and green regions). When the competing strategy S_1 falls in the pink region strategy S_2 will take over. When S_1 falls in the green region, it will eliminate S_2. The blue/yellow regions show contour plots of the value of the intermediate equilibrium $\tilde{x}$. In these regions the populations could stably coexist (blue) or be bistable (yellow) where the the initial population densities determine which strategy is eliminated.

For most choices of S_2, the boundaries between these regions are defined by two curves: the line through S_2 and $(1, 0)$, and a *'critical curve'* which depends on the choice of S_2, and runs from about $(p = 1/4, q = 0)$ to $(p = 1, q = 1/3)$. Figure 4.4 shows these regions for two choices of $\tilde{s}$. These figures show characteristic regions and dynamics that generally hold when S_2 is far enough above (Fig 4.4a) or below (Fig 4.4b) the critical curve. Strategies that are well above the critical curve are replaced by less cooperative strategies (in the green region of Fig 4.4a). Strategies that are well below the critical curve are replaced by more generous strategies (in the green region of Fig 4.4b). When S_2 competes with a strategy on the other side of the curve the two populations could either coexist at an intermediate level (blue regions in Fig 4.4) or be bistable with the strategy with a high enough initial population density eliminating the other (yellow region in 4.4).The contour lines show the value of $\tilde{x}$ which define the fraction of S_1 in the mixed equilibrium in the blue region and the threshold initial population density for strategy S_1 in the yellow region.

This population model predicts that the population will move from more cooperative strategies (like *AllC*) to less cooperative strategies (like *AllD*). Likewise the population will move from more aggressive retaliatory strategies (like not-so-nice TFT, $(0.8, 0)$) towards more generous retaliatory strategies (like $GTFT$). When the strategy S_2 is near the curved boundary, the regions become more complex but the possible dynamics are still the same. Figure 4.5 shows two examples of the regions that arise when S_2 is near the critical curve.

The critical curve plays an important role for the dynamics, so it is important that we understand how this curve changes with the choice of S_2. This curve

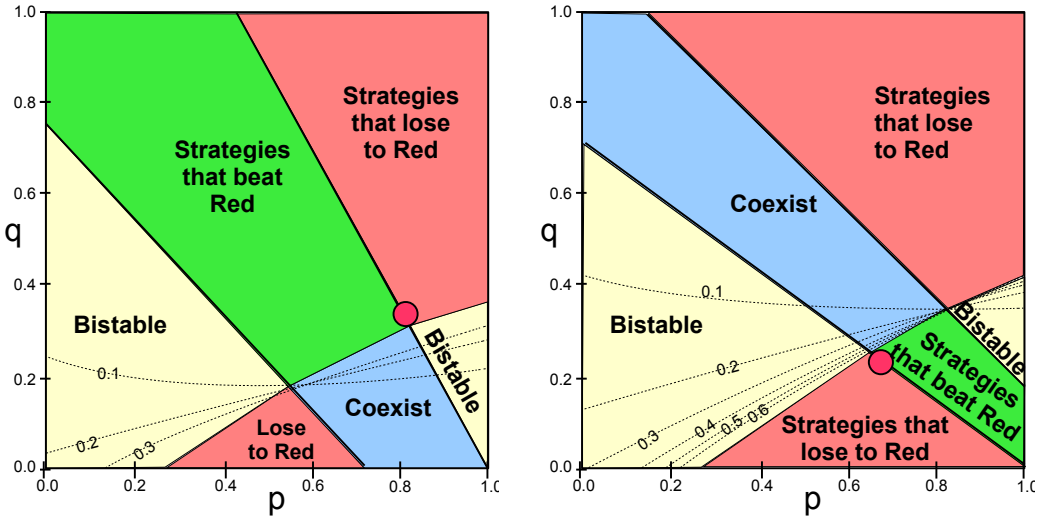

(a) $\tilde{s}$ is just above the critical curve

(b) $\tilde{s}$ is just below the critical curve

Figure 4.5: Population dynamics for two competing strategies close to the critical curve. When S_2 (the red dot) is close to the critical curve, a bifurcation occurs and a new pair of regions appear. These figures illustrate examples of the population dynamics that occur when S_2 is close to the critical curve. In a) S_2 is just above the critical curve and in b) S_2 is just below the critical curve. There is another bifurcation when S_2 crosses the critical curve.

occurs when the non-trivial ($x \neq 0, x \neq 1$) fixed point $\tilde{x}$ equals one. In Figure 4.6 the critical lines for a range of strategies S_2 are overlaid. We find that the critical curves are contained in an envelope bounded below by the critical curve for the strategy *AllC*, $(1, 1)$,

$$f_1 = \frac{4p - 3 + \sqrt{5 - 4p}}{4} \tag{4.5}$$

and above by the critical curve for strategy *AllD*, $(0, 0)$,

$$f_2 = \frac{6p - 5 + \sqrt{13 - 12p}}{6} \tag{4.6}$$

Both of these curves are shown in black in figure 4.7. There is a third important line which is where the critical curve is when points are very close to the curve (either above or below). This line is the critical curve f for the strategy $(1, 0)$ and

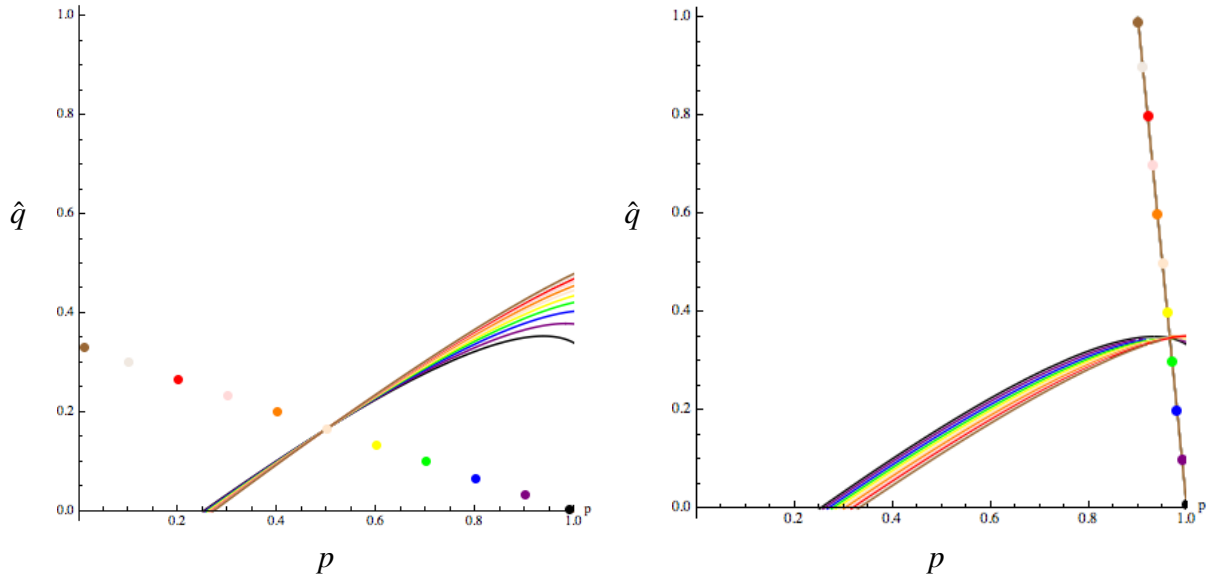

Figure 4.6: Plots of the critical curves for eleven strategies along a line. The strategies are plotted as colored dots with the associated critical curve shown in the same color. The critical curve divides the strategy space into two regions with qualitatively different population dynamics between the set strategy and strategies in that region. As $\tilde{s}$ moves along each ray starting near $(1, 0)$ the critical curve changes only slightly, with most variation further from the ray of interest.

is plotted in gray in Figure 4.7. We find that the equation for this line is

$$f = \frac{1}{9}\left(p - 9(1-p) + \frac{18(1-p) + p^2}{\beta} + \beta\right) \tag{4.7}$$

where $\beta = 27(1-p)p + p^3 + 9\sqrt{3}^3\sqrt{-(1-p)^2(24(1-p)+p^2)}$.

Nowak and Sigmund discovered similar curves when they looked at the adaptive dynamics of this game. They discovered that if the population evolves (collectively) toward nearby strategies with the highest individual fitness, then the population's strategy will become more cooperative when below this critical curve, and will become less cooperative when above the critical curve [75]. This matches what we see using the more general replicator equations which

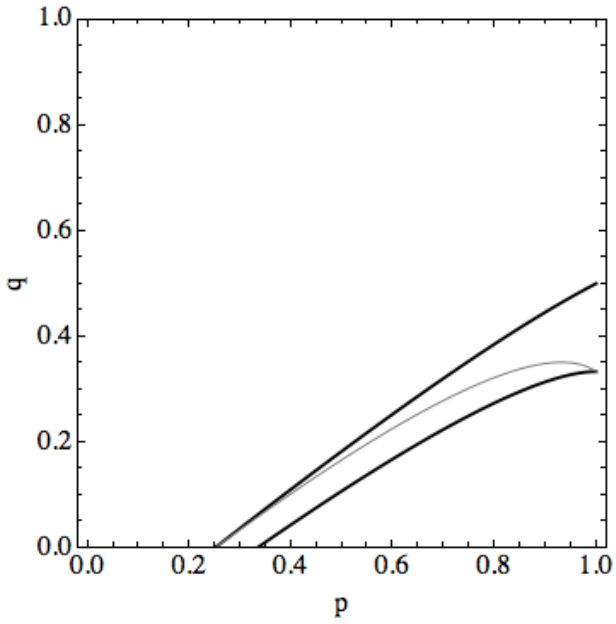

Figure 4.7: The envelope functions f_1 (4.5) and f_2 (4.6) for the critical curves that define regions with distinct dynamics are plotted in black. The grey line, f (4.7), is the boundary that is actually approached as the strategies get close (or into) the envelope region.

consider not only evolution to nearby strategies but the ability of any strategy to invade and flourish.

In summary, we find that for two strategy populations, when generous strategies are too generous *AllD* will prevail. Thus, counterintuitively, for populations to stably maintain cooperation it is important that individuals be only somewhat forgiving of non-cooperation. Some level of forgiveness in the TFT strategy is helpful when there are mistakes, but forgiving defection too often provides an opening for *AllD* to take over. We see this in the two-strategy interactions in that when the population is below the critical curve (*i.e.* not too forgiving), more cooperative strategies will vanquish their less cooperative counterparts. When strategies are above the curve (*i.e.* more forgiving), less cooperative

strategies will prevail.

4.3 Dynamics of three strategies

Now that we have a careful classification of the dynamics of a two player interaction, it is time to move on to the realm of three-strategy types. The interactions for three strategies have been well characterized but are very complicated and it is hard to draw conclusions from the current analysis [100]. For this reason, we reanalyze the system of equations for three particular strategies of interest and provide results for this reduced system. These strategies are non-cooperation (*AllD*: $(0,0)$), tit-for-tat with occasional mistakes ($\epsilon - TFT : (1-\epsilon, \epsilon)$), and generous tit-for-tat ($GTFT : (1, \hat{q})$). The parameter ϵ is the probability that $\epsilon - TFT$ will make a mistake and not copy their opponent's last move. $\hat{p}$ is the probability that generous TFT ($GTFT$) forgives the opponent and cooperates after being defected against. We explore the effects of different levels of forgiveness ($\hat{q}$) and mistakes (ϵ) on the population dynamics.

We use the standard replicator equations to represent the population dynamics. Let the fraction of the population that are $AllD, \epsilon - TFT$, and $GTFT$, be x_1, x_2, x_3, respectively with $x_3 = 1 - x_1 - x_2$. The replicator equations express the change in the population densities, *i.e.* $\dot{x}_1, \dot{x}_2, \dot{x}_3$ (explicitly defined in equations 4.1 and 4.2). We find the fixed points, by solving $\dot{x_1} = 0$ and $\dot{x_2} = 0$ for x_1 and x_2. There are seven possible fixed points (x_1^*, y_2^*) for this system. The three trivial fixed points representing populations consisting of a single-strategy are always present: all defectors $(1,0)$, all $\epsilon - TFT(0,1)$, and all $GTFT(0,0)$. Three of the

fixed points, when they exist, are a mix of two strategies: $(x_1, 1-x_1), (x_1, 0), (0, x_2)$. The last fixed point, when it is in the region, is a mix of all three strategies: *i.e.* (x_1, x_2), where $x_1 + x_2 < 1$. We then compute the Jacobian matrix analytically and calculate the trace and determinant at each of these fixed points to determine the stability of each point. We determine the location and stability of each fixed point analytically as a function of $\hat{q}$ and ϵ and consider the dynamics within the region $0 \leq \hat{q} \leq 1, 0 \leq \epsilon \leq .2$. The range for ϵ is restricted to be small because it is supposed to be a strategy close to TFT, and this is only true for small values of ϵ. Figure 4.8 shows stability diagram for $GTFT$ in terms of the parameters $\hat{q}$ and ϵ.

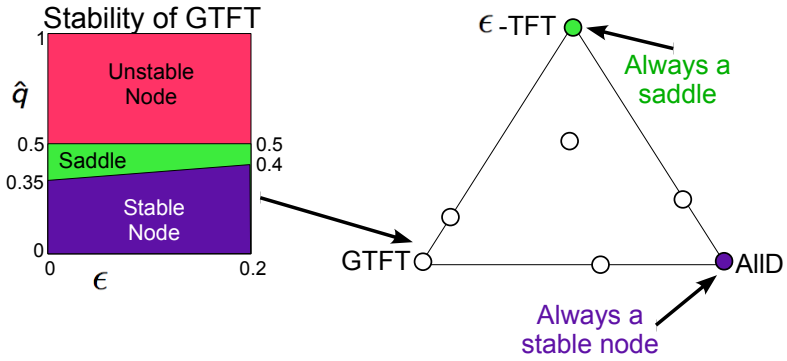

Figure 4.8: The triangle shows a diagram of the fixed population proportions. The triangle's corners represent the single-strategy populations. Along the edges the population consists of two strategies. The one interior fixed point is a mix of all three strategies. An example stability diagram is included for $GTFT$ over reasonable values of ϵ and $\hat{q}$.

We see that $\epsilon - TFT$ is always a saddle (*i.e.* never an end state) and that *AllD* is always a stable node, so for all reasonable ϵ and $\hat{q}$, there is always the possibility that the population will be taken over by *AllD* if there is a high enough initial density of defectors. Generous TFT is stable when it is not too generous ($\hat{q} < .35$). This matches the results of Nowak and Sigmund where a mixed population of 100 randomly chosen strategies will initially be taken over by a

strategy close to *AllD*, then, if there is a strategy close enough to TFT, this retaliatory strategy will prevail for a short time until it is finally taken over by a more generous strategy ($GTFT$) with $\hat{p} \approx 0.3$ that prevails for the rest of time [79]. This strategy is generous enough to end costly retaliatory cycles fairly quickly, but is retaliatory enough to not be overly sensitive to exploitation by defectors and is not taken over by any other strategies.

Figure 4.9 shows a bifurcation diagram of the regions with qualitatively different dynamics as well as representative phase portraits for each part of the state space. In all cases defectors will become prevalent if the initial population of *AllD* is large enough (what we mean by large enough depends on the choices of ϵ and q). As we change ϵ and $\hat{q}$, the second stable node changes. For less generous (small $\hat{q}$) $GTFT$ strategies, the population converges to all $GTFT$ if the initial density of *AllD* is small enough. For intermediate levels of generosity (the orange region of Fig 4.9), the second stable fixed point is a mix of $\epsilon - TFT$ and $GTFT$. When $GTFT$ is very forgiving and $\epsilon - TFT$ does not make many mistakes (the white region of Fig 4.9), the second stable fixed point is a mix of all three strategies. The conceptual diagrams in Figure 4.9 do not show the locations of the fixed points accurately, as the fixed points change with $\hat{q}$ and ϵ.

4.4 Discussion

In this work we find that for both two and three strategy populations, when generous strategies are too generous *AllD* will prevail. Thus, counterintuitively, for populations to stably maintain cooperation it is important that individuals

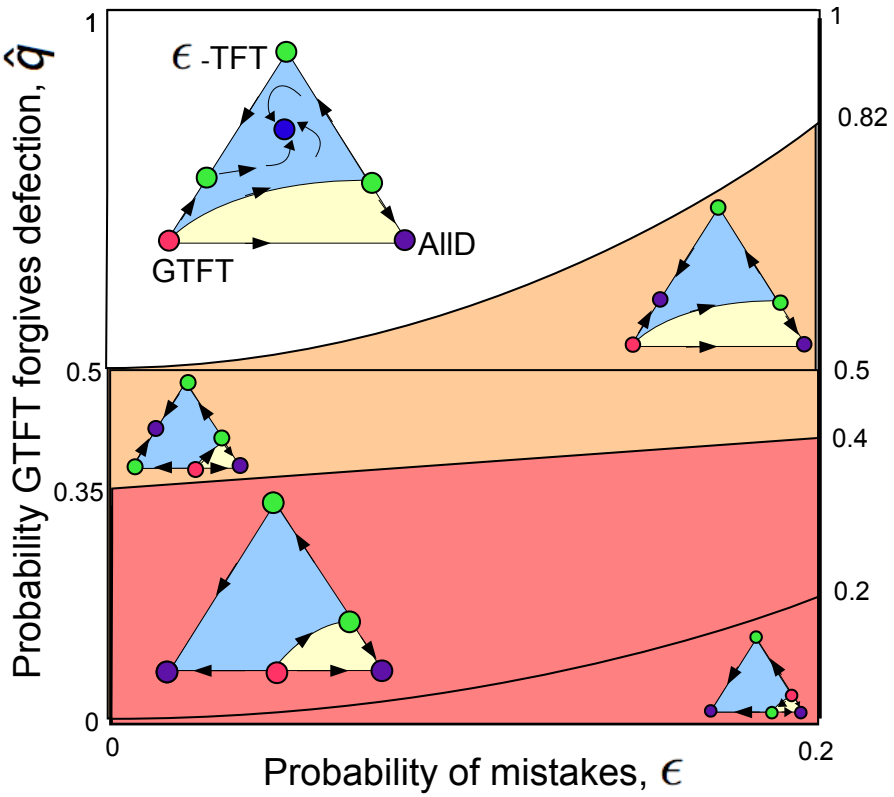

Figure 4.9: Bifurcation diagram of $\epsilon - q$ parameter space for the population densities of strategies *AllD* (proportion x_1, $p = 0, q = 0$), $\epsilon - TFT$ (proportion y, $p = 1 - \epsilon, q = \epsilon$), and $GTFT$ (proportion $x_3 = 1 - x_1 - x_2$, $p = 1, q = \hat{q}$). The associated stabilities of each fixed point sketched in the region where green points are saddles, blue points are stable spirals, purple points are stable nodes, red points are unstable nodes, and orange points (non shown here) are unstable spirals. Only the general location of the fixed point (*e.g.* on a certain edge) is accurate. The exact locations depend on the parameters $\hat{q}$ and ϵ.

be only somewhat forgiving of non-cooperation. Some level of forgiveness in the TFT strategy is helpful when there are mistakes, but forgiving defection too often provides an opening for *AllD* to take over. We see this in the two-strategy interactions in that when the population is below the critical curve (*i.e.* not too forgiving), more cooperative strategies will vanquish their less cooperative counterparts. When strategies are above the curve (*i.e.* more forgiving), less

cooperative strategies will prevail.

The next phase of this work is to consider three competing strategies with mutation. The addition of mutation may add enough complexity to produce stable cycles of cooperation, where the population oscillates between almost everyone being cooperative to almost everyone being non-cooperative to almost everyone being retaliatory (with occasional mistakes) and back to almost everyone being cooperative. These cycles of cooperation have been reported for more complex populations [78, 80, 58], and raise questions about long term stability of cooperative strategies. Now that we have a better analytical understanding of the interactions between strategies, our goal is to find the simplest situation where true limit cycles occur so that we can analytically describe the minimal requirements for cooperative cycles. We will start by considering three competing stochastic strategies with mistakes in the retaliatory strategy and mutation between subpopulations. A slightly more complex variant of this system has been shown to have population cycles, so we think that it is reasonable to think that a population with three competing stochastic strategies reproducing according to the replicator-mutator equations might be the simplest system which will exhibit cooperative cycles.

Bibliography

[1] *Mathematica edition: Version 9.0*, Wolfram Research, Inc., Champaign, Illinois, 2010.

[2] D. R. Ardia, J. E. Gantz, B. C. Schneider, and S. Strebel, *Costs of immunity in insects: an induced immune response increases metabolic rate and decreases antimicrobial activity*, Functional Ecology **26** (2012), 732–739.

[3] R. Axelrod, *Effective choice in the prisoner's dilemma*, Journal of Conflict Resolution **24** (1980), no. 1, 3–25.

[4] ———, *More effective choice in the prisoner's dilemma*, Journal of Conflict Resolution **24** (1980), 379–403.

[5] ———, *The emergence of cooperation among egoists*, American Political Science Review **75** (1981), no. 2, 306–318.

[6] R. Axelrod and W. D. Hamilton, *The evolution of cooperation*, Science **211** (1981), no. 4489, 1390–1396.

[7] Y. Ayal and R. F. Green, *Optimal egg distribution among host patches for parasitoids subject to attack by hyperparasitoids*, The American Naturalist **141** (1993), no. 1, 120–138.

[8] M. A. Becher and R. F. A. Moritz, *A new device for continuous temperature measurement in brood cells of honeybees (Apis mellifera)*, Apidologie **40** (2009), no. 5, 577–584.

[9] J. Bendor, R. M. Kramer, and S. Stout, *When in doubt… cooperation in a noisy prisoner's dilemma*, The Journal of Conflict Resolution **35** (1991), no. 4, 691–719.

[10] C. Bernstein and G. Driessen, *Patch-marking and optimal search patterns in the parasitoid Venturia canescens*, Journal of Animal Ecology **65** (1996), no. 2, 211–219.

[11] S M Blower and H Dowlatabadi, *Sensitivity and Uncertainty Analysis of Complex Models of Disease Transmission: An HIV Model, as an Example*, International Statistical Review **62** (1994), no. 2, 229–243.

[12] F S Bodenheimer, *Studies in animal populations II: seasonal population-trends of the honey-bee*, The Quarterly Review of Biology **12** (1937), no. 4, 406–425.

[13] A. Bouskila, I. C. Robertson, M. E. Robinson, B. D. Roitberg, B. Tenhumberg, A. J. Tyre, and E. van Randen, *Submaximal oviposition rates in a myramid parasitoid: Choosiness should not be ingnored*, Ecology **76** (1995), no. 6, 1990–1993.

[14] C. J. Briggs and J. Latto, *The window of vulnerability and its effect on relative parasitoid abundance*, Ecological Entomology **21** (1996), no. 2, 128–140.

[15] J. Brodeur and G. Boivin, *Functional ecology of immature parasitoids.*, Annual Review of Entomology **49** (2004), 27–49.

[16] B. Bujok, M. Kleinhenz, S. Fuchs, and J. Tautz, *Hot spots in the bee hive*, Naturwissenschaften **89** (2002), no. 7, 299–301.

[17] N Calderone and B Johnson, *The within-nest behaviour of honeybee pollen foragers in colonies with a high or low need for pollen*, Animal behaviour (2002), no. 63, 749–758.

[18] S Camazine, *Self-organizing pattern formation on the combs of honey bee colonies*, Behavioral Ecology and Sociobiology **28** (1991), no. 1, 61–76.

[19] S Camazine, J Deneubourg, N Franks, J Sneyd, G Theraulaz, and E Bonabeau, *Self-Organization in Biological Systems* , Princeton studies in complexity, Princeton University Press, January 2001.

[20] Scott Camazine, James Sneyd, Michael J Jenkins, and J D Murray, *A mathematical model of self-organized pattern formation on the combs of honeybee colonies*, Journal of Theoretical Biology **147** (1990), no. 4, 553–571.

[21] E. L. Charnov, *Optimal foraging, the marginal value theorem*, Theoretical Population Biology **9** (1976), no. 2, 129–136.

[22] D. Cohen, *Optimizing reproduction in a randomly varying environment*, Journal of Theoretical Biology **12** (1966), no. 1, 119.

[23] J. T. Costa, *The other insect societies*, The Belknap Press of Harvard University Press, 2006.

[24] C. Couchoux, K. J. Montovan, S. D. van Nouhuys, and Seppa, *How effective is Hyposoter horticola's deterrent post-oviposition marking? behavioral and genetic approaches*, In prep for Behavioral Ecology.

[25] C. Couchoux and S. van Nouhuys, *Effects of intraspecific competition and host-parasitoid developmental timing on foraging behaviour of a parasitoid wasp*, In prep.

[26] K Crailsheim, L Schneider, N Hrassnigg, G Buhlmann, U Brosch, R Gmeinbauer, and B Schoffmann, *Pollen consumption and utilization in worker honeybees (Apis mellifera carnica): Dependence on individual age and function*, Journal of Insect Physiology **38** (1992), no. 6, 409–419.

[27] J. Cronin and D. Strong, *Substantially Submaximal Oviposition rates by a Mymarid Egg Parasitoid in the Laboratory and Field*, Ecology **74** (1993), no. 6, 1813–1825.

[28] L. B. Crowder and W. E. Cooper, *Habitat structural complexity and the interaction between bluegills and their prey*, Ecology **63** (1982), no. 6, 1802–1813.

[29] M. Doebeli and C. Hauert, *Models of cooperation based on the prisoner's dilemma and the snowdrift game*, Ecology Letters **8** (2005), no. 7, 748–766.

[30] G. Driessen and C. Bernstein, *Patch departure mechanisms and optimal host exploitation in an insect parasitoid*, Journal of Animal Ecology **68** (1999), no. 3, 445–459.

[31] F. C. Dyer, *The biology of the dance language*, Annu. Rev. Entomol. **47** (2002), 917–949.

[32] Stephen P Ellner and John Guckenheimer, *Dynamic models in biology*, 1 ed., Princeton University Press, March 2006.

[33] P. Eslin and G. Prevost, *Racing against host's immunity defenses: a likely strategy for passive evasion of encapsulation in Asobara tabida parasitoids*, Journal of Insect Physiology **46** (2000), no. 8, 1161–1167.

[34] M. Fehler, M. Kleinhenz, F. Klügl, F. Pupper, and J. Tautz, *Caps and gaps: a computer model for studies on brood incubation strategies in honeybees (Apis mellifera carnica)*, Naturwissenschaften **94** (2007), no. 8, 675–680.

[35] S. A. Field and M. A. Keller, *Short-term host discrimination in the parasitoid wasp Trissolcus basalis Wollaston (hymenoptera: Scelionidae)*, Australian Journal of Zoology **47** (1999), no. 1, 19–28.

[36] T. P. Friedlander, *Egg mass design relative to surface-parasitizing parasitoids, with notes on Asterocampa clyton (lepidoptera: Nymphalidae)*, Journal of Research on the Lepidoptera **24** (1985), 250–257.

[37] J. H. Gillespie, *Natural selection for within-generation variance in offspring number*, Genetics **76** (1974), no. 3, 601–609.

[38] ———, *Natural selection for variances in offspring numbers: A new evolutionary principle*, The American Naturalist **111** (1977), no. 981, 1010–1014.

[39] J. P. Gillespie, M. R. Kanost, and T. Trenczek, *Biological mediators of insect immunity*, Annu. Rev. Entomol. **42** (1997), 611–643.

[40] H. C. J. Godfray, M. P. Hassell, and R. D. Holt, *The population dynamic consequences of phenological asynchrony between parasitoids and their hosts*, Journal of Animal Ecology **63** (1994), 1–10.

[41] K. J. Griffiths, *The importance of coincidence in the functional and numerical responses of two parasites of european pine sawfly, Neodiprion sertifer.*, Canadian Entomologist **101** (1969), 673–713.

[42] P. Grodzicki and M. Caputa, *Social versus individual behaviour: a comparative approach to thermal behaviour of the honeybee (Apis mellifera l.) and the american cockroach (Periplaneta americana l.)*, Journal of Insect Physiology **51** (2005), no. 3, 315–322.

[43] A. H. Grossman, A Janssen, E. F de Brito, E. G. Cordeiro, J. O. Fonseca, E. R. Lima, A. Pallini, and M. W. Sabelis, *Parasitoid increases survival of its pupae by inducing hosts to fight predators*, PLoS ONE **3** (2008), no. 6, e2276.

[44] I. Hanski, *Eco-evolutionary spatial dynamics in the glanville fritillary butterfly.*, Proc. Natl. Acad. Sci. **108** (2011), no. 35, 14397–14404.

[45] I. Hanski, J. Alho, and A. Moilanen, *Estimating the parameters of survival and migration of individuals in metapopulations*, Ecology **81** (2000), 239–251.

[46] D. D. Hart, S. L. Kohler, and R. G. Carlton, *Harvesting of benthic algae by territorial grazers: The potential for prudent predation*, OIKOS **60** (1991), no. 3, 329–335.

[47] M. P. Hassell, *The spatial and temporal dynamics of host-parasitoid interactions*, Oxford University Press, 2000.

[48] G. E. Heimpel, J. A. Rosenheim, and M. Mangel, *Egg limitation, host quality, and dynamic behavior by a parasitoid in the field.*, Ecology **77** (1996), 2410–2420.

[49] B. Heinrich, *Experimental behavioral ecology and sociobiology*, no. 31, ch. The social physiology of temperature regulation in honeybees, pp. 393–406, Fortschritte der Zoologie, 1985.

[50] S. W. Hitchcock, *Number of fall generations of Ooencyrtus kuwanai (how.) in gypsy moth eggs.*, Journal of Economic Entomology **52** (1959), no. 4, 764–765.

[51] J. Hofbauer and K Sigmund, *Evolutionary game dynamics*, Bulletin of the American Mathematical Society **40** (2003), no. 4, 479–519.

[52] C. Höller and R. Hörmann, *Patch marking in the aphid hyperparasitoid, Dendrocerus carpenteri: the information contained in patch marks*, Oecologia **94** (1993), no. 1, 128.

[53] M. T. Hondo, T. Onodera, and N. Morimoto, *Parasitoid attack on a pyramid shaped egg mass of the peacock butterfly Inachis io geisha (lepidoptera: Nymphalidae).*, Applied Entomology and Zoology **30** (1995), no. 2, 271–276.

[54] K. R. Hopper, *Risk-spreading and bet-hedging in insect population biology*, Annual Review of Entomology **44** (1999), 535–560.

[55] S. F. Hubbard and R. M. Cook, *Optimal foraging by parasitoid wasps*, Journal of Animal Ecology **47** (1978), no. 2, 593–604.

[56] S. F. Hubbard, G. Marris, A. Reynolds, and G. W. Rowe, *Adaptive patterns in the avoidance of superparasitism by solitary parasitic wasps*, The Journal of Animal Ecology **56** (1987), no. 2, 387–401.

[57] J. A. C. Humphrey and E. S. Dykes, *Thermal energy conduction in a honey bee comb due to cell-heating bees*, Journal of Theoretical Biology **250** (2008), no. 1, 194–208.

[58] L. A. Imhof, D. Fudenberg, and M. A. Nowak, *Evolutionary cycles of cooperation and defection*, PNAS **102** (2005), no. 31, 10797–10800.

[59] Michael J Jenkins, James Sneyd, Scott Camazine, and J D Murray, *On a simplified model for pattern formation in honey bee colonies*, Journal of Mathematical Biology **30** (1992), no. 3, 281–306.

[60] B. R. Johnson, *Pattern formation on the combs of honeybees: increasing fitness by coupling self-organization with templates*, Proceedings of the Royal Society B **276** (2009), 255–261.

[61] M. Kankare, S. D. van Nouhuys, O. Gaggiotti, and I. Hanski, *Metapopulation genetic structure of two coexisting parasitoids of the Glanville fritillary butterfly*, Oecologia **143** (2005), 77–84.

[62] M. Kleinhenz, B. Bujok, S. Fuchs, and J. Tautz, *Hot bees in empty broodnest cells: heating from within*, The Journal of Experimental Biology **206** (2003), 4217–4231.

[63] Fredi Kronenberg and H Craig Heller, *Colonial thermoregulation in honey bees (Apis mellifera)*, Journal of Comparative Physiology B **148** (1982), no. 1, 65–76.

[64] M. S. Kuussaari, J. Hellmann, and M. C. Singer, *On the wings of checkerspots: A model system for population biology*, ch. Larval biology of checkerspot butterflies, pp. 138 – 160, Oxford University Press, 2004.

[65] M. D. Lavine and M. R. Strand, *Insect hemocytes and their role in immunity*, Insect Biochemistry and Molecular Biology **32** (2002), no. 10, 1295–1309.

[66] G. C. Lei, V. Vikberg, and M. Kuussaari, *The parasitoid complex attacking Finnish populations of the Glanville fritillary Melitaea cinxia, and endangered butterfly*, Journal of Natural history **31** (1997), 635–648.

[67] V. C. Maiorana, *Reproductive value, prudent predators, and group selection*, The American Naturalist **110** (1976), no. 973, 486–489.

[68] P. Marrow, R. Law, and C. Cannings, *The coevolution of predator-prey interactions: Esss and red queen dynamics*, Proceedings of the Royal Society of London Series B **250** (1992), 133–141.

[69] MATLAB, *version 7.14.0 (r2012a)*, The MathWorks Inc., Natick, Massachusetts, 2012.

[70] A. L. Mattila, A. Duplouy, M. Kirjokangas, R. Lehtonen, P. Rastas, and I. Hanski, *High genetic load in an old isolated butterfly population*, Proceedings of the National Academy of Sciences **109** (2012), no. 37, E2496–E2505.

[71] Michael D. McKay, *Latin hypercube sampling as a tool in uncertainty analysis of computer models*, Proceedings of the 24th conference on Winter simulation (New York, NY, USA), WSC '92, ACM, 1992, pp. 557–564.

[72] J. C. Munger, *Long-term yield from harvester ant colonies: Implications for horned lizard foraging strategy*, Ecological Society of America **65** (1984), no. 4, 1077–1086.

[73] A. T. Nicholson, *Supplement: the balance of animal populations*, Journal of Animal Ecology **2** (1933), no. 1, 131–178.

[74] W J Nolan, *The brood-rearing cycle of the honeybee (Department bulletin / United States Department of Agriculture)*, U.S. Dept. of Agriculture, 1925.

[75] M. Nowak and K. Sigmund, *The evolution of stochastic strategies in the prisoner's dilemma*, Acta Applicandae Mathematicae **20** (1990), 247–265.

[76] M. A. Nowak, *Five rules for the evolution of cooperation*, Science **314** (2006), 1560–1563.

[77] _____, *Evolving cooperation*, Journal of Theoretical Biology **299** (2012), 1–8.

[78] M. A. Nowak and K. Sigmund, *Oscillations in the evolution of reciprocity*, Journal of Theoretical Biology **137** (1989), 21–26.

[79] _____, *Tit for tat in heterogeneous populations*, Nature **355** (1992), 250–253.

[80] _____, *Chaos and the evolution of cooperation*, Proc. Natl. Acad. Sci. **90** (1993), 5091–5094.

[81] C. R. Nufio and D. R. Papaj, *Host marking behavior in phytophagous insects and parasitoids*, Entologia Experimentalist et Applicata **99** (2001), 273–293.

[82] O. Ovaskainen, *Habitat-specific movement parameters estimed using mark-recapture data and a diffusion model*, Ecology **85** (2004), 242 – 257.

[83] F. Pennacchio and M. R. Strand, *Evolution of developmental strategies in parasitic hymenoptera.*, Annual Review of Entomology **51** (2006), 233–258.

[84] G. H. Pyke, *Optimal foraging theory: a critical review*, Annual Review of Ecological Systems **15** (1984), 523–575.

[85] D. L. J. Quicke, *Parasitic wasps*, London Chapman and Hall, 1997.

[86] R Development Core Team, *R: A language and environment for statistical computing*, R Foundation for Statistical Computing, Vienna, Austria, 2011.

[87] K. H. Redford, *Feeding and food preference in captive and wild giant anteaters (Myrmecophaga tridactyla)*, J. Zool., Lond. (A) **205** (1985), 559–572.

[88] M. E. Ritchie, *Optimal foraging and fitness in columbian ground squirrels*, Oecologia **82** (1990), no. 1, 56–67.

[89] N. E. Sanchez, P. C. Pereyra, and M. G. Luna, *Spatial patterns of parasitism of the solitary parasitoid pseudapanteles dignus (hymenoptera: Braconidae) on tuta absoluta (lepidoptera: Gelechiidae).*, Environmental Entomology **38** (2009), no. 2, 365–374.

[90] W. M. Schaffer and M. L. Rosenzweig, *Hommage to the red queen. i. coevolution of predators and their victims*, Theoretical Population Biology **14** (1978), 135–157.

[91] T. Schmickl and K. Crailsheim, *HoPoMo: A model of honeybee intracolonial population dynamics and resource management*, Ecological Modeling **204** (2007), 219–245.

[92] P. Schmid-Hempel, *Variation in immune defense as a question of evolutionary*

ecology, Proceedings of the Royal Society of London Series B **270** (2003), no. 1513, 357–366.

[93] T D Seeley, *The ecology of temperate and tropical honeybee societies*, American Scientist **71** (1983), no. 3, 264–272.

[94] T D Seeley and R A Morse, *The nest of the honey bee (Apis mellifera L.)*, Insectes Sociaux **23** (1976), no. 4, 495–512.

[95] T. D. Seeley, P. K. Visscher, and K. M. Passino, *Group decision-making in honey bee swarms*, American Scientist **94** (2006), no. 2, 220–229.

[96] Thomas D Seeley, *Social foraging in honey bees: how nectar foragers assess their colony's nutritional status*, Behavioral Ecology and Sociobiology **24** (1989), no. 3, 181–199.

[97] M. R. Shaw, C. Stefanescu, and S. van Nouhuys, *Ecology of butterflies of europe*, ch. 11: Parasitoids of European Butterflies, pp. 130–156, Cambridge University Press, 2009.

[98] M. J. Smith, *Group selection and kin selection*, Nature **201** (1964), 1145–1147.

[99] D. C. Speirs, T. N. Herratt, and S. F. Hubbard, *Parasitoid diets: Does superparasitism pay?*, Trends in Ecology and Evolution **6** (1991), no. 1, 22–25.

[100] P. F. Stadler and P. Schuster, *Dynamics of small autocatalytic reaction networks- i. bifuc=rcations, preformence and exclusion*, Bulletin of Mathematical Biology **52** (1990), no. 4, 485–508.

[101] P. T. Starks and D. C. Gilley, *Heat shielding: A novel method of colonial thermoregulation in honey bees*, Naturwissenschaften **86** (1999), 438–440.

[102] L. L. Stelinski, R. Oakleaf, and C. Rodriguez-Saona, *Oviposition-deterring pheromone deposited on blueberry fruit by the parasitic wasp, Diachasma alloeum*, Behaviour **144** (2007), 429–445.

[103] D. W. Stephens and J. Krebs, *Foraging theory*, Princeton University Press, 1986.

[104] Jurgen J Tautz, Sven S Maier, Claudia C Groh, Wolfgang W Rossler, and Axel A Brockmann, *Behavioral performance in adult honey bees is influenced by the temperature experienced during their pupal development.*, PNAS **100** (2003), no. 12, 7343–7347.

[105] A. Traulsen and M. A. Nowak, *Evolution of cooperation by multilevel selection*, PNAS **103** (2006), no. 29, 190952–10955.

[106] S. van Nouhuys, M. C. Singer, and M. Nieminen, *Spatial and temporal patterns of caterpillar performance and the suitability of two host plant species*, Ecological Entomology **28** (2003), 193–202.

[107] S. D. van Nouhuys and J. Ehrnsten, *Wasp behavior leads to uniform parasitism of host available only a few hours per year*, Behavioral Ecology **15** (2004), no. 4, 661–665.

[108] S. D. van Nouhuys and I. Hanski, *Colonization rates and distances of a host butterfly and two specific parasitoids in a fragmented landscape*, Journal of Animal Ecology **71** (2002), 639–650.

[109] ———, *Metacommunities of butterflies, their host plants and their parasitoids*, Metacommunities: spatial dynamics and ecological communities (M. Holyoak, M. A. Leibold, and R. D. Holt, eds.), University of Chicago Press, Chicago, Il., USA, 2005, pp. 99–121.

[110] S. D. van Nouhuys and R. Kaartinen, *A parasitoid wasp uses landmarks while monitoring potential resources*, Proceedings of the Royal Society B **275** (2008), 377–385.

[111] S. D. van Nouhuys and G. C. Lei, *Parasitoid and host metapopulation dynamics: The influences of temperature mediated phenological asynchrony*, Journal of Animal Ecology **73** (2004), 526–535.

[112] J. Varaldi, P. Fouillit, M. Boulétreau, and F. Fleury, *Superparasitism acceptance and patch-leaving mechanisms in parasitoids: a comparison between two sympatric wasps*, Animal Behaviour **69** (2005), no. 6, 1227–1234.

[113] L. Vega, A. Torres, W. Hoffmann, and I. Lamprecht, *Thermal investigations associated with the behaviour patterns of resting workers of Bombus atratus (hymenoptera: Apidae)*, Journal of Thermal Analysis and Calorimetry **104** (2011), no. 1, 233–237.

[114] D. L. Venable, *Bet hedging in a guild of desert annuals*, Ecology **88** (2007), no. 5, 1086–1090.

[115] R. M. Weseloh, *Influence of gypsy moth egg mass dimensions and microhabitat distribution on parasitism by Ooencyrtus kuwanai*, Annals of the Entomological Society of America **65** (1972), 64–69.

[116] ———, *Spatial distribution of the gypsy moth [lepidoptera: Lymantriidae] and some of its parasitoids within a forest environment*, Entomophaga **17** (1972), 339–351.

[117] G. C. Williams, *Adaptation and natural selection: a critique of some current evolutionary thought*, Princeton University Press, 1966.

[118] D. S. Wilson, *Prudent predation: a field study involving three species of tiger beetles*, Oikos **31** (1978), 128–136.

[119] Mark L Winston, *The biology of the honey bee*, Harvard Univ Pr, January 1987.

[120] V. C. Wynne-Edwards, *Evolution through group selection*, Blackwell Scientific, Oxford, 1986.

APPENDIX A

HYPOSOTER HORTICOLA EXPERIMENTAL AND MODELING DETAILS

A.1 General Experimental procedures

Unless noted otherwise, the hosts used in experiments are obtained from a lab population of *M. cinxia* which are augmented each year with *M. cinxia* collected during the spring population census, and reared to pupation under controlled laboratory conditions. This produces adult *M. cinxia, H. horticola* and *M. stigmaticus*. After adults emerge, the female *H. horticola* are maintained in the laboratory, fed honey water (3:1), until they are needed for the experiment (at least 2 weeks).

The adult butterflies are few honey water (3:1), mated, and allowed to lay egg clusters on potted plants. To do this the *M. cinxia* butterflies are placed in cages (3 females + 8 non-sibling males) for one day to mate. After mating, 2 females are put in a cage with a host plant (*Plantago lanceolata* or *Veronica spicata*) to lay eggs. The laying cages are checked daily and when an egg cluster is found, the plant is removed. The plants with egg clusters are stored until the eggs are close to susceptible. They are then exposed to parasitism in the laboratory or are placed in a habitat patch in the field to be parasitized by *H. horticola*.

For parasitism in the laboratory, a female wasp is placed in a 40 by 40 by 50 cm cage containing a plant with susceptible butterfly eggs on it and allowed to parasitize the egg cluster. We observed each of the parasitism event. After the

wasp has parasitized and left the host egg cluster, we move the egg cluster to a Petri dish and wait 1 to 3 days for the host eggs to hatch. Host larvae are then typically dissected to determine the parasitism rate in each host egg cluster.

A.2 Experiment 2: Åland, Estonia, Morocco Population comparison study

For this experiment, host caterpillars were collected from several nests of each of two populations in the Moroccan highlands in autumn 2011, and several populations throughout Åland. They were kept in diapause under laboratory conditions until spring 2012. In the spring of 2012, we collected 11 post-diapause *M. cinxia* nests from Paldiski, Estonia.[1]. Then we reared all the caterpillars in the laboratory until they pupated. This produced adult *M. cinxia* from Åland, Morocco and Estonia, adult *H. horticola* from Åland and Estonia, and adult *M. stigmaticus* from Åland.

To obtain host egg clusters from all three origins, *M. cinxia* butterflies from each region were placed in cages (3 females + 8 non-sibling males from the same region) for one day to mate. After mating, 2 females (from the same region) were put in a cage with a host plant (*Veronica spicata*) to lay eggs. The laying cages were checked daily and when an egg cluster was found, the plant was removed. The plants with egg clusters were stored until the eggs were susceptible and used in the behavioral experiment. After adults emerge, the female

[1]This study was designed and performed by XX: Saskya? Christelle?

Host origin	Wasp origin	n	$\mu_p \pm \sigma_p$
Åland	Åland	11	28% ± 21%
Åland	Estonia	14	35% ± 18%
Estonia	Åland	10	43% ± 17%
Estonia	Estonia	14	38% ± 18%
Morocco	Åland	15	28% ± 18%

Table A.1: Summary of results from the Åland, Estonia, Morocco parasitism comparison study. n is the number of host clusters parasitized and dissected for that group. μ_p is the mean fraction parasitized for each group, and σ_p is the standard deviation of the fractions parasitized for each group.

H. horticola were maintained in the laboratory, fed honey water (3:1), until they were approximately two weeks old and were then used in the experiment to parasitize a single egg cluster. The adult *M. stigmaticus* were not used in this experiment.

For each trial of the experiment, a female wasp was put in a 40 by 40 by 50 cm cage containing a plant with susceptible butterfly eggs on it and allowed to parasitize the egg cluster. We used a different wasp for each host cluster and observed each of the parasitism events. After the wasp had parasitized and left the host egg cluster, we moved the egg cluster to a Petri dish and waited 1 to 3 days for the host eggs to hatch. When the host larvae were 1-2 weeks old, we dissected them to determine the parasitism rate in each host egg cluster. In total 64 egg clusters were parasitized, each by a different wasp from the chosen population. See table A.1 for more details and summary results.

A.3 Probing efficiency

The probing efficiency (b) is an important parameter for the optimal foraging model. It is not possible to estimate this parameter directly because of the tiny size of the eggs, mounded host egg architecture, and indistinguishable nature of probing and ovipositing. Instead, we use the model developed in section 3.2.6, $p = 1 - e^{-bt/\alpha}$ to relate the total time spent probing a single cluster (t) and number of eggs in the cluster (α) to the fraction of eggs parasitized (p).[2]

We observed Åland *H. horticola* wasps probing and ovipositing into 36 host egg clusters under laboratory conditions. The total time spent probing the eggs (t) was recorded for each cluster. After the hosts emerged, they were counted and dissected to determine the number of hosts parasitized in each cluster. We performed logistic regression in the statical package R [86] using glm with a binomial error function and logic link function. We fit a model that predicts the parasitism of individual eggs based on the average time per egg ($t/alpha$) spent at the cluster. We find that the best estimate for b is 0.96 ($p < 0.001$), and the 95% confidence interval for b is [0.81, 1.12].

A.4 Experiment 6: Detecting previous parasitism

To calculate the expected probability of multiply parasitized hosts we first consider the expectations according to the poisson process. The probability that a

[2]The data for this analysis was collected by K. J. Montovan and C. Couchoux and analyzed by K. J. Montovan.

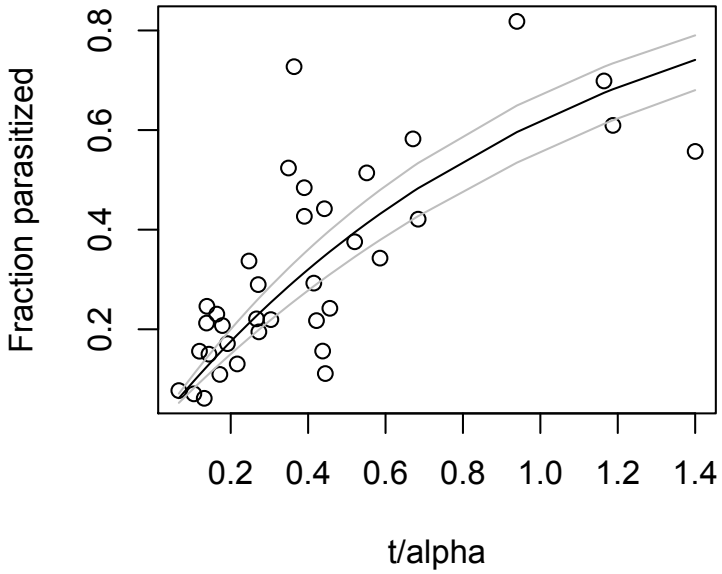

Figure A.1: Plot of the fraction of each cluster parasitized as a function of the average time per egg (t/α) that the wasp spent at the cluster. The black curve is the best fit line with $b = 0.96$, and the grey lines correspond to the curves bounding the 95% confidence interval for b ($b = .81$ and $b = 1.12$).

host is probed k times is

$$P(n = k) = \frac{\lambda^k}{k!} e^{-\lambda}$$

where λ is the mean number of probes per host. The wasp probes b eggs per minute so in t minutes the wasp probes bt eggs, which is divided by the number of eggs in the host cluster (α), *i.e.* $\lambda = \frac{bt}{\alpha}$.

If the wasp is unable to detect prior parasitism in a host, then the probability that a host egg is parasitized only once is

$$P(n = 1) = \lambda e^{-\lambda}.$$

If the wasp instead detects the prior parasitism with probability z and does not lay an egg when prior parasitism is detected, then the probability that a host

egg is parasitized only once is

$$\begin{aligned}
\hat{P}(n=1) &= \lambda e^{-\lambda} + z\frac{\lambda^2}{2!}e^{-\lambda} + z^2\frac{\lambda^3}{3!}e^{-\lambda} + \ldots \\
&= \lambda e^{-\lambda}\left(1 + \frac{z\lambda}{2!} + \frac{(z\lambda)^2}{3!} + \ldots\right) \\
&= \frac{\lambda e^{-\lambda}}{z\lambda}\left(z\lambda + \frac{(z\lambda)^2}{2!} + \frac{(z\lambda)^3}{3!} + \ldots\right) \\
&= \frac{e^{-\lambda}}{z}\sum_{j=1}^{\infty}\frac{(z\lambda)^j}{j!} \\
&= \frac{e^{-\lambda}}{z}(e^{z\lambda} - 1)
\end{aligned}$$

For our models we assume that the fraction of the cluster parasitized is $p = 1 - e^{-\lambda}$. We can then rewrite the above probabilities of superparasitism in terms of p.

$$\hat{P}(n=1) = \frac{1-p}{z}((1-p)^{-z} - 1) \tag{A.1}$$

Then the probability that an egg is multiply parasitized is

$$\hat{P}(n>1) = p - \frac{1-p}{z}((1-p)^{-z} - 1) \tag{A.2}$$

We determine the parameter z using the nonlinear (weighted) least-squares estimates to fit our data on the frequency of superparasitism to our model (the data are shown in Figure 3.5). We find that z is significantly different from zero indicating that the wasps do detect previously parasitized hosts and effectively avoid superparasitism some of the time ($p - value < 0.0001$). The estimate is $z = 0.74714$, *i.e.* the wasps detect previous parasitism approximately 75% of the time.